United States
Environmental Protection
Agency

Industrial Environmental Research
Laboratory
Research Triangle Park NC 27711

EPA-600/2-79-195
October 1979

Research and Development

EPA

Hyperfiltration Processes for Treatment and Renovation of Textile Wastewater

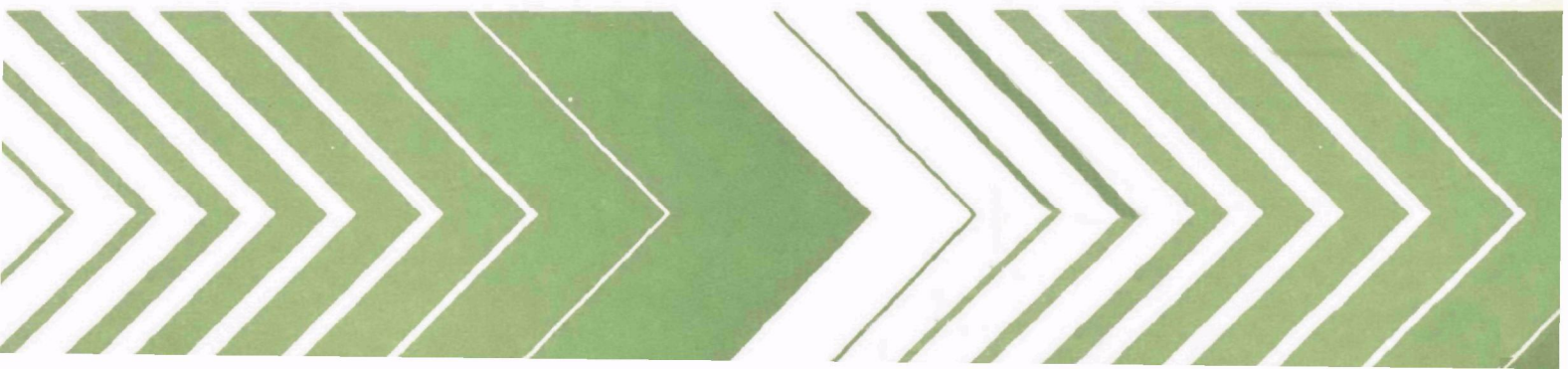

RESEARCH REPORTING SERIES

Research reports of the Office of Research and Development, U.S. Environmental Protection Agency, have been grouped into nine series. These nine broad categories were established to facilitate further development and application of environmental technology. Elimination of traditional grouping was consciously planned to foster technology transfer and a maximum interface in related fields. The nine series are:

1. Environmental Health Effects Research
2. Environmental Protection Technology
3. Ecological Research
4. Environmental Monitoring
5. Socioeconomic Environmental Studies
6. Scientific and Technical Assessment Reports (STAR)
7. Interagency Energy-Environment Research and Development
8. "Special" Reports
9. Miscellaneous Reports

This report has been assigned to the ENVIRONMENTAL PROTECTION TECHNOLOGY series. This series describes research performed to develop and demonstrate instrumentation, equipment, and methodology to repair or prevent environmental degradation from point and non-point sources of pollution. This work provides the new or improved technology required for the control and treatment of pollution sources to meet environmental quality standards.

EPA REVIEW NOTICE

This report has been reviewed by the U.S. Environmental Protection Agency, and approved for publication. Approval does not signify that the contents necessarily reflect the views and policy of the Agency, nor does mention of trade names or commercial products constitute endorsement or recommendation for use.

This document is available to the public through the National Technical Information Service, Springfield, Virginia 22161.

EPA-600/2-79-195

October 1979

Hyperfiltration Processes for Treatment and Renovation of Textile Wastewater

by

S. M. Ko and J. A. Tevepaugh

Lockheed Missiles and Space Co.
Huntsville Research and Engineering Center
Huntsville, AL 35807

Contract No. 68-02-2614
Task No. 009
Program Element No. 1BB-610

EPA Project Officer: Max Samfield

Industrial Environmental Research Laboratory
Office of Environmental Engineering and Technology
Research Triangle Park, NC 27711

Prepared for

U.S. ENVIRONMENTAL PROTECTION AGENCY
Office of Research and Development
Washington, DC 20460

ABSTRACT

A computer program for design and simulation of a multi-stage hyperfiltration system for renovation of textile wastewater has been developed. The program is capable of practical design, parametric simulation and cost projection of the multi-stage hyperfiltration system with tapered innerstages. The mathematical model is formulated based on Sourirajan's preferential sorption and solute diffusion theory. Experimental rejection and flux data of a test hyperfiltration module are required as input parameters. Empirical correlations and test results available from recent EPA-sponsored programs are utilized to calculate membrane transport parameters. Computed results for sample cases using cellulose acetate and dynamic membranes are presented. Various design and operating parameters are considered in the numerical computations to show effects of these parameters on economics of the system. This simulation program has been developed in a general manner and is readily adaptable for evaluation of other RO*/hyperfiltration applications.

---

* Reverse Osmosis

This report was submitted in fulfillment of Contract 68-02-2614, Task 009, by the Lockheed Missile & Space Company Huntsville Research & Engineering Center under the sponsorship of the U.S. Environmental Protection Agency. This report covers the period November 19, 1978 to August 31, 1979 and work was completed as of August 31, 1979.

TABLE OF CONTENTS

FIGURES

TABLES

LIST OF SYMBOLS

A	pure water permeability of membrane
A_o	constant
B	constant
C	molar concentration of solution
C_1	solvent concentration in membrane
C_1^*	concentration of water in solution on low pressure side
C_2	molar concentration of boundary solution
ΔC_2	solute concentration gradient across membrane
C_3	molar concentration of product solution
ΔC_A	difference in solute concentration in feed and product solutions
C_{A1}	molar concentration of solute in bulk
C_{A3}	molar concentration of solute in product
C_{AM}	solute concentration in membrane
D	diffusivity
D_1	solvent diffusion coefficient
D_2	solute diffusion coefficient
D_{AB}	diffusivity of solute in feed solution
D_{AM}	diffusivity of solute in membrane phase
f	Fanning friction factor
F	flow rate

g_c	conversion factor
J_1	solvent flux
J_2	solute flux
K	mass transfer coefficient
l	effective thickness of concentrated boundary layer
L	channel length
L_A	solute permeability
L_B	filtration coefficient
m_1	molarity of feed solution
m_3	molarity of product solution
M	average molecular weight of solution
M_A	molecular weight of component
M_B	molecular weight of water
N_A	solute flux
N_B	solvent flux
P	bulk pressure
ΔP	difference in bulk pressure across membrane
PR	product rate
PWP	pure water permeability
Q	permeability
r	tube radius
rj	rejection
R	gas constant

R_e	Reynolds number
S	solute transport parameter
S_A	surface area
Sc	Schmidt number
Sh	Sherwood number
t	channel thickness
T	temperature
TCM	mass transfer coefficient of solute
$\bar{u}$	average axial velocity
v_w	permeation velocity
V_1	partial molar volume of water
x	axial distance
X_{A2}	mole fraction of solute in concentrated boundary solution on high pressure side of membrane
X_{A3}	mole fraction of solute in product solution
α	constant
β	constant
δ	solubility parameter
δ_t	effective membrane thickness
λ	mass transfer coefficient on high pressure side divided by solute mass transfer coefficient
π	osmotic pressure
$\Delta\pi$	diiference in osmotic pressure across membrane
σ	Staverman reflection coefficient

ACKNOWLEDGEMENTS

The authors are grateful to Dr. J.L. Gaddis of Clemson University and Dr. C.A. Brandon of Carre, Inc., for their contribution to this study, in particular, their comments on the mathematical model. The EPA project officer was Dr. Max Samfield and his support and interest in this study is gratefully acknowledged.

1. INTRODUCTION

Hyperfiltration (also termed reverse osmosis) as a textile wastewater treatment and renovation process has been studied under EPA/IERL/RTP* sponsorship to investigate the technical feasibility and the economic practicability of the separation process. A recent investigation (Ref.1) of a pilot scale hyperfiltration facility at LaFrance Industries, a division of Riegel Textile Corporation, successfully demonstrated the feasibility of dynamic hyperfiltration membranes for the in-plant recycle and reuse of composite textile dyeing and finishing wastewater. The applicability of the concept to a variety of composite textile wastewaters has been confirmed in a more recent study (Ref.2) at eight different textile mills encompassing eight different subcategories of the textile mills point source category (Ref.3). The scope of these studies, however, was limited to testing and evaluating a few commercial membranes using plant composite wastewater and the mixed dyehouse effluent. Furthermore, optimization of process parameters in regard to more favorable economics, energy conservation, byproduct recovery and effluent control of the process system were not investigated in detail.

* Environmental Protection Agency. Industrial Environmental Research Laboratory, Research Triangle Park, N.C.

Textile finishing wastewater contains a variety of chemicals depending upon the particular dyeing and finishing operations. The type of chemicals in the wastewater greatly affects the performance of the membranes. The effectiveness of membranes is also sensitive to the temperature of the wastewater being treated. In the interest of energy recovery, high temperature operation of the process is desirable. Thus, a parametric investigation of the separation process directed toward efficient and cost effective design of the treatment system is required to provide the optimum performance and design information essential in the development of a full-scale system. Since experimental investigations of these parameters are not practical, such a parametric study necessitates a theoretical analysis of fundamental mechanisms involved in the hyperfiltration process and the development of a computer model of the process system. Unfortunately, however, direct extension of general reverse osmosis theory to mixed solute systems is complicated due to nonavailability of pertinent fundamental physiochemical properties of both membranes and solutes, and possible complex interactions of chemicals in such a system. Thus, the transport properties of solutes in the composite wastewater must be calculated from experimental flux and rejection data. Where such data are not available, these transport parameters may be estimated using empirical correlations (Refs.4 and 5).

In the following sections a discussion of hyperfiltration

theory and associated transport parameters is followed by a description of a computer model for design and simulation of a multi-stage hyperfiltration system. Results of a parametric study of the multi-stage system using the computer model are presented and significant conclusions summarized. In Appendix A, experimental membrane rejection and flux data are presented in tabular and graphic form. A report authored by Mr. A. Schindler of Research Triangle Institute on osmosis membrane separation efficiencies is included as Appendix B. A listing of the computer code is contained in Appendix C.

2. CONCLUSIONS

Governing equations describing the hyperfiltration of solvents and solutes can be derived from phenomenological considerations. These equations can be used to predict the performance of actual membranes provided experimental data and correlations are available for determining membrane transport parameters. These parameters are membrane and solute dependent.

A mathematical model formulated from Sourirajan's preferential sorption and solute diffusion theory is adequate for predicting membrane performance. The computer code provides reasonable design and simulation results (pressure, flow rate, rejection, recovery factor, concentration polarization) for a single module with multiple innerstages using both cellulose acetate and dynamic membranes. Given accurate cost information, the economic model realistically depicts the impact of various design parameters on unit cost.

The computer model is capable of predicting system performance as well as analyzing system economics to find an optimum set of design parameters. Reliability of the computer results is largely dependent on the availability of rigorous cost information

for the system as well as the accuracy of the test module data and membrane specifications.

3. THEORY OF HYPERFILTRATION

Phenomenology

Hyperfiltration (reverse osmosis) is a separation process which utilizes the selective sorbability of the solvent from a solution by semipermeable, microporous membranes. Figure 1 shows a schematic of steady state concentration profiles of the solvent (water) and the solute across the membrane. Due to relatively high affinity of the membrane to solvent molecules, a concentration gradient is established in the interface region. Adsorbed pure water molecules are permeated through the microporous structure of the membrane at a rate which is determined by the characteristics of the membrane and the pressure exerted to overcome the osmotic pressure.

Solute, on the other hand, diffuses to both directions from the interface. The selective permeation of water molecules will develope high solute concentration in the vicinity of the interface and thus develop a maximum concentration. This provides a driving force for the solute diffusion in both directions from the interface.

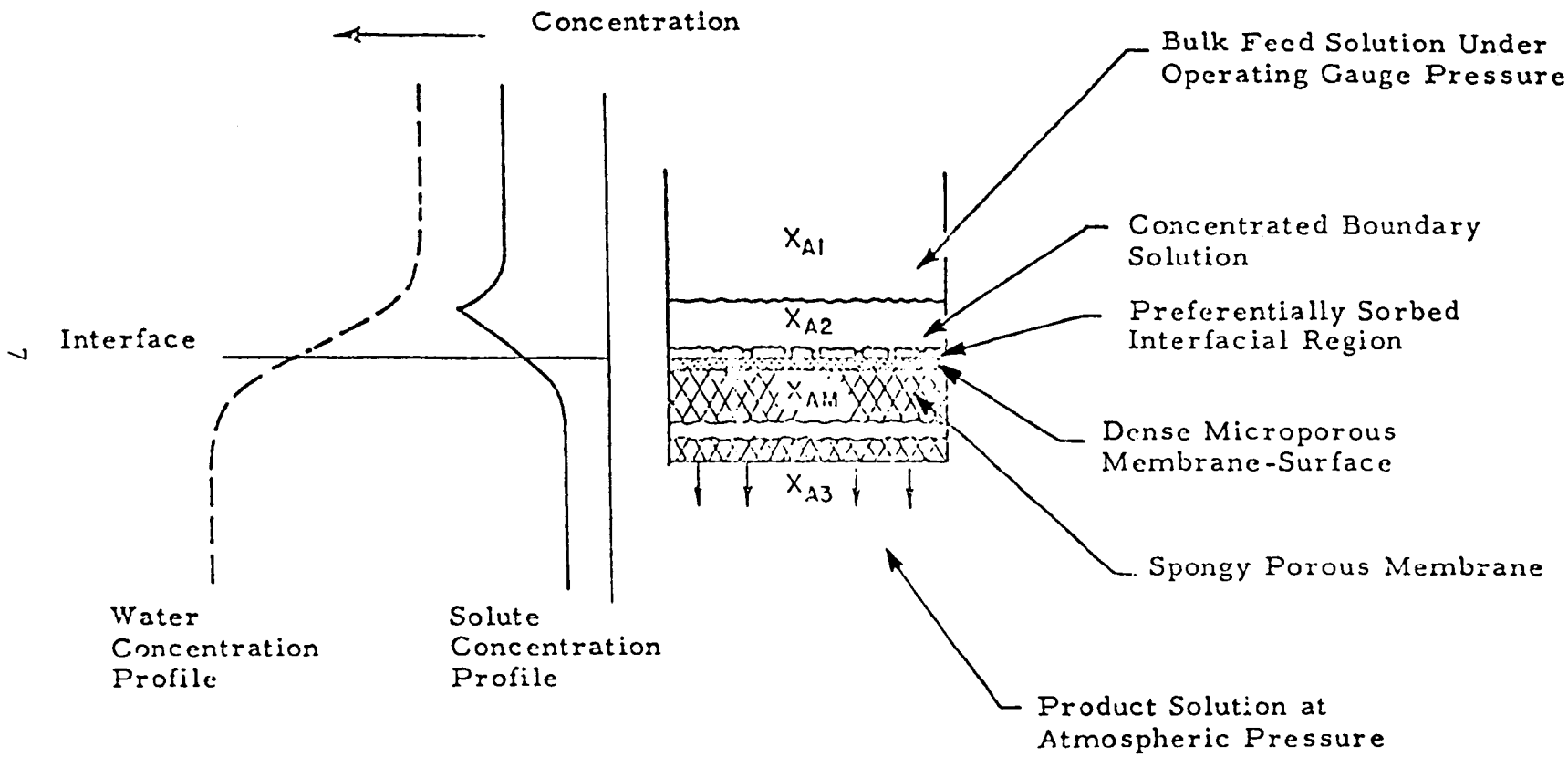

Figure 1. Concentration profiles of water and solute for steady state operation of reverse osmosis process.

It is necessary to define a quantity to express the overall degree of permeation in general, regardless of the actual transport mechanism. Permeability may be defined in terms of concentration or pressures in the general form,

$$F = Q S_A\left(\frac{r_1 - r_2}{\ell}\right)$$

where

Q = permeability

S_A = area

F = flow rate

The concentration gradients of solutes and the solution pressure are important forces primarily responsible for inducing fluxes of solute and solvent.

Each flux can be associated with the various forces using a finite number of the linear phenomenological coefficients. Diffusion models are generally one of two types, diffusion or pore. The diffusion model is very convenient, particularly in the case where the molecular size of a chemical species is of the same order as that of another species from which it is to be separated. If the molecular sizes are quite different as in ultrafiltration, a porous membrane with a suitable average pore size is commonly chosen to effect the separation (pore model). The membrane is viewed as a homogeneous medium with a finite thickness. When the membrane is associated with a solution, the membrane phase itself is considered as a solution in which the "component" of the membrane segment is very sluggish and almost stationary. Thus,

Three transport coefficients are involved in the transport process. The relative magnitude of these coefficients will determine the shape of concentration gradients and the efficiency of the hyperfiltration process. They are:

- Water permeability constant through the membrane
- Solute transport coefficient through the membrane
- Mass transfer coefficient of the solute in the solution

These transport coefficients can be obtained from a set of experimental measurements of the product water rate, pure water permeability of the membrane (normally given by the membrane manufacturer) and solute separation efficiency. The mass transfer coefficient of the solute can also be obtained from empirical correlations published in the literature.

Preferential Sorption/Diffusion Theory

Permeation is a phenomena in which a species or component is passing through another substance, usually but not necessarily by means of diffusion. In fact, permeation is a phenomenological definition which encompasses a variety of transport mechanisms. Driving forces which cause permeation include:

- concentration gradient
- pressure gradient
- electric potential
- temperature gradient

the well established solution theory can be applied directly to the system.

Nonequilibrium Flow Model

Katchalsky and Curran (Ref.6) developed equations governing membrane permeability from phenomenological considerations of nonequilibrium flow. The solvent flux N_B, was determined to be,

$$N_B = L_B \quad (\Delta P - \sigma \Delta \pi)$$

and similarly the solute flux, N_A, was determined to be,

$$N_A = C_{AM} \ (1-\sigma) \ N_B + L_A \Delta C_A$$

where,

L_B = filtration coefficient (represents velocity of fluid per unit pressure difference)

L_A = solute permeability (measured at $N_B = 0$)

σ = Staverman reflection coefficient (measure of membrane selectivity depending on properties of both the membrane and solute)

ΔP = difference in bulk pressure across the membrane

$\Delta \pi$ = difference in osmotic pressure across the membrane

C_{AM} = solute concentration in membrane

ΔC_A = diiference in solute concentration in feed and product solutions

Substituting for N_B, the solute flux may be written,

$$N_A = C_{AM}L_B \left[\Delta P(1-\sigma) - \sigma\Delta\pi(1-\sigma)\right] + L_A\Delta C_A$$

For the special case of a nonselective membrane ($\sigma=0$), the solute flux is,

$$N_A = C_{AM}L_B\Delta P + L_A\Delta C_A$$

For the special case of an ideal semipermeable membrane, $\sigma=1$, and the solute flux reduces to the expression

$$N_A = L_A\Delta C_A$$

The coefficients, L_A, L_B, and σ can be determined from experimental measurements. Thus, membrane permeability can be calculated from phenomenological considerations provided the necessary constants can be determined experimentally.

4. TRANSPORT PARAMETERS

Two parameters have been suggested by Sourirajan for characterizing membranes. These parameters are the pure water permeability constant, A, and a mass transfer coefficient, $D_{AM}/K\delta$. The parameter, A, is a measure of the overall porosity of a film and is independent of any solute. The parameter, $D_{AM}/K\delta$, is a mass transfer coefficient with respect to solute transfer.

Permeability

The parameter, A, is pressure dependent according to the relationship,

$$A = A_o \exp(-\alpha P)$$

where A_o is A at P=0 and α is a constant. The parameter, A (gm-moles-water/cm^2-sec-atm), may be further defined,

$$A = \frac{PWP}{M_B x S_A x 3600 x P} = \frac{N_B}{P - \pi(X_{A_2}) + \pi(X_{A_3})}$$

where,

PWP = pure water permeability (gm/hr)

M_B = molecular weight of water (gm/mole)

S_A = surface area of membrane (cm^2)

P = operating pressure (atm)

N_B = solvent water flux (gm-mole/cm^2-sec)

π = osmotic pressure (atm)

X_{A2} = mole fraction of solute in concentrated boundary solution on high pressure side of membrane

X_{A3} = mole fraction of solute in product solution

the term, N_B, may be obtained from the following equation,

$$N_B = (PR)\left[1 - \frac{1}{\left(1 + \frac{1000}{m_1 \quad (1-f)M_A}\right)}\right] \Big/ M_B \cdot S \cdot 3600$$

where,

(PR) = product rate (gm/hr-cm^2)

m_1 = molarity of feed solution (moles of solute/1000 gm water, $m_1 = ppm/1000M_A$ where M_A is the solute molecular weight)

f = separation = $1 - \frac{m_3}{m_1}$ = rejection

m_3 = molarity of product solution

Values for the terms, N_B and X_{A_2} at different pressures are not usually available for commercial membranes. In order to obtain approximate values for A, the osmotic pressure, $\pi(X_{A_3})$ was assumed zero and the osmotic pressure, $\pi(X_{A_2})$ was assumed equal to $\pi(X_{A_1})$, the osmotic pressure of the feed solution.

Solute Mass Transfer Coefficient

The parameter, $D_{AM}/K\delta$, is pressure dependent according to the relationship,

$$D_{AM}/K\delta \quad \alpha P^{-\beta}$$

where β is a constant. For many solutes, D_{AM}/KS is independent of feed concentration and feed flow rate at any given operating pressure. The solute mass transfer coefficient is further defined,

$$\frac{D_{AM}}{K\delta} = \frac{N_B}{\left(\frac{1-X_{A_3}}{X_{A_3}}\right)\ (C_2X_{A_2} - C_3X_{A_3})}$$

where,

D_{AM} = diffusivity of solute in membrane phase (ft^2/sec)

K = mass transfer coefficient (cm/sec)

δ = solubility parameter

C_2 = molar density of boundary solution ($gm\text{-}mole/cm^3$)

C_3 = molar density of product solution ($gm\text{-}mole/cm^3$)

Values for the term, C_2, at different pressures are not usually available for commercial membranes. In order to obtain approximate values for $D_{AM}/K\delta$, it was assumed that C_2 is equal to the molar density of pure water, X_{A2} is equal to X_{A1}, and the mole fractions, X_A, are,

$$X_A = ppmx10^{-6}\left(\frac{M_B}{M_A}\right)$$

Mass Transfer Coefficient

The mass transfer coefficient of the solute in solution is given by the expression,

$$TCM = \frac{Sh\,D}{2r}$$

where,

Sh = Sherwood number (mass diffusivity/molecular diffusivity)

D = diffusivity

r = tube radius

Sherwood number depends on membrane geometry and flow conditions, i.e., whether the flow is turbulent or laminar. The flow is considered turbulent for Reynolds numbers greater than 2100 (based on hydraulic diameter). For turbulent flow, the Sherwood number is assumed independent of axial distance from the tube entrance and for a tubular membrane is calculated with an expression developed by Gill and Sherwood,

$$Sh = 0.18Re^{7/8}Sc^{1/4}\left[0.127\left(1-\frac{60}{Re^{.875}}\right)\right]^{0.5}$$

where,

Re = Reynolds number

Sc = Schmidt number

and for a sheet membrane is calculated with an expression developed by Linton and Sherwood,

$$Sh = 0.44Re^{7/12} \left(\frac{Sct}{2L}\right)^{0.333}$$

t = channel thickness

L = channel length

For laminar flow, the Sherwood number is a function of axial distance and for a tubular membrane is calculated with an expression developed by Lebeque and modified by Sourirajan,

$$Sh = 1.95 \left(\frac{ReSc2r}{x}\right)^{0.333}$$

and for a sheet membrane,

$$Sh = 2.24 \left(\frac{ReSc2t}{x}\right)^{0.333}$$

where x is the axial distance from the tube entrance.

Macroscopic Parameters

Several macroscopic parameters are required in order to define the membrane transport. The diffusion model for membrane transport assumes that Fick's law is obeyed and that uncoupled flow occurs (the flow of one component is unaffected by the flow of other components within the membrane). The solvent flux, J_1, is given by the expression,

$$J_1 = \frac{D_1 C_1 V_1}{RT\lambda} (\Delta P - \Delta \pi)$$

where, C_1 = solvent concentration in membrane

D_1 = solvent diffusion coefficient

V_1 = partial molar volume of water

ΔP = bulk pressure difference across the membrane

$\Delta\pi$ = osmotic pressure difference across the membrane

R = gas constant

T = temperature

λ = mass transfer coefficient on high pressure side divided by the solute mass transfer coefficient

The solute flux, J_2, is given by the expression,

$$J_2 = \frac{-D_2 k (\Delta C_2)}{\lambda}$$

where,

k = distribution coefficient (g/cm^3 of solute in the membrane divided by the g/cm^3 of solute in the surrounding solution)

D_2 = solute diffusion coefficient

ΔC_2 = solute concentration gradient across the membrane

Performance of the membrane is also characterized by the rejection, rj,

$$rj = \left[1 + \frac{D_2 k \, RTC_1^*}{D_1 C_1 V_1 (\Delta P - \Delta\pi)} \right]^{-1}$$

where,

C_1^* = concentration of water in solution on the low pressure side of the membrane

The utilization of the preceding parameters in the membrane systems model is described in the following chapter.

5. MEMBRANE SYSTEMS MODEL

In the following paragraphs a mathematical model of hyperfiltration processes is developed. The model includes a mathematical description of membrane behavior and the economics of a hyperfiltration system. A description is presented of the hyperfiltration system to be simulated and the computer code developed from the mathematical model.

Mathematical Model

The model described herein is based on Sourirajan's preferential sorption and solute diffusion theory (Ref.7) which applies simple boundary film theory (Refs. 8 and 9) to obtain the concentration polarization of the solute (Ref. 10). The effect of pressure drop due to friction losses and momentum changes on the performance of the system (Refs. 11 and 12) is included in the model.

Membrane model: The model described herein is based on Sourirajan's preferential sorption and solute diffusion theory (Ref. 1) which applies simple boundary film theory (Refs. 2 and 3) to obtain

the concentration polarization of the solute (Ref.4). The effect of pressure drop due to friction losses and momentum changes on the performance of the system (Refs.5 and 7) is included in the model.

Consider a tubular hyperfiltration module shown in Fig. 2. From the overall material balance for the differential control volume, the change in average axial velocity ($\bar{u}$) can be written as

$$-\frac{d\bar{u}}{dx} = \frac{2}{r} v_w \tag{5.1a}$$

where v_w is the permeation velocity of product water through the membrane in ft/sec. Similarly, the solute material balance can be written as

$$-\frac{d(\bar{u} C_{A1})}{dx} = \frac{2}{r} v_w C_{A3} \tag{5.2a}$$

where C_{A1} and C_{A3} are the molar densities of solute in the bulk and the product, respectively.

Now, an expression for the pressure drop in a tube in terms of friction losses and momentum changes may be obtained from an energy balance (Ref. 5).

$$-\frac{dP}{dx} = CM \frac{\bar{u}^2 f}{g_c r} + \frac{\bar{u}}{g_c} \frac{d\bar{u}}{dx} \tag{5.3a}$$

or substituting (5.1a) yields

$$-\frac{dP}{dx} = CM \frac{\bar{u}^2 f}{g_c r} - \frac{2 v_w \bar{u}}{g_c r} \tag{5.3b}$$

where C is the molar density of solution (lb mole/ft^3), M is the average molecular weight of solution, f is the Fanning friction factor, and g_c is the conversion factor.

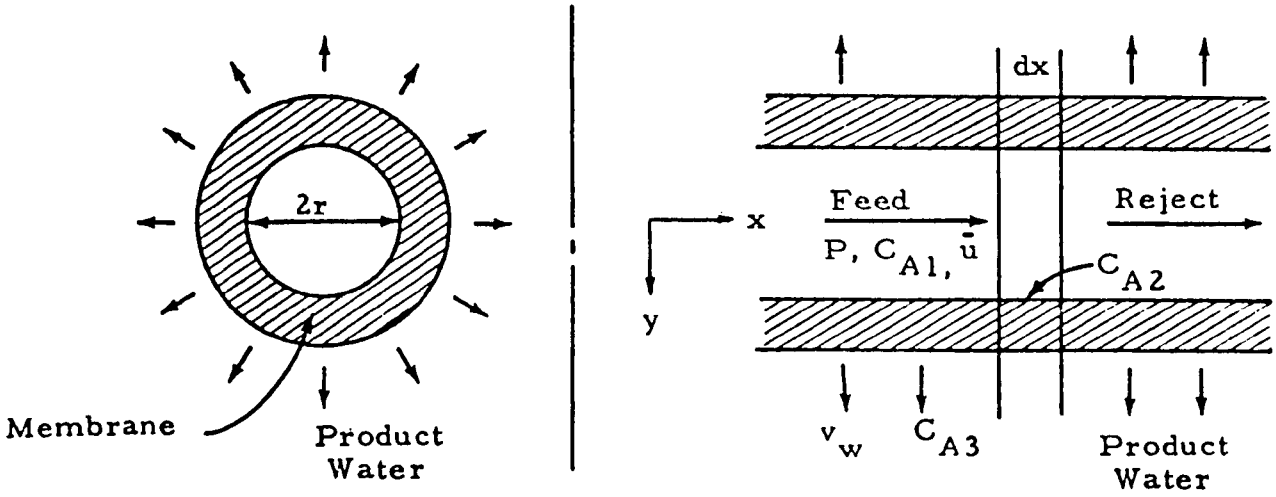

Fig. 2 - A Tubular Hyperfiltration Module

By solving Eqs. (5.3a) and (5.3b) simultaneously, one can compute output variables, $\tilde{u}$, P and C_{A1} for the differential volume for a given set of dependent variables, product rate (V_w) and solute transport (C_{A3}). These dependent variables can be related to the feed rate ($\tilde{u}$), the system operating pressure (P) and the concentration of feed stream (C_{A1}) by transport mechanisms of solute in the high pressure side of the membrane.

The transport of product water through the membrane (Refs. 1 and 4) is proportional to the effective operating pressure of the system (see Fig. 2a),

$$N_B = A P_{eff} = A \left[P - \left\{\pi|_{X_{A2}} - \pi|_{X_{A3}}\right\}\right] \qquad (5.4a)$$

where A is the pure water permeability of the membrane, π is the osmotic pressure at given solute concentration and P is the system operating pressure, N_B is the product water flux through the membrane. X_{A2} and X_{A3} are the mole fractions of the solute at the high pressure and product water sides of the membrane. Equation (5.4a) can be written in terms of mole fraction by assuming a linear dependency of osmotic pressure on mole fraction. This is true for most dilute solutions.

$$\pi = BX \qquad (5.4b)$$

where B is a constant with units of pressure. Substituting, we have

$$N_B = AP \left[1 - \frac{B}{PC} (C_{A2} - C_{A3})\right] \qquad (5.4c)$$

or dividing both sides of Eq. (5.4c) by C,

$$v_w = \frac{N_B}{C} = \frac{AP}{C}\left[1 - \frac{B}{PC}(C_{A2} - C_{A3})\right] \qquad (5.4d)$$

The transport of the solute through the membrane is given by (Ref. 1)

$$N_A = \left(\frac{D_{AM}}{\delta_t}\right)(C_{A2}^* - C_{A3}^*) \qquad (5.5a)$$

where C_{A2}^* and C_{A3}^* are the molar densities of the solute in the membrane phase in equilibrium with the respective solution phases, D_{AM} is the diffusivity of solute in the membrane phase in ft^2/sec, and δ_t is the effective thickness of membrane. The equilibrium concentration can be written as

$$C_A = KC_A^* \qquad (5.5b)$$

where K is a characteristic constant determined by the properties of membrane and solute. Substituting (5.5b) into (5.5a) yields

$$N_A = \left(\frac{D_{AM}}{K\delta}\right)(C_{A2} - C_{A3}) \qquad (5.5c)$$

$\left(\frac{D_{AM}}{K\delta}\right)$ is the solute transport parameter (ft/sec) uniquely determined by the characteristics of specific membrane/solute combination.

Dividing (5.5c) by (5.4c) yields

$$\frac{N_A}{N_B} = \frac{C_{A3}}{C} = \frac{\left(\frac{D_{AM}}{\delta K}\right)(C_{A2} - C_{A3})}{AP\left[1 - \frac{B}{PC}(C_{A2} - C_{A3})\right]}$$

or

$$\frac{C_{A2} - C_{A3}}{C_{A3}} = \frac{1}{\frac{B}{PC} C_{A3} + (\frac{D_{AM}}{\delta K})/(AP/C)} \qquad (5.5d)$$

Now, for a simultaneous solution of equations (5.4d) and (5.5D) one must have an expression for the solute concentration in the boundary layer (C_{A2}). The net rate of solute transport to the membrane within the thin boundary layer is given by (Refs. 1 and 4),

$$N_A = \frac{C_{A3}}{C} (N_A + N_B) = \text{Bulk flux} - \text{solute diffusion flux back to the bulk}$$

$$= \frac{C_A}{C} (N_A + N_B) - D_{AB} \frac{d C_A}{dy}$$

or

$$\frac{dC_A}{dy} \quad \left(\frac{N_A + N_B}{C D_{AB}}\right) C_A = \left(\frac{N_A + N_B}{C D_{AB}}\right) C_{A3} \qquad (5.6a)$$

with boundary conditions

$$C_A = C_{A1} \quad \text{at} \quad y = 0$$

$$C_A = C_{A2} \quad \text{at} \quad y = \ell$$

where D_{AB} is the diffusivity of solute in the feed solution, and ℓ is the effective thickness of the concentrated boundary layer.

Solving the differential equation (5.6a) and defining the mass transfer coefficient of solute in the feed solution,

$$k = D_{AB}/\ell \qquad (5.6b)$$

we have

$$\log_e\left(\frac{C_{A2} - C_{A3}}{C_{A1} - C_{A3}}\right) = \frac{N_A + N_B}{kC} \qquad (5.6c)$$

or solving for N_A

$$N_A = k\, C_{A3} \log_e \frac{C_{A2} - C_{A3}}{C_{A1} - C_{A3}} \qquad (5.6d)$$

From (5.5c) and (5.6d) we write

$$\left(\frac{D_{AM}}{K\delta}\right)\left(\frac{C_{A2} - C_{A3}}{C_{A3}}\right) = k \log_e \frac{C_{A2} - C_{A3}}{C_{A1} - C_{A3}} \qquad (5.6e)$$

Substituting (5.5d) into (5.6e) and solving for C_{A1} yields

$$C_{A1} = C_{A3}\, q\ ,$$

where

$$q = 1 + \frac{1}{\gamma^* C_{A3} + \theta} \exp \frac{1}{\lambda(\gamma^* C_{A3} + \theta)} \qquad (5.6f)$$

$$\left.\begin{aligned} \lambda &= k/\left(\frac{D_{AM}}{K\delta}\right) \\ \gamma^* &= \frac{B}{CP} \\ \theta &\doteq \left(\frac{D_{AM}}{K\delta}\right)/v_w^* \\ v_w^* &= \frac{AP}{C} \end{aligned}\right\} \qquad (5.6g)$$

The set of equations summarized in Fig. 3b can be solved simultaneously to obtain output conditions of the differential section for a given input (or initial) conditions at the inlet of the differential section. By repeating the procedure one can

compute the overall performance of the module.

To predict the overall performance of the hyperfiltration system, the following input data are required:

1. Design specifications for the system, i.e., geometry of the module,
2. Initial process conditions at the inlet of the system, i.e., flow rate, feed concentration, pressure, temperature and pH,
3. Physical properties of feed stream, i.e., viscosity and osmotic pressure (π) as functions of solute concentration and temperature,
4. An empirical expression for the mass transfer coefficient (k) as a function of Reynolds number, and Schmidt number (Section 4),
5. Membrane parameters:
   a. Permeability constant (A) as a function of pressure and temperature, (Section 4), and
   b. Solute transport parameter ($D_{AM}/K\delta$) as a function of pressure, temperature and pH (Section 4).

Items 1 and 2 are defined by the system design specifications. Item 3 may be obtained from published data in the literature. In the event when these data are not available from the literature, experimental measurements are necessary. Item 4 can be obtained from the literature. Item 5, membrane parameters, must be obtained through a series of experimental measurements. Variables to be monitored in an experimental system for this purpose are solute rejection, product rate and system pressure. The experimental data then can be used to compute membrane parameters using the system of equations presented in Fig. 3b.

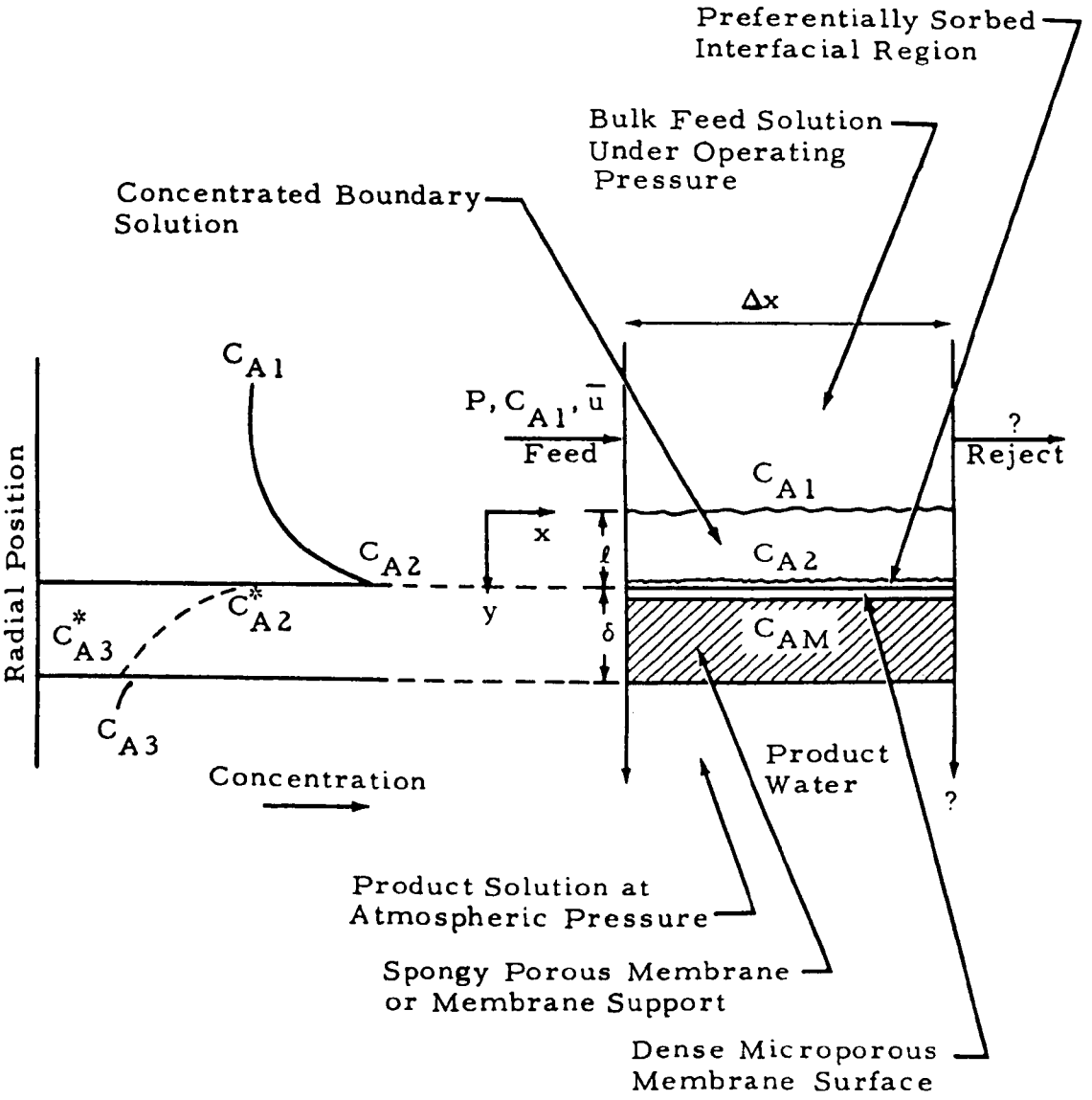

Fig. 3 - Concentration Profile of the Differential Hyperfiltration Module Under Steady State (C^*_{A2} and C^*_{A3} denote solute concentrations in the membrane phase in equilibrium with respective concentrations in the liquid phases.)

List of Equations

$$-\frac{d\bar{u}}{dx} = \frac{2}{r} v_w, \qquad (1a), \qquad -\frac{d(\bar{u} C_{A1})}{dx} = \frac{2}{r} v_w C_{A3}$$

$$-\frac{dP}{dx} = CM \left(\frac{\bar{u}^2 f}{g_c r} - \frac{2 v_w \bar{u}}{g_c r}\right)$$

$$v_w = v_w^* \left(1 - \frac{\gamma^* C_{A3}}{\gamma^* C_{A3} + \theta}\right)$$

$$C_{A2} = C_{A3} \left(1 + \frac{1}{\gamma^* C_{A3} + \theta}\right)$$

$$C_{A1} = C_{A3} \left\{1 + \frac{1}{\gamma^* C_{A3} + \theta} \exp\left(-\frac{1}{\lambda (\gamma^* C_{A3} + \theta)}\right)\right\}$$

$$\lambda = k \Big/ \left(\frac{D_{AM}}{K\delta}\right), \quad \gamma^* = \frac{B}{CP}$$

$$\theta = \left(\frac{D_{AM}}{K\delta}\right) \Big/ v_w^*, \quad v_w^* = \frac{AP}{C}$$

Fig. 3b- Summary of the Hyperfiltration Model

Consider a tubular hyperfiltration module shown in Fig. 1. From the overall material balance for the differential control volume, the change in average axial velocity ($\bar{u}$) can be written as

$$-\frac{d\bar{u}}{dx} = \frac{2}{r} v_w \qquad (5.1a)$$

where v_w is the permeation velocity of product water (permeate) through the membrane (ft/sec). Similarly, the solute material balance can be written as

$$-\frac{d(\bar{u}C_{A1})}{dx} = \frac{2}{r} v_w C_{A3} \qquad (5.2a)$$

where C_{A1} and C_{A3} are the molar concentrations of solute in the bulk and the product, respectively.

Now, an expression for the pressure drop in a tube in terms of friction losses and momentum changes may be obtained from an energy balance (Ref. 11).

$$-\frac{dP}{dx} = CM\frac{\bar{u}^2 f}{g_c r} + \frac{\bar{u}}{g_c}\frac{d\bar{u}}{dx}$$

or substituting (1) yields

$$-\frac{dP}{dx} = CM\frac{\bar{u}^2 f}{g_c r} - \frac{2 v_w \bar{u}}{g_c r} \qquad (5.3a)$$

where C is the molar density of solution (lb mole/ft^3), M is the average molecular weight of solution, f is the Fanning friction factor, and g_c is the conversion factor.

By solving Eqs. (5.1a), (5.2a) and (5.3a) simultaneously, one can compute output variables, $\bar{u}$, P and C_{A1} for the differential

volume for a given set of dependent variables, product rate (v_w) and solute transport (C_{A3}). These dependent variables can be related to the feed rate ($\bar{u}$), the system operating pressure (P) and the concentration of feed stream (C_{A1}) by transport mechanisms of solute and permeate (product water) through the membrane and associated concentration polarization of solute in the high pressure side of the membrane. To obtain the expressions for v_w and C_{A3}, let us consider a differential section of the tubular hyperfiltration module shown in Fig.3a. The figure shows a schematic of steady state concentration profile of the solute across the membrane. Due to relatively high affinity of the membrane to solvent (water) molecules, a concentration gradient is established in the interface region. Adsorbed water molecules are permeated through the microporous structure of the membrane at a rate which is determined by the characteristics of the membrane and the pressure exerted to overcome the osmotic pressure. Solute, on the other hand, diffuses to both directions from the interface. The preferential sorption of water molecule will develop high solute concentration right in the vicinity of the interface and thus develop a maximum concentration. This provides a driving force for the solute diffusion to both directions from the interface.

The transport of product water through the membrane (Refs. 7 and 10) is proportional to the effective operating pressure of the system. The effective pressure is defined to be the difference between the operating pressure and the osmotic pressure

exerted by the concentrated boundary layer. Assuming a linear dependency of osmotic pressure on mole fraction, we obtain the following expression. Detailed derivation of the expression is available in Ref. 13.

$$v_w = \frac{N_B}{C} = \frac{AP}{C}\left[1 - \frac{B}{PC}(C_{A2} - C_{A3})\right] \qquad (5.4d)$$

N_B is the permeate water flux through the membrane (lb mole/ft^2 -sec), C is the molar concentration of the bulk solution (lb-mole/ft^3), A is the pure water permeability of the membrane (lb mole/ft^2 -sec-psi), P is the operating pressure (psi), and B is a proportionality constant for osmotic pressure (psi)*.

The expression for C_{A3} can be obtained by integrating the differential equation obtained from a differential solute material balance within the concentrated boundary layer. A detailed derivation and solution of the boundary equation are presented in Ref. 13. The resulting expression is:

$$\frac{C_{A1}}{C_{A3}} = 1 + \frac{1}{C_{A3}\,B/CP + CS/AP}\exp\left|-\frac{1}{k/S\,(C_{A3}\,B/CP + SC/AP)}\right| \qquad (5.7)$$

S is the solute transport parameter* (ft/sec) and k is the mass transfer coefficient of the solute in the solution phase (ft/sec).

---

*Note that the constant B is a very small number for organic solutes found in textile wastewaters. For such cases, the osmotic pressure term can be neglected and the flux can be written simply as: $v_w = AP/C$.

*S is used to denote the solute transport parameter which is represented by $(D_{AM}/K\delta)$ by Sourirajan (Ref. 7). D_{AM} is the diffusivity of solute in the membrane phase (ft^2/sec). K is a characteristic constant which represents preferential sorbability of the solute on a given membrane surface. S is uniquely determined by the characteristics of specific membrane/ solute combination.

The set of equations, (5.1a) - (5.3a), (5.4d), and (5.7), can be numerically solved to obtain output conditions from the differential section of the module for a given input (or initial) conditions at the inlet of the differential section. By repeating the procedure one can compute the overall performance of the module.

The relative magnitude of the three transport coefficients will determine the shape of concentration profile and the efficiency of the hyperfiltration process. The transport coefficient can be obtained from a set of experimental measurements of the product water rate, pure water permeability of the membrane (normally given by the membrane manufacturer) and solute rejection efficiency. These parameters are temperature and pressure dependent. The dependencies can be expressed by the following equations (Refs. 14 and 15.):

$$A \propto \exp(-\alpha P)$$

$$S \propto P^{-\beta} \exp(-\gamma/T)$$

α , β and γ are constants, which can be calculated from experimental results. Empirical correlations published in the literature can be used to calculate the solute mass transfer coefficient (Ref. 16).

Economic model: The incremental cost for producing unit quantity of permeate water is considered to analyze the system economics. The cost elements contributing to the incremental product cost are amortized capital cost, UCC ($/Kgal), and O&M costs ($/Kgal). The amortized capital cost is calculated based on the installed system capital cost per unit membrane area ($/ft^2 of membrane surface). The O&M costs include membrane replacement cost. UMRC ($/Kgal), pumping power cost, UPP ($/Kgal), and other O&M costs, UMOMC ($/Kgal). The credits to the product cost are credit from recovered water, CRW ($/Kgal), and credit from recovered energy, CRE ($/Kgal). The credit from recovered chemicals from the concentrate usually requires additional process modifications.

The unit incremental cost for product water, UCPW ($/Kgal), is written as:

$$UCPW = UCC + UMRC + UPP + UMOMC - CRW - CRE \qquad (6)$$

The unit costs can be obtained from vendors or actual estimations.

Description of System and Method

In practical applications of the reverse osmosis process, a certain multistage design concept is desirable to achieve desired levels of product recovery and solute rejection. Three such concepts with tapered inner stages are presented in Fig. 4.

Note that the innerstages are tapered with respect to the number of modules rather than the physical shape of the membrane support structure. The tapered innerstage design increases efficiency of the system since it reduces the concentration polarization in the boundary layer. The feed rate at the inlet of each module is maintained at the design value by reducing the number of modules within an innerstage. The number of modules for an innerstage is determined by the flow rate fed to the particular innerstage. As the bulk flow rate decreases due to permeation of water through the membrane, the level of polarization in a module increases. Minimizing the concentration polarization increases the efficiency of solute rejection as well as the product rate. The rejection increases due to reduced solute concentration in the boundary layer while higher effective operating pressure is responsible for the improvement in the product rate.

The single stage concept employs direct recycle of a portion of the reject stream to concentrate the reject to the specified design value. In this case, the system is operated at a somewhat higher concentration than the concentration of the feed. In the two-stage concept shown in Fig. 4b, the first stage is used as a purification stage, and the second as a concentration stage. Since the permeate from the second stage has a higher concentration than the design product concentration, it is recycled to the first stage. In the two-stage case, the concentration of the combined feed to the first stage is lower than the incoming

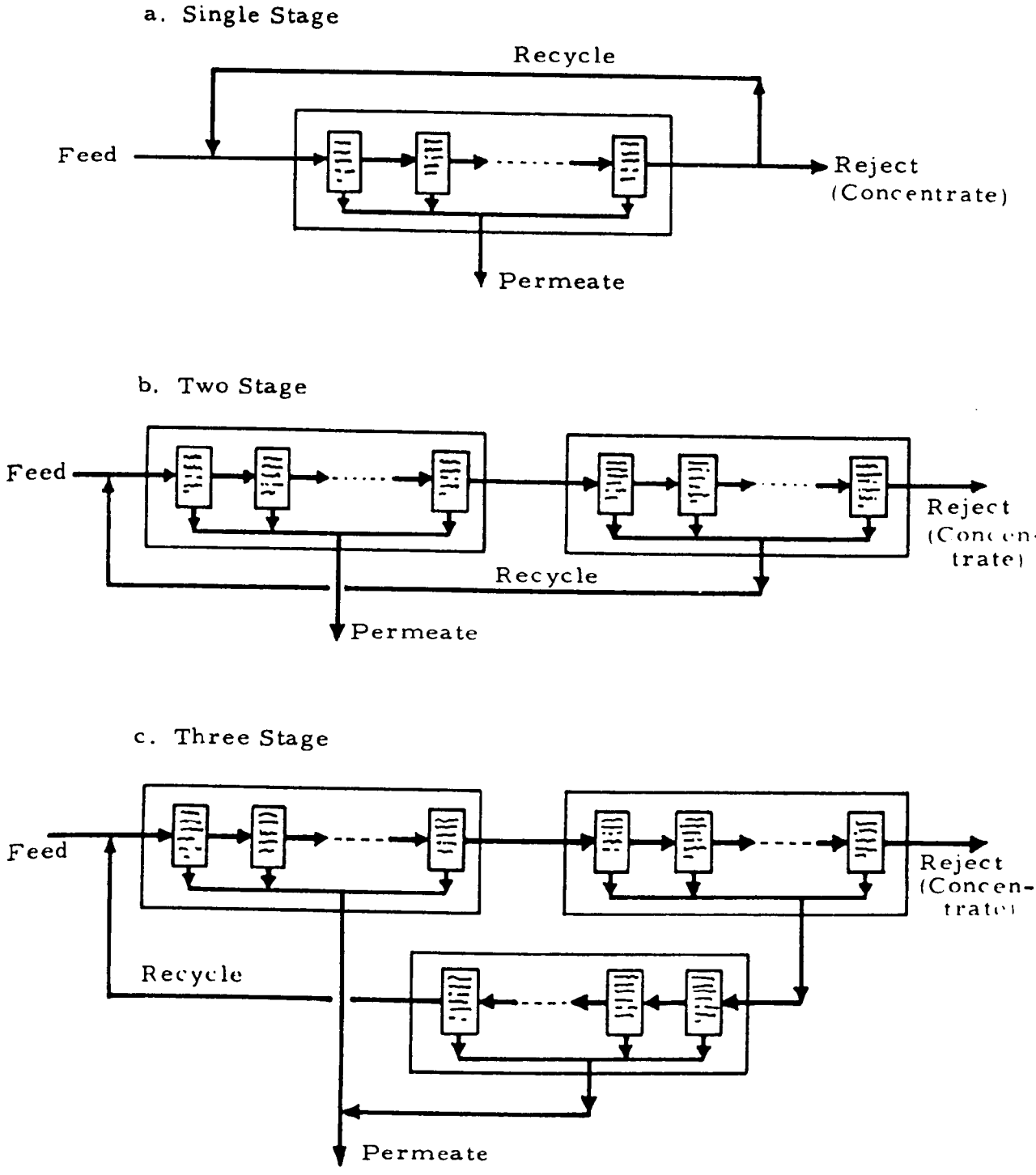

Fig. 4 - Schematic Diagrams of Tapered Multistage Hyperfiltration Systems

feed concentration to the hyperfiltration system. An additional stage is employed in the three-stage concept. The purpose of this stage is to concentrate the permeate from the second stage back to the feed concentration. This scheme provides higher system efficiency because of the reduced number of modules required for the system.

For a given design rejection and product recovery factor, the best system efficiency can be obtained when the recycle flow rate is the minimum and the concentration of the recycle stream is the same as the feed stream. Numerical results indicated that the three-stage concept reduces the total number of modules by 30 and 10 percent over the single and two-stage system, respectively. For this reason, the three-stage concept is chosen as the system model.

For the reasons discussed above the tapered innerstage design is chosen for the system design purposes. Note that the innerstages are tapered with respect to the number of modules rather than the physical shape of the membrane support structure.

A schematic flow chart for the design simulation of the three-stage tapered hyperfiltration system is shown in Fig.5. A computer program developed to solve the system of equations presented in the previous section was utilized to obtain design and economic results for the staged system. The numerical procedure for simulation of a single module employs an iterative

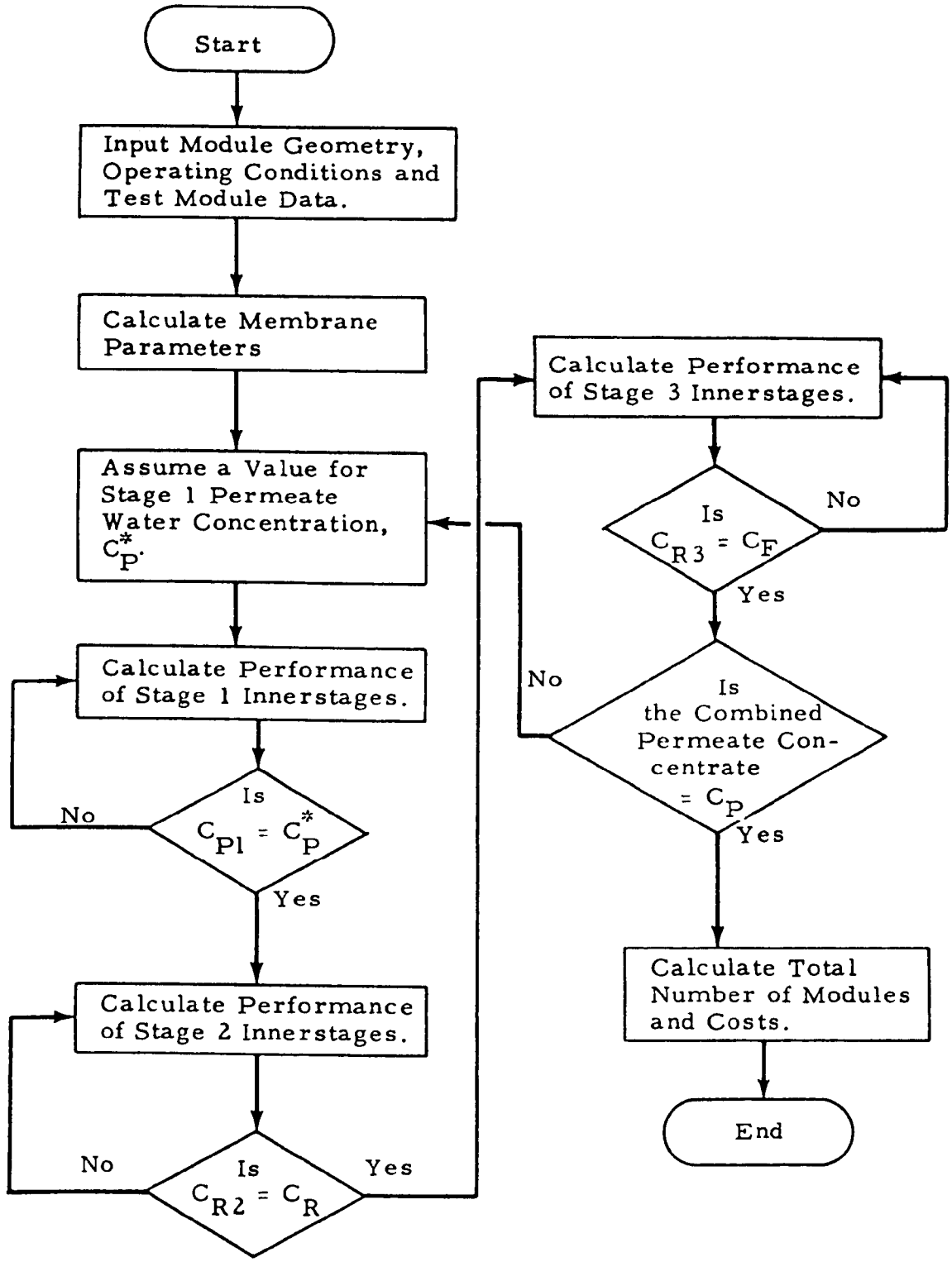

Fig. 5 - Flow Chart of the Three-Stage Hyperfiltration Design Program (Subscripts P, R and F denote permeate, rejected concentrate, and feed, respectively.)

scheme based on the Newton-Raphson method over a number of finite subsections of the module. A similar iterative procedure is utilized to match the concentrations and flow rates to and from each stage.

6. PARAMETRIC RESULTS

The numerical results of a single module performance simulation are shown in Fig. 6. The case shown in the figure simulates a tubular Westinghouse module with a cellulose acetate membrane on the inside tube wall. The operating conditions and the geometry are indicated in the figure. The pressure drop for the 100 ft. module is approximately 1 percent. The initial rejection is 96 percent and slightly decreases as the concentration polarization increases by 8 percent. Approximately 10 percent of the feed is recovered as permeate water and the resulting decline of the flow rate is 10 percent.

From the single module simulation results, it is apparent that at least eight stages in series are required to obtain 80 percent product water recovery if the feed concentration is low enough. For a normal textile wastewater, however, a considerably higher number of stages are required due to additional purification necessary to achieve the overall design rejection and product rate. This will be evident in the following discussions on the system design simulation of two sample cases.

Table 1 summarizes the three stage design simulation results

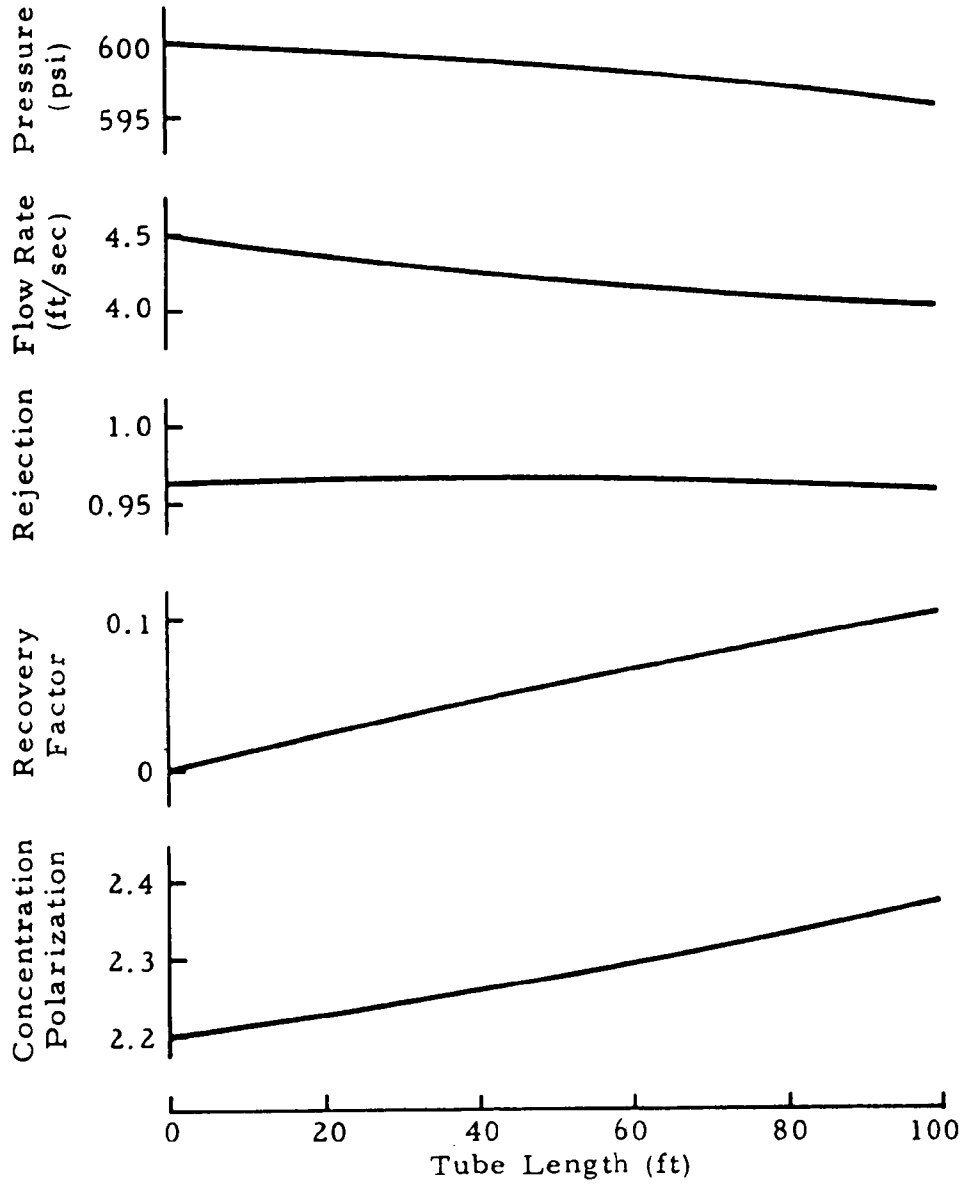

Fig. 6 - Performance Simulation of a Single Tubular Hyperfiltration Module (Feed Rate = 10 gpm, Temperature = 70 F, Tube Diameter = 1 in., Cellulose Acetate Membrane (by Westinghouse) with Flux = 4.75×10^{-5} ft/sec, Feed Concentration = 2.0×10^{-5} lb-mole/ft^3)

Table 1

SUMMARY OF COMPUTER DESIGN SIMULATION RESULTS FOR TWO SAMPLE HYPERFILTRATION SYSTEMS OF ONE MILLION GALLONS PER DAY CAPACITY

Item	Cellulose Acetate Membrane	ZR(IV)-PAA Dynamic Membrane
Design Parameters		
Test Tube Rejection	0.96	0.96
Test Tube Flux (ft/sec)	4.75×10^{-5}	11.3×10^{-5}
Permeability (lb-mole/ft^2-sec-psi)	2.07×10^{-9}	2.88×10^{-9}
Solute Transport Parameter (ft/sec)	1.23×10^{-6}	2.53×10^{-6}
Design Tube Diameter (in.)	1	1
Design Tube Length (ft)	100	100
Design Product Recovery Factor	0.8	0.8
Design Rejection	0.95	0.95
Design Feed Concentration (lb-mole/ft^3)	2.0×10^{-5}	2.0×10^{-5}
Design Temperature (F)	70	150
Design Pressure (psi)	600	1,000
Design Results		
Number of Innerstages, Stage 1	19	7
Stage 2	11	5
Stage 3	42	15
Number of Modules, Stage 1	846	339
Stage 2	213	101
Stage 3	204	99
Total Number of Modules	1,263	539
Total Membrane Area (ft^2)	31,727	13,540
Economic Results*		
Total Installed Capital Cost ($)	539,350	2,301,700
Capital Amortization Cost (cents/Kgal	24	102
Membrane Replacement Cost (cents/Kgal)	79	2
Pumping Power Cost (cents/Kgal)	15	25
Other O&M Costs (cents/Kgal)	10	20
Credit for Recovered Water (cents/Kgal)	40	40
Credit for Recovered Energy (cents/Kgal)	0	67
Total Unit Cost (cents/Kgal)	88	42

*The unit cost basis are obtained from a recent study estimation (Ref. 2). More detailed cost breakdown is described in the reference.

for two sample one million gallons per day hyperfiltration systems. One is a Cellulose Acetate (CA) membrane system (Westinghouse) operating at 600 psi and 70 F. The other is a Zr(IV)-PAA (poly-acrylic acid) dynamic membrane system (Selas) operating at 1000 psi and 150 F. These two membranes are selected because of readily available design and cost information (Refs. 1 and 2) . The transport parameters are calculated from experimentally measured rejection and flux data from the references. The two systems are designed for a product recovery factor and rejection of 0.8 and 0.95, respectively. The unit cost information was obtained from vendors and recent study estimations (Refs. 1 and 2).

The computed total numbers of modules of 1 in. in diameter and 100 ft long for the CA and dynamic membranes are 1263 and 539, respectively. The corresponding membrane areas required are 31,727 and 13,540 sq. ft. The higher surface area requirement for the CA membrane system is due to the smaller permeability of water through the membrane. The unit cost for producing a thousand gallons of permeate water is 88 cents for the CA system and 42 cents for the dynamic membrane system. It is noted that the major cost element for the CA system is the membrane replacement cost, while the capital amortization cost makes the largest cost contribution. The credit from recovered energy is significant enough to cause the dynamic membrane to be attractive. It should be noted that the design and operation conditions used are for illustration purposes and do not represent a typical case.

To demonstrate the range of applicability of the developed model and to investigate the effects of various design parameters on the economics of the system, a series of parametric studies was performed. The results are shown in Figs. 7 and 8.

Figure 7 shows the effects of design product rate factor and solute rejection on the unit cost. The effect of design product rate factor on the unit cost is relatively moderate. The design rejection factor has a more pronounced effect on the cost of the dynamic membrane system. Significantly lower unit cost can be obtained at slightly lower design rejection for the dynamic membrane. On the other hand, the effect of design rejection is less significant in the CA membrane. Thus, a proper combination of these two membrane systems may be desirable when a higher design rejection is necessary due to more stringent quality requirements for reuse of the permeate water.

Figure 8 shows the effects of operating temperature on the unit cost with operating pressure as a parameter. Due to characteristics of the membranes, the effects are shown only for the respective applicable operating temperature and pressure ranges. It is shown that the unit cost is generally lower at higher temperature and pressure. Unit cost is a stronger function of temperature and pressure than product recovery factor and rejection (Fig.7).

The unit cost does not include credit from possible reuse of the chemicals contained in the concentrated reject stream. A net

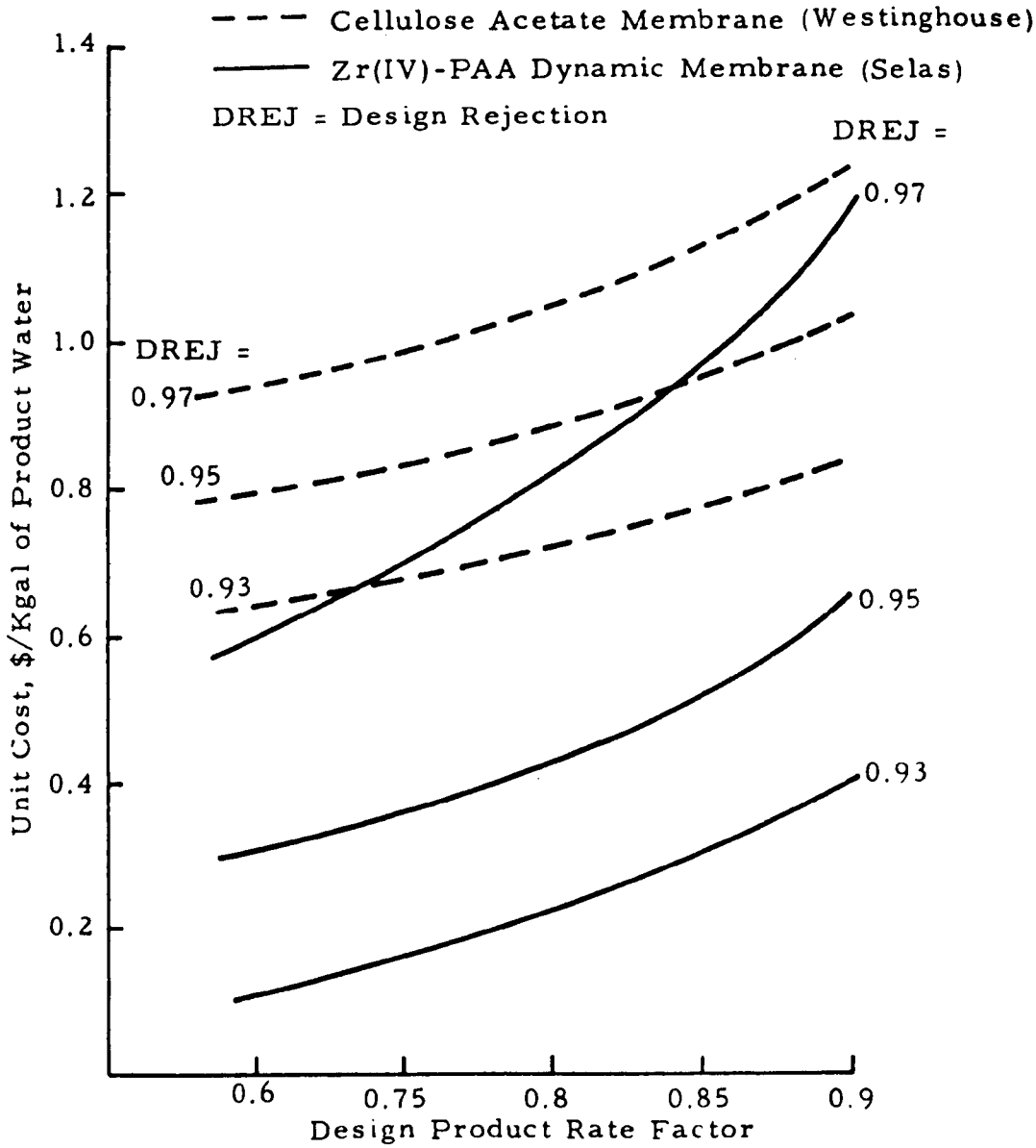

Fig. 7 - Effect of Design Product Rate Factor and Rejection on Unit Cost (Feed Rate = 10 gpm, Tube Diameter = 1 in., Temperature = 70 F for CA Membrane and 150 F for Dynamic Membrane, Pressure = 600 psi for CA Membrane and 1000 psi for Dynamic Membrane)

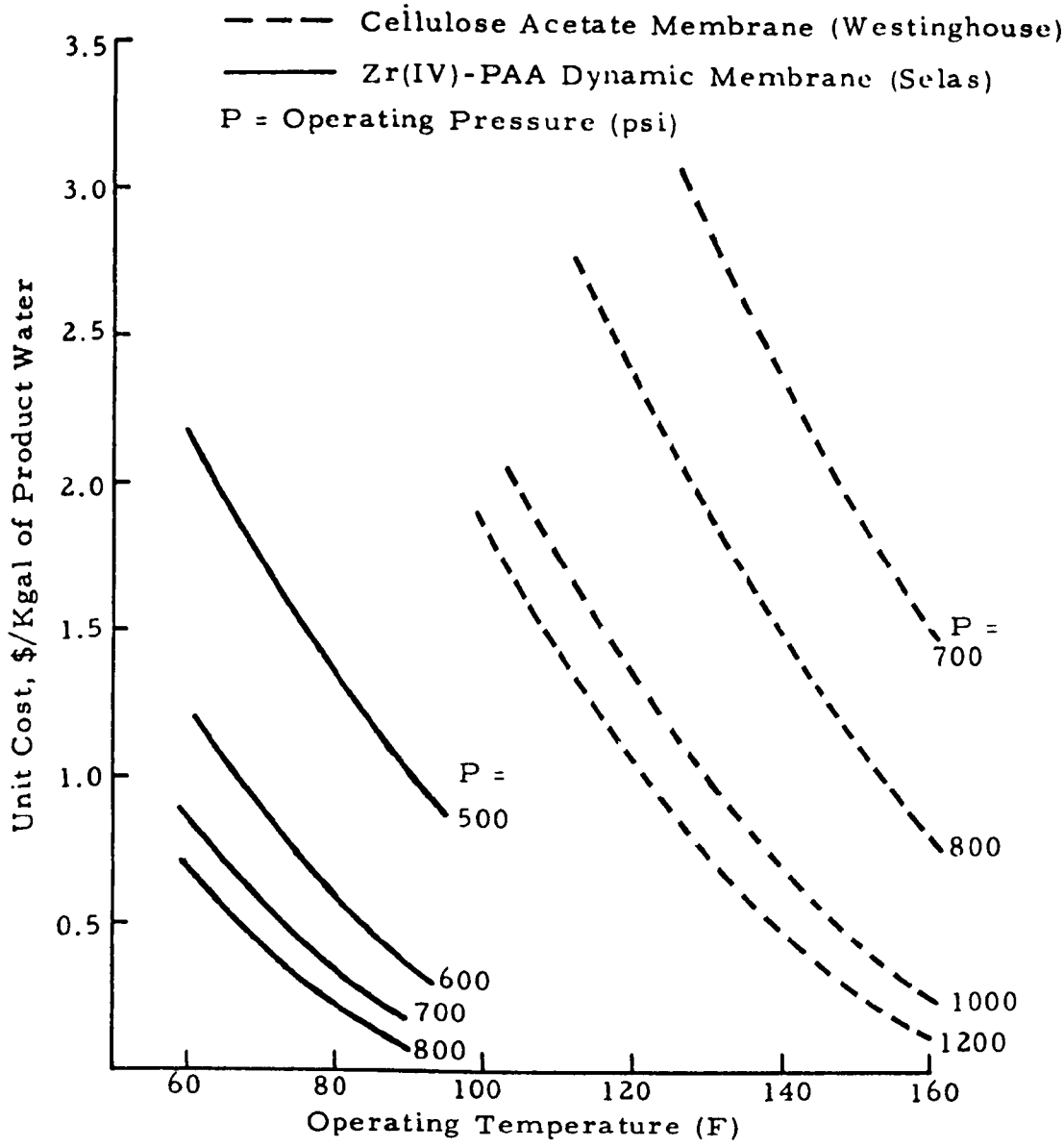

Fig. 8 - Effect of Operating Temperature and Pressure on Unit Cost (Feed Rate = 10 gpm, Tube Diameter = 1 in., Design Rejection = 0.95, Design Product Rate Factor = 0.8)

saving can be realized if the chemical credit is included in the computation of the unit cost. Although high temperature and pressure operation is desirable in the interest of achieving lower unit cost or even net savings, it is limited by excessive maintenance costs at high operating temperature and pressure. Membrane lifetime is diminished by operation at high temperatures and very high pressures (several hundred atmospheres) thus increasing maintenance costs. For the range of temperatures and pressures investigated, a flat estimated average maintenance cost was assumed. At higher temperatures and pressures, a functional relationship between these operating variables and maintenance cost should be developed and included in the computations.

REFERENCES

1. Brandon, C.A., and J.J. Porter, "Hyperfiltration for Renovation of Textile Finishing Plant Wastewater," EPA-600/2-76-060, March 1976.

2. Brandon, C.A., J.J. Porter and D.K. Todd, "Hyperfiltration for Renovation of Composite Wastewater at Eight Textile Finishing Plants, " EPA-600/2-78-047, March 1978.

3. Development Document for Effluent Limitations Guidelines and New Source Performance Standards for the Textile Mills Point Source Category," EPA-440/1-74-022-a, June 1974.

4. Shindler, A., Unpublished results developed under EPA/RTP sponsorship.

5. Spencer, H.G., and J.L. Gaddis, "Hyperfiltration of Nonelectrolytes: Dependence of Rejection on Solubility Parameters," Paper presented at EPA Symposium on Textilw Industry Technology, 5-8 December 1978.

6. Katchalsky, A. and P.F. Curran, Nonequilibrium Thermodynamics in Biophysics, Harvard University Press, Cambridge Massachusetts, 1965.

7. Sourirajan, S., Reverse Osmosis, Academic Press, New York, 1970, pp. 176-184.

8. Sourirajan, S., Reverse Osmosis, Academic Press, New York, 1970, pp. 185-188.

9. Brian, P.L.T., "Mass Transport in Reverse Osmosis," in Desalination by Reverse Osmosis, edited by Ulrich Merten, The MIT Press, Cambridge, 1971.

10. Pusch, W., "Concentration Polarization in Hyperfiltration Systems," in Reverse Osmosis Membrane Research, edited by H.K. Lonsdale and H.E. Podall, Plenum Press, New York, 1972, pp. 43-57.

11. Griffith, W.L., R.M. Keller, and K.A. Kraus, "Parametric Study of Hyperfiltration in Tubular Systems with High Permeability Membranes," Desalination, Vol. 4, 1968, pp. 203-308.

12. Johnson, J.S., Jr., L. Dresner and K.A. Kraus, "Hyperfiltration (Reverse Osmosis)," in Principles of Desalination, edited by K.S. Speigler, Academic Press, New York, 1966, pp. 345-439.

13. Ko, S.M., and P.G. Grodzka, "Study of Hyperfiltration Processes for Treatment and Renovation of Textile Wastewater," to be published.

14. Sourirajan, S., Reverse Osmosis, Academic Press, New York, 1970, pp. 191-202.

15. Gaddis, J.L., Private communication dated 24 May 1978.

16. Hwang, S.T., and K. Kammermeyer, Membranes in Separations, Wiley-Interscience, New York, 1975, pp. 351-359.

Appendix A

EXPERIMENTAL REJECTION/FLUX DATA *

* The experimental rejection data presented in Tables 1-8 and Figs. A-1 through A-18 were obtained from: CARRE, Inc., "Compilation of Toxic Rejection Data for Membranes". Prepared for EPA, December, 1977.

Table A-1

REJECTION OF SPECIFIC COMPOUNDS BY THE SELAS DYNAMIC Zr(IV)-PAA MEMBRANE OPERATING ON TEXTILE WASTEWATER

Solution (underlined solutes in consent decree)	Rejection (%)	pH	Concentration (mg/l)	Number of Data 70-80%	80-90%	90-100%	Total
COD	71 - 99	5.2 - 12	1600 - 7100	1	7	27	35
BOD	74 - 99	5.2 - 12	25 - 2300	3	6	29	38
TOC	82 - 98	5.2 - 12	175 - 2000	0	6	26	32
Dissolved Solids	62 - 99	5.2 - 12	670 - 128000	2	8	21	32
Total Solids	63 - 96		2500 - 215000				40
Volitile Solids	70 - 99	5.2 - 12	370 - 2700	2	6	21	29
Color	89 - 100	5.2 - 12	120 - 3400*	1	1	19	21
Phenol	86 - 100	6.6 - 9.6	0.66 - 315	1	2	4	7
Iron	97 - 99	5.2 - 9.6	8.25 - 20	0	0	6	6
Nickel	80 - 98	5.2 - 9.6	0.7 - 3.87	0	3	7	10
Chromium	89 - 99	5.9 - 12	0.7 - 23	0	1	7	8
Zinc	94 - 99	5.2 - 7.5	2.1 - 18	0	0	13	13
Copper	92 - 99	5.2 - 9.3	1.2 - 5.5	0	0	14	14
Manganese	90 - 98	6.1 - 7.4	0.5 - 1.02	0	0	4	4

*Concentration in Pt-Co Units

Data compiled from: Brandon, C. A., Porter, J. J., and Todd, D. K., "Hyperfiltration for Renovation of Composite Wastewater at Eight Textile Finishing Plants." Final Report, EPA Grant No. S802973, Clemson University report in preparation.

Table A-2
REJECTION OF SPECIFIC COMPOUNDS BY THE WESTINGHOUSE
TUBULAR CELLULOSE ACETATE MEMBRANE
OPERATING ON TEXTILE WASTE WATER

Solute (underlined solutes in consent decree)	Rejection (%)	pH	Concentration (mg/l)	Number of Data 70-80%	80-90%	90-100%	TOTAL
COD	89-99	5.8-7.1	1765-8664	0	2	6	8
BOD	87-99	5.8-7.1	128-1800	0	2	6	8
TOC	82-96	5.8-6.2	345-1800	0	1	4	5
Dissolved Solids	82-97	5.8-7.1	2804-6303	0	0	3	3
Volatile Solids	90-98	5.8-7.1	630-3504	0	0	5	5
Color	91-98	5.8-7.1	220-2000*	0	0	5	5
Phenol	9-99	6.8-7.1	0.54-0.65	0	0	1	2
Iron	96.5	5.8	8.48	0	0	1	1
Nickel	-	-	-	-	-	-	-
Chromium	-	-	-	-	-	-	-
Zinc	-	-	-	-	-	-	-
Copper	-	-	-	-	-	-	-
Manganese	67-99	5.8-7.1	0.12-1.34	1	2	1	5

*Concentration in Pt-Co Units

Data compiled from: Brandon, C. A., Porter, J. J., and Todd, D. K., "Hyperfiltration for Renovation of Composite Wastewater at Eight Textile Finishing Plants." Final Report, EPA Grant No. S802973, Clemson University report in preparation.

Table A-3
REJECTION OF SPECIFIC COMPOUNDS BY THE UOP
SPIRAL-WOUND CELLULOSE ACETATE MEMBRANE
OPERATING ON TEXTILE WASTE WATER

Solute (underlined solutes in consent decree)	Rejection (%)	pH	Concentration (mg/l)	Number of Data 70-80%	80-90%	90-100%	TOTAL
COD	89-99	5.2-9.4	27-2303	0	2	18	20
BOD	89-100	4.9-9.4	500-8664	0	1	21	22
TOC	83-99	4.9-9.4	232-2000	0	3	11	14
Dissolved Solids	90-99	4.9-8.0	670-12120	0	0	22	22
Volatile Solids	89-99	4.9-7.2	630-3504	0	1	13	14
Color	98-100	3.6-8.0	65-2000*	0	0	17	17
Phenol	20-98	6.8-7.1	0.54-35.0	0	1	1	3
Iron	94-99	5.2-6.8	8.25-12.0	0	0	5	5
Nickel	80-83	5.2-6.8	1.02-1.20	0	2	0	2
Chromium	97	6.8	3.6	0	0	1	1
Zinc	89-99	3.6-7.5	3.02-18.3	0	1	9	10
Copper	92-99	3.6-7.5	1.78-5.51	0	0	6	6
Marganese	98-99	4.9-6.2	0.47-1.32	0	0	5	5

*Concentration in Pt-Co Units.

Data compiled from: Brandon, C. A., Porter, J. J., and Todd, D. K., "Hyperfiltration for Renovation of Composite Wastewater at Eight Textile Finishing Plants." Final Report, EPA Grant No. S802973, Clemson University report in preparation.

Table A-4
REJECTION OF SPECIFIC COMPOUNDS BY THE DUPONT
MEMBRANE OPERATING ON TEXTILE WASTE WATER

Solute (underlined solutes in consent decree)	Rejection (%)	pH	Concentration (mg/l)	Number of Data 70-80%	80-90%	90-100%	TOTAL
COD	98.3	6.4	2776	0	0	1	1
BOD	98.4	6.4	1138	0	0	1	1
TOC	97.2	6.4	1058	0	0	1	1
Dissolved Solids	99.2	6.4	8906	0	0	1	1
Volatile Solids	96.7	6.4	1950	0	0	1	1
Color	99.1	6.4	1571*	0	0	1	1
Phenol							
Iron	85	6.4	1.0	0	1	0	1
Nickel	-	-	-	-	-	-	-
Chromium	-	-	-	-	-	-	-
Zinc	-	-	-	-	-	-	-
Copper	95.7	6.4	0.92	0	0	1	1
Manganese	-	-	-	-	-	-	-

*Concentration in Pt-Co Units.

Data compiled from: Brandon, C. A., Porter, J. J., and Todd, D. K., "Hyperfiltration for Renovation of Composite Wastewater at Eight Textile Finishing Plants." Final Report, EPA Grant No. S802973, Clemson University report in preparation.

Table A-5
REJECTION OF SPECIFIC COMPOUNDS BY THE
UNION CARBIDE 3NJR MEMBRANE
OPERATING ON TEXTILE WASTE WATER

Solute (underlined solute in consent decree)	Rejection (%)	pH	Concentration (mg/l)	Number of Data 70-80%	80-90%	90-100%	TOTAL
COD	-	-	-	-	-	-	-
BOD	-	-	-	-	-	-	-
TOC	15.2	8.1	330	0	0	0	1
Dissolved Solids	7.3	8.1	23853				1
Volatile Solids	55.7	8.1	804				1
Color							
Phenol							
Iron							
Nickel							
Chromium	61.0	8.1	0.172				1
Zinc	54.1	8.1	1.64				1
Copper	55.9	8.1	0.397				1
Manganese							

*Concentration in Pt-Co Units.

Data compiled from: Brandon, C. A., Porter, J. J., and Todd, D. K., "Hyperfiltration for Renovation of Composite Wastewater at Eight Textile Finishing Plants." Final Report, EPA Grant No. S802973, Clemson University report in preparation.

Table A-6
REJECTION OF SPECIFIC COMPOUNDS BY THE
SELAS Zr(IV)-Na_2SiO_3 MEMBRANE
OPERATING ON TEXTILE WASTE WATER

Solute (underlined solute in consent decree)	Rejection (%)	pH	Concentration (mg/l)	Number of Data 70-80%	80-90%	90-100%	TOTAL
COD	71-98	7.1-10.7	933-17,800	1	1	2	4
BOD	88-98	7.1-10.7	295-6200	0	1	4	5
TOC	85-92	8.0-10.7	330-440	0	2	2	4
Dissolved Solids	41-97	7.1-10.7	17810-23853	0	0	1	5
Volatile Solids	81-98	8.0-10.7	213-10870	0	1	2	3
Color	99-100	7.4-10.7	4000-30,000*	0	0	3	3
Phenol	16-97	7.1-8.1	1.4-241	0	0	1	3
Iron	67-95	7.1-10.7	2.9-9.02	1	1	1	4
Nickel	90.6	7.1	2.12	0	0	1	1
Chromium	93-100	7.1-10.7	0.129-1.38	0	0	5	5
Zinc	89-99	7.1-10.7	1.64-7.76	0	2	3	5
Copper	94-100	7.1-10.7	0.243-1.59	0	0	5	5
Manganese	99.7	7.1	3.97	0	0	1	1

*Concentration in Pt-Co Units

Data compiled from: Brandon, C. A., Porter, J. J., and Todd, D. K., "Hyperfiltration for Renovation of Composite Wastewater at Eight Textile Finishing Plants." Final Report, EPA Grant No. S802973, Clemson University report in preparation.

Table A-7
REJECTION OF SPECIFIC COMPOUNDS BY THE
WESTINGHOUSE TUBULAR POLYSULFONE MEMBRANE
OPERATING ON TEXTILE WASTE WATER

Solute (underlined solute in consent decree)	Rejection (%)	pH	Concentration (mg/l)	Number of Data 70-80%	80-90%	90-100%	TOTAL
COD	17-75	3.6-12	468-5020	2	0	0	8
BOD	65-71	6.4-12	1180-1800	1	0	0	2
TOC	49-82	5.9-12	762-1338	2	1	0	8
Dissolved Solids	23-69	3.6-12	3705-12840	0	0	0	9
Volatile Solid	30-72	3.6-11.6	370-2698	1	0	0	8
Color	25-96	5.9-12	200-3409*	1	2	2	8
Phenol	11-24	6.4-7.0	0.140-0.210	0	0	0	3
Iron	48-97	3.6-9.2	3.80-7.75	1	0	1	3
Nickel	15.8	3.6	0.76	0	0	0	1
Chromium	82-93	5.9-12.0	1.4-23.0	0	2	3	5
Zinc	33-99	3.6-7.0	3.60-9.91	0	0	4	6
Copper	76-97	3.6-12.0	0.92-5.51	2	0	6	8
Manganese	50-75	5.9-7.0	0.08-0.40	1	0	0	5

*Concentration in Pt-Co Units

Data compiled from: Brandon, C. A., Porter, J. J., and Todd, D. K., "Hyperfiltration for Renovation of Composite Wastewater at Eight Textile Finishing Plants." Final Report, EPA Grant No. S802973, Clemson University report in preparation.

Table A-8
REJECTION OF SPECIFIC COMPOUNDS BY THE
Zr(IV)-PAA MEMBRANE ON STAINLESS STEEL
OPERATING ON TEXTILE WASTE WATER

Solute (underlined solute in consent decree)	Rejection (%)	pH	Concentration (mg/l)	Number of Data 70-80%	80-90%	90-100%	TOTAL
COD BOD TOC Dissolved Solids Total Solids Volatile Solids Color Phenol Iron	38-88 0-97		3000-9200 0.65-7.10	6 0	2 3	0 5	10 10
Nickel Chromium	11-100		12-281	3	0	4	9
Zinc Copper Manganese	48-99		0.07-0.96	0	2	5	9

*Concentration in Pt-Co Units

Data compiled from: Brandon, C. A., Porter, J. J., and Todd, D. K., "Hyperfiltration for Renovation of Composite Wastewater at Eight Textile Finishing Plants." Final Report, EPA Grant No. S802973, Clemson University report in preparation.

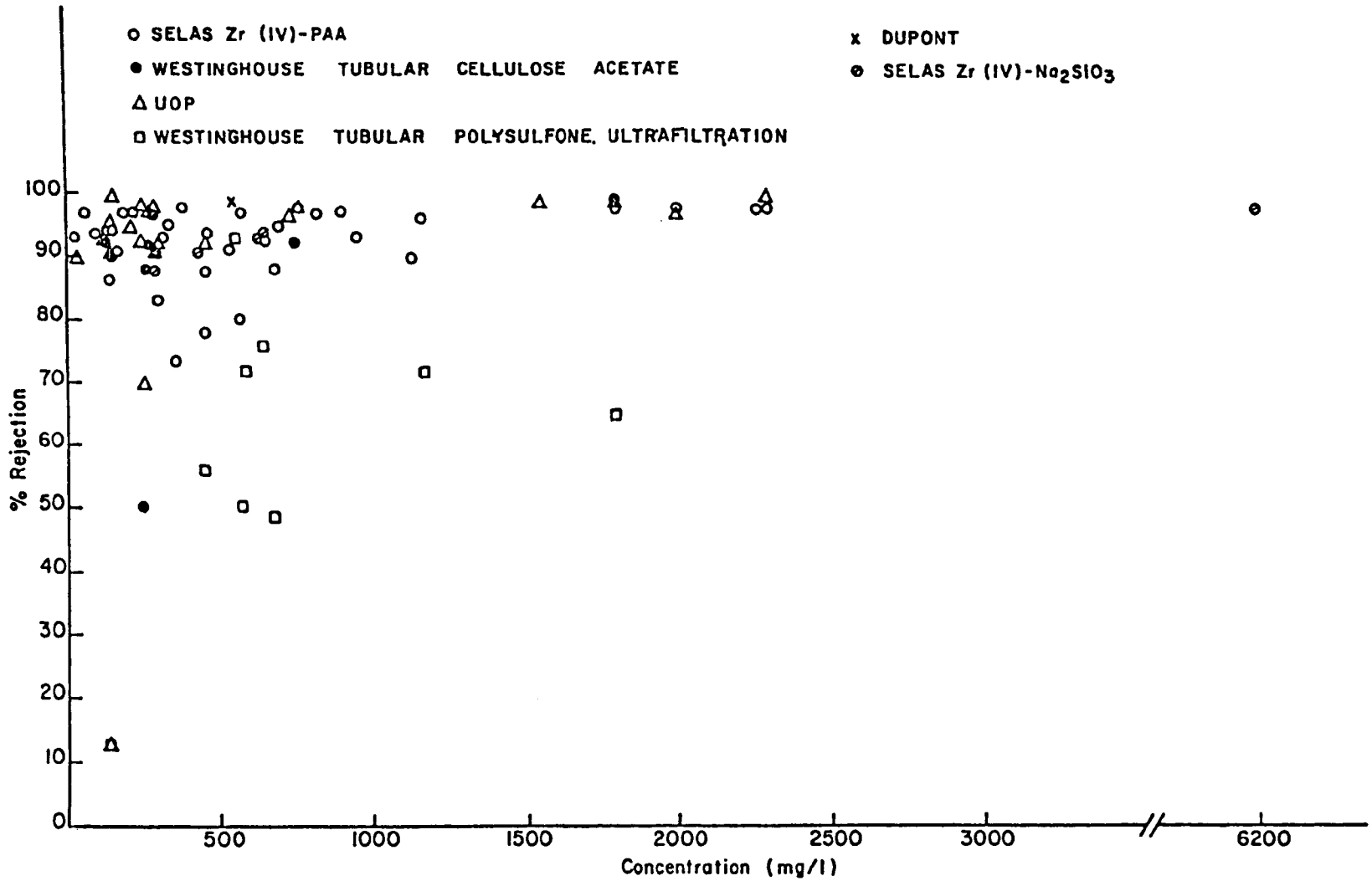

Figure A-1 Percent Rejection versus Concentration for Biochemical Oxygen Demand$_5$ (BOD$_5$).

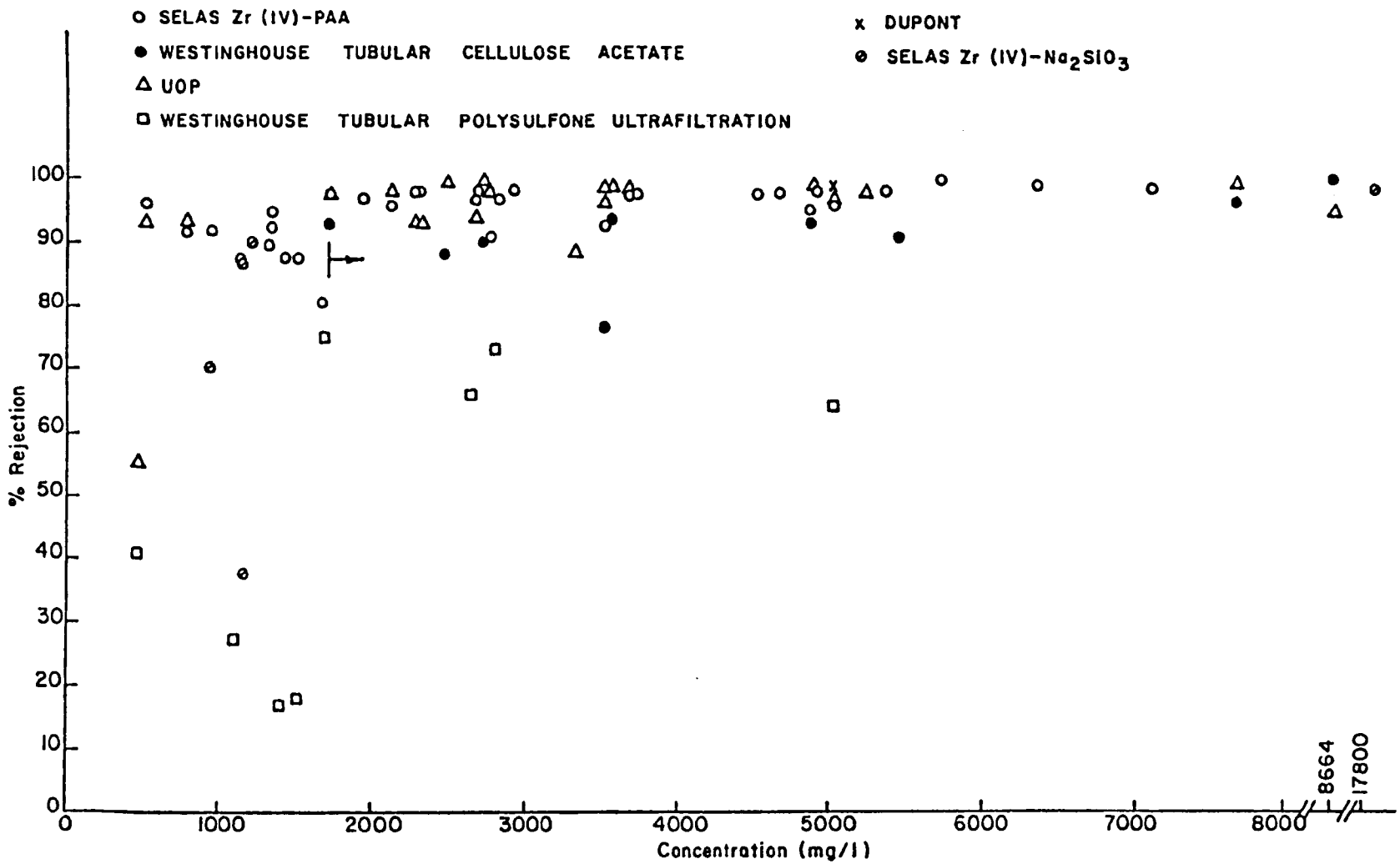

Figure A-2 Percent Rejection versus Concentration for Chemical Oxygen Demand (COD).

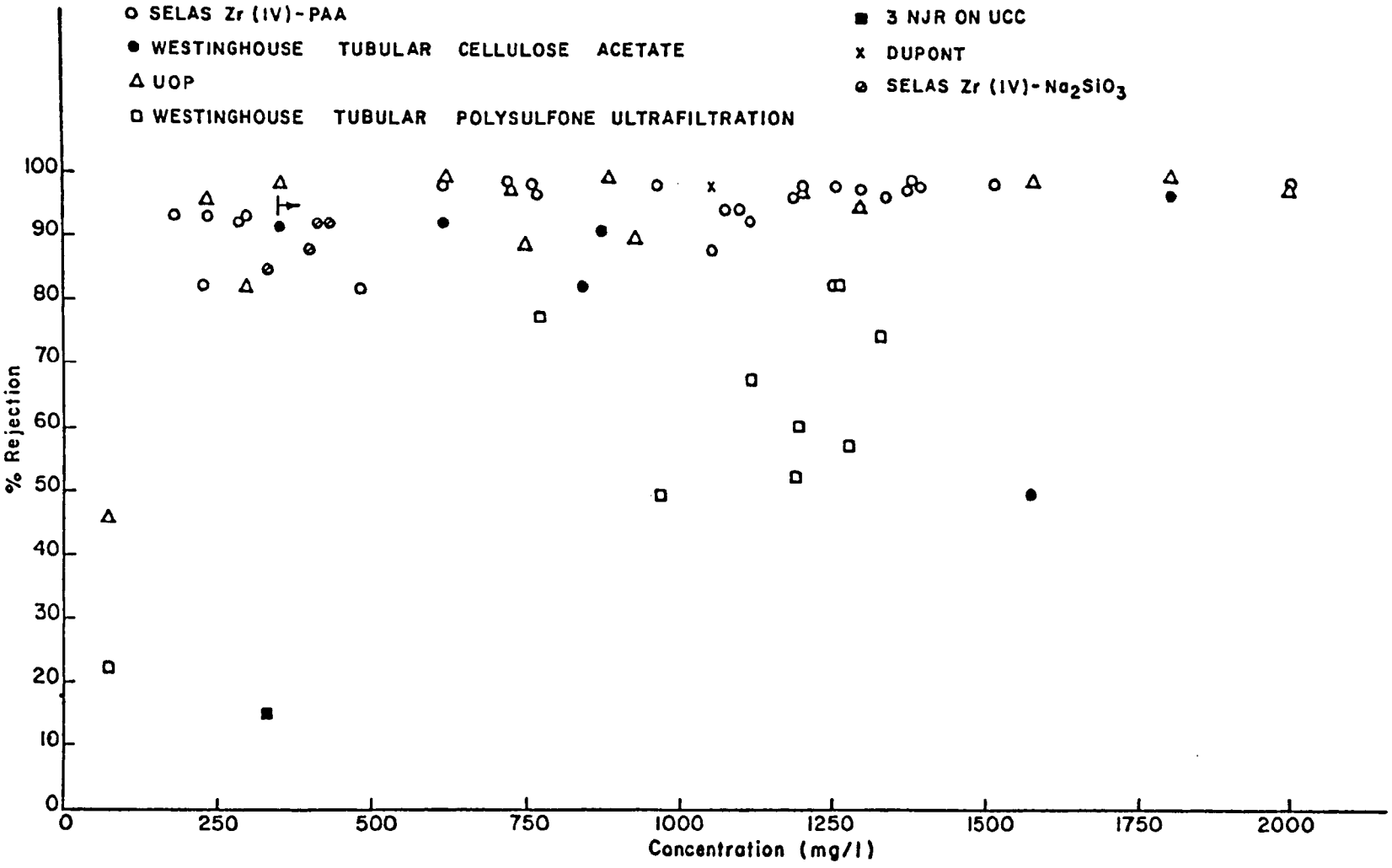

Figure A-3 Percent Rejection versus Concentration for Total Organic Carbon (TOC).

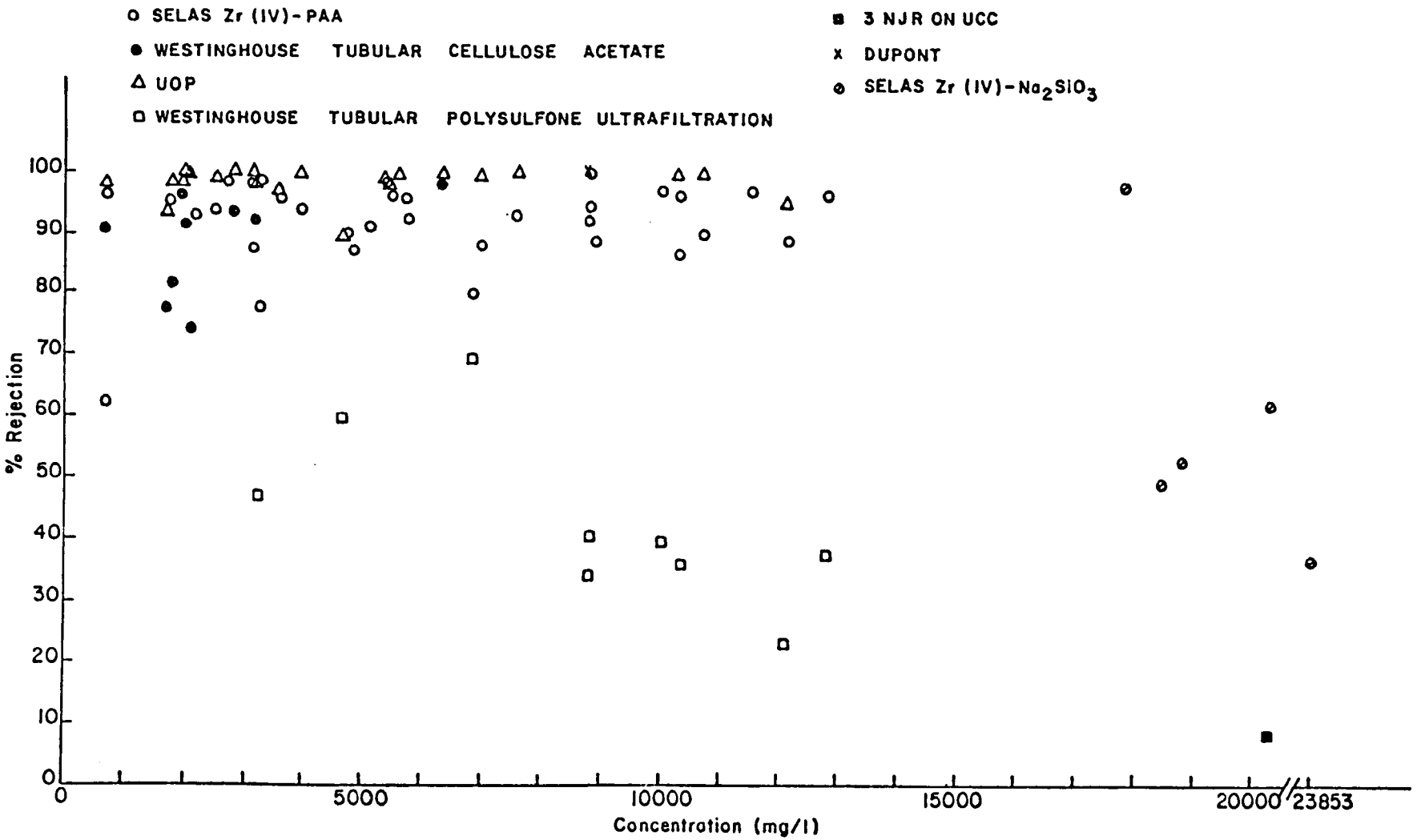

Figure A-4 Percent Rejection versus Concentration for Dissolved Solids.

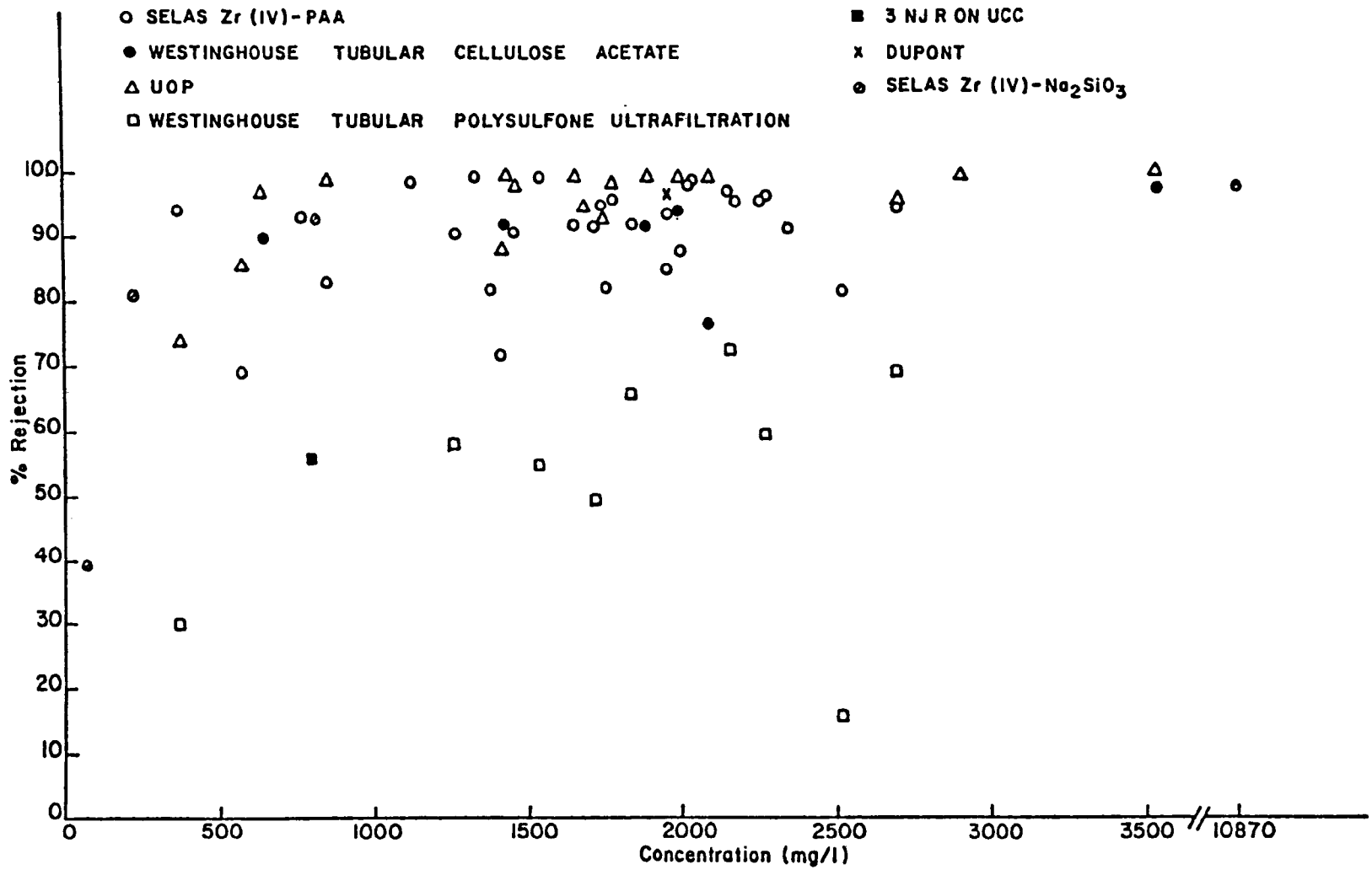

Figure A-5 Percent Rejection versus Concentration for Volatile Solids.

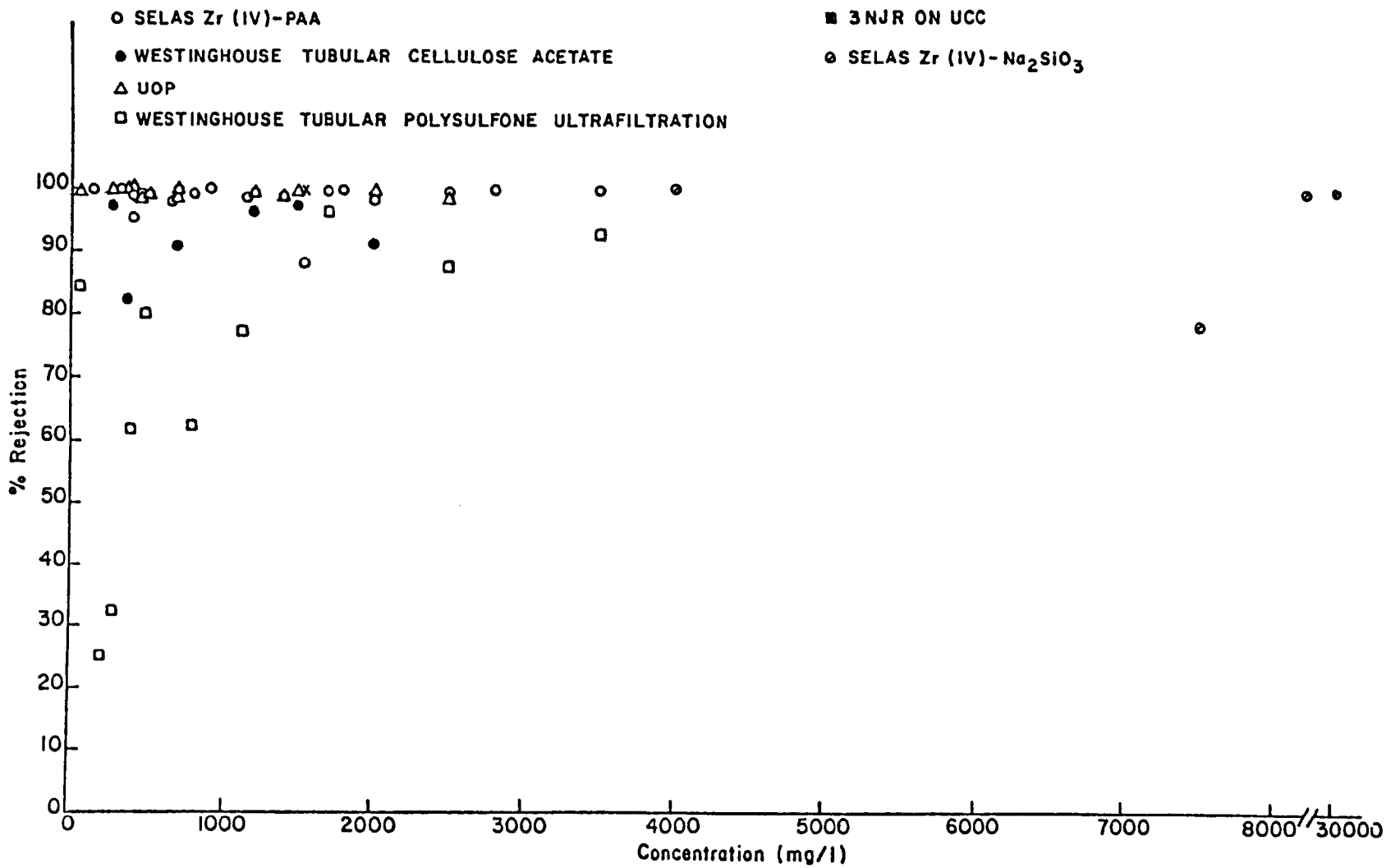

Figure A-6 Percent Rejection versus Concentration for Color.

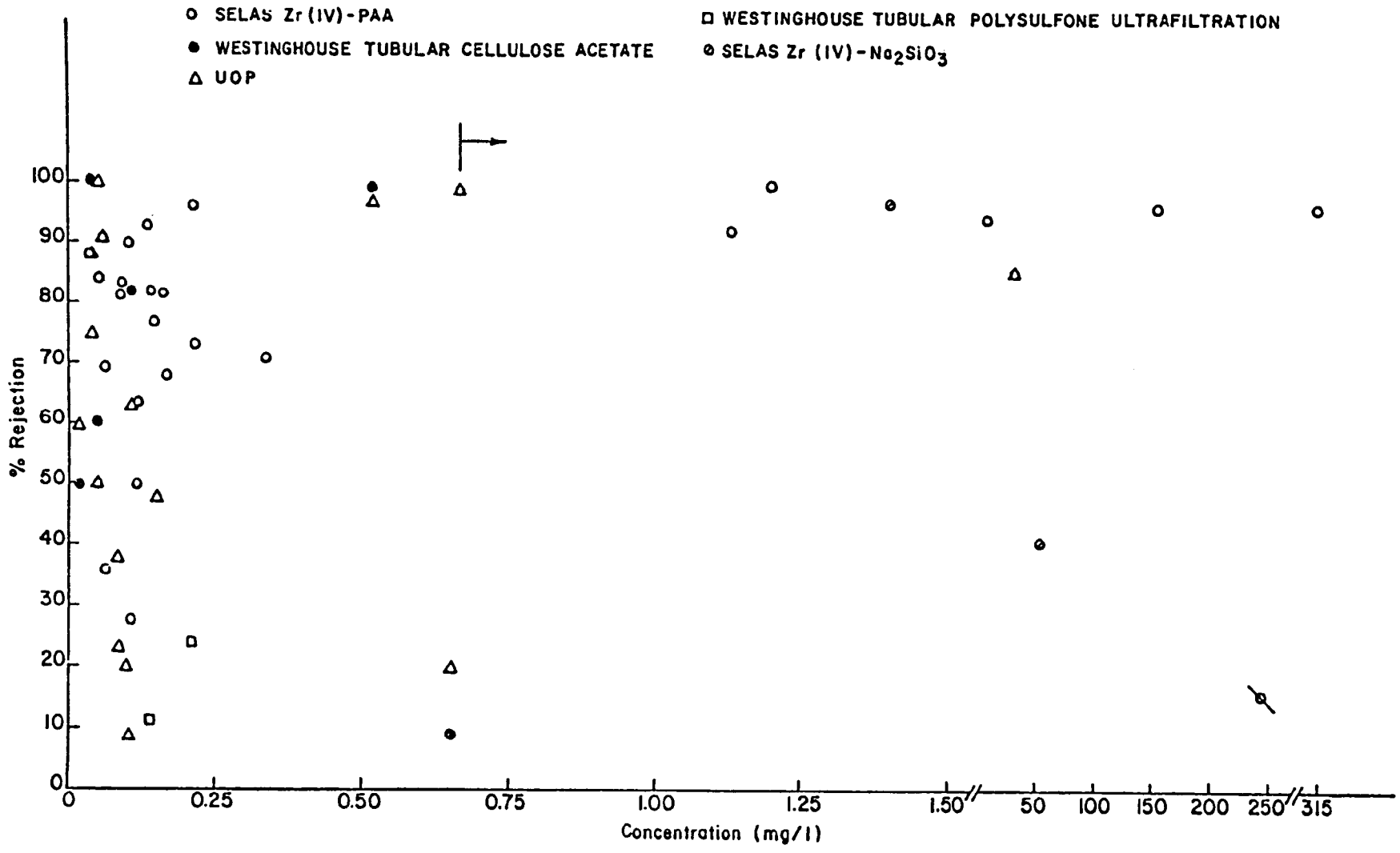

Figure A-7 Percent Rejection versus Concentration for Phenol.

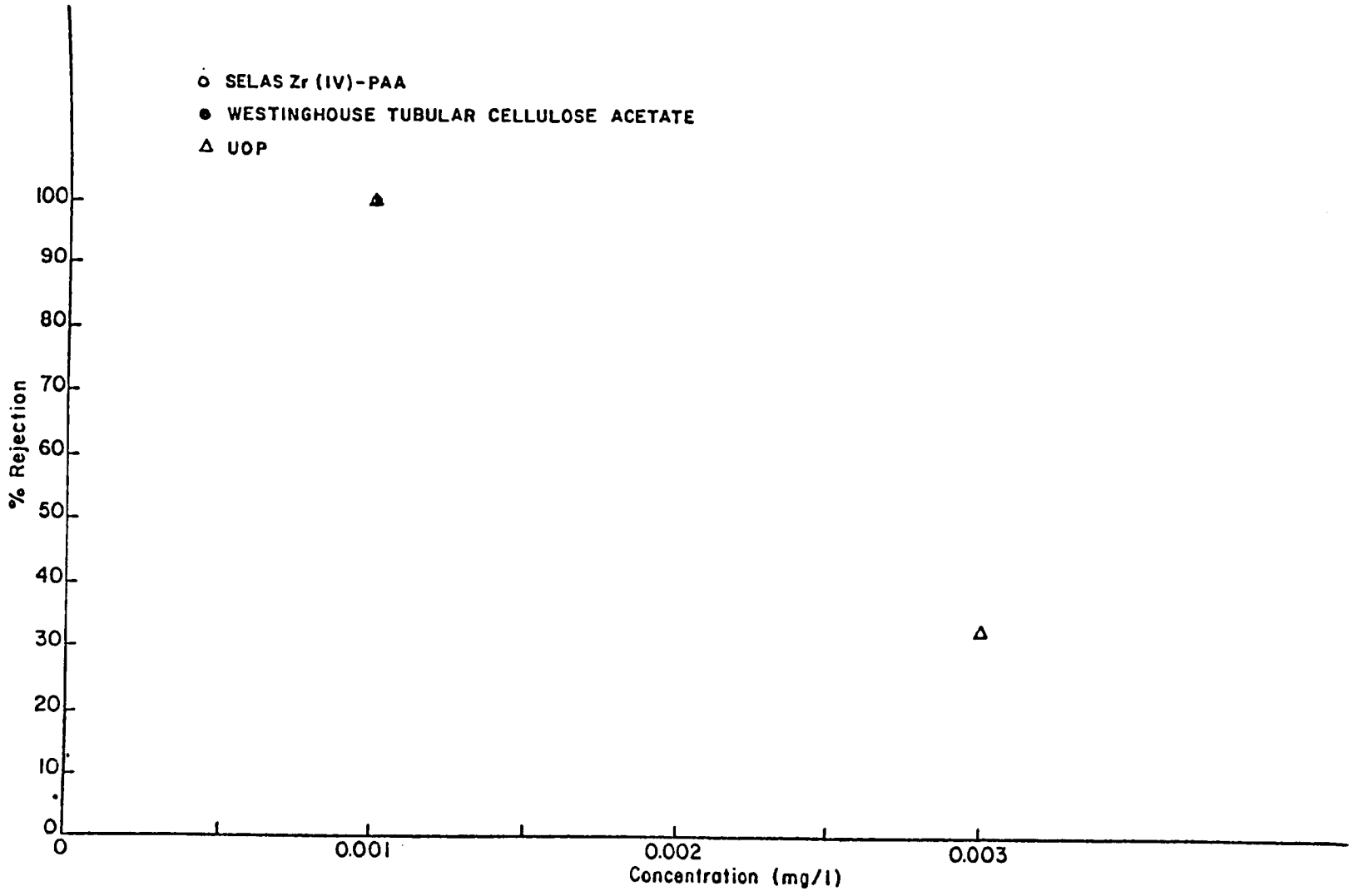

Figure A-8 Percent Rejection versus Concentration for Mercury.

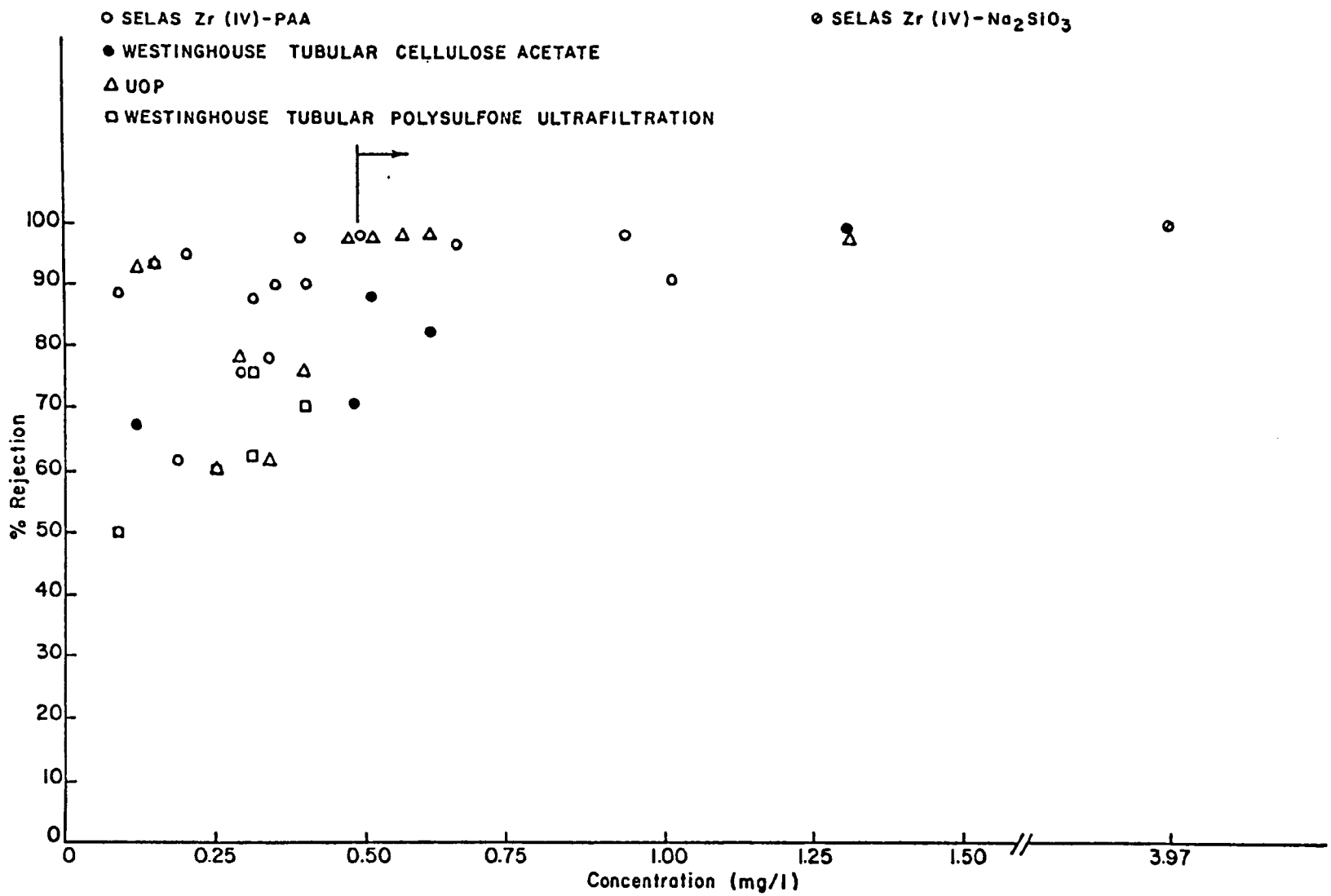

Figure A-9 Percent Rejection versus Concentration for Manganese.

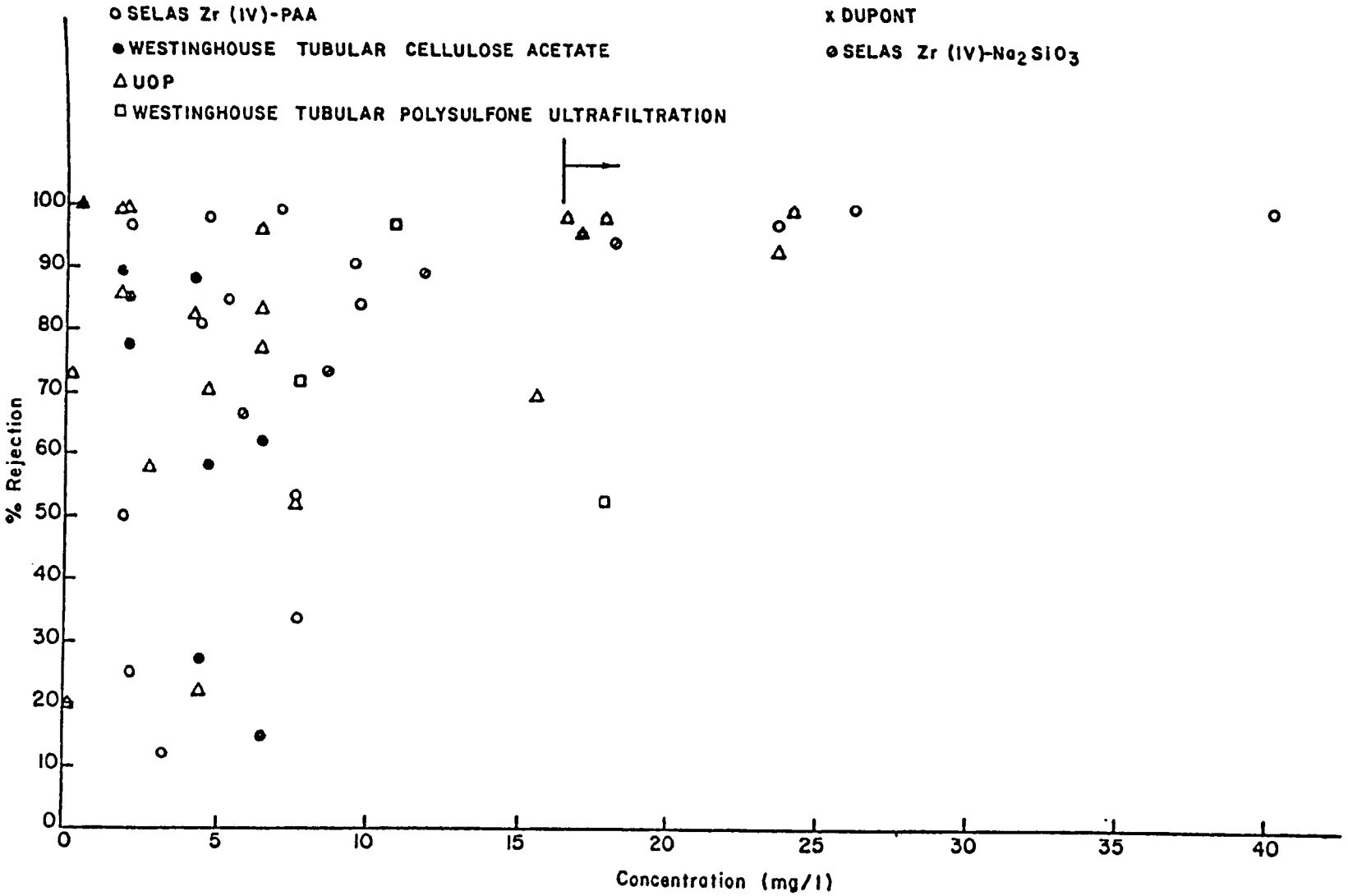

Figure A-10 Percent Rejection versus Concentration for Iron.

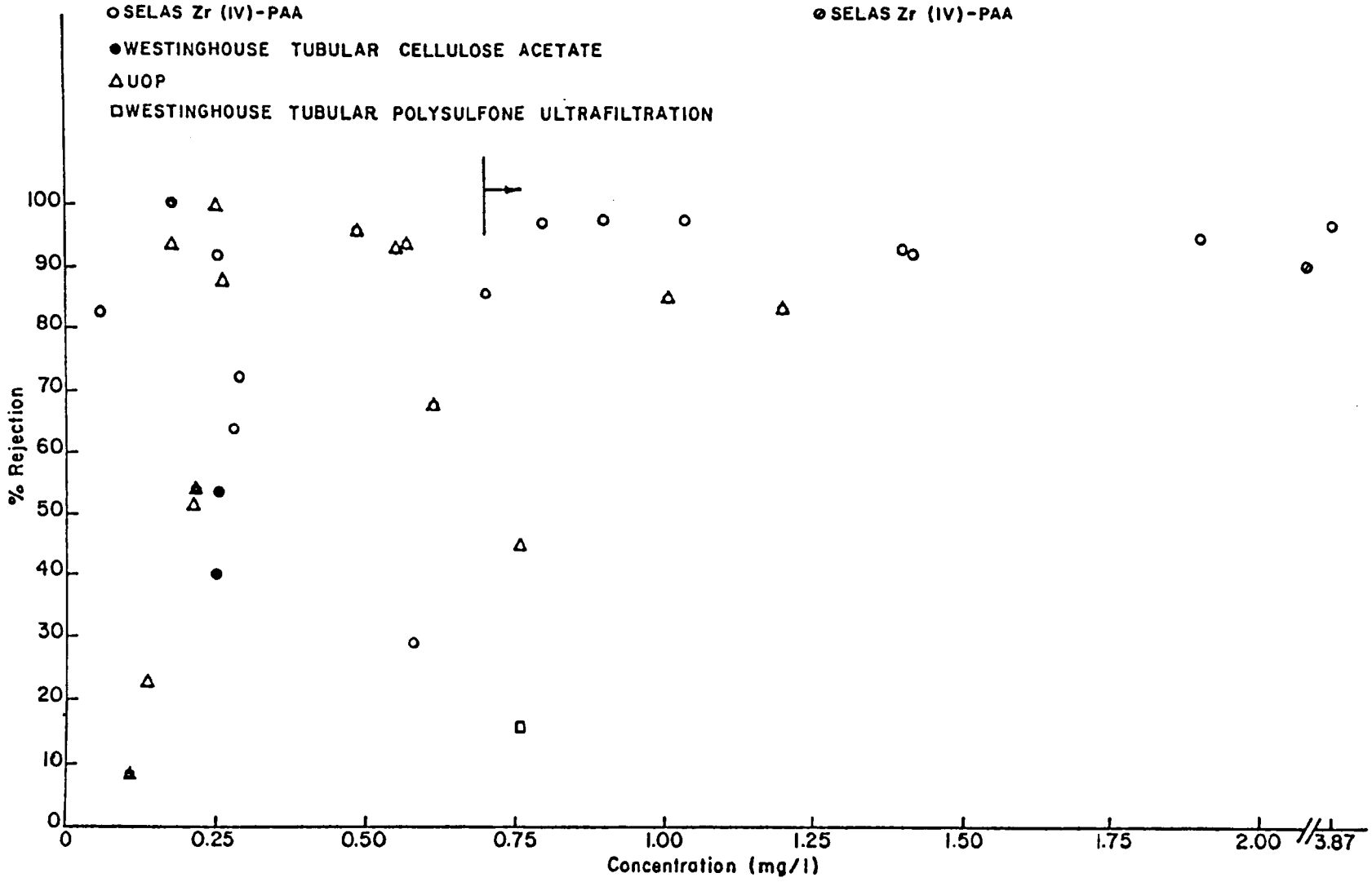

Figure A-11 Percent Rejection versus Concentration for Nickel.

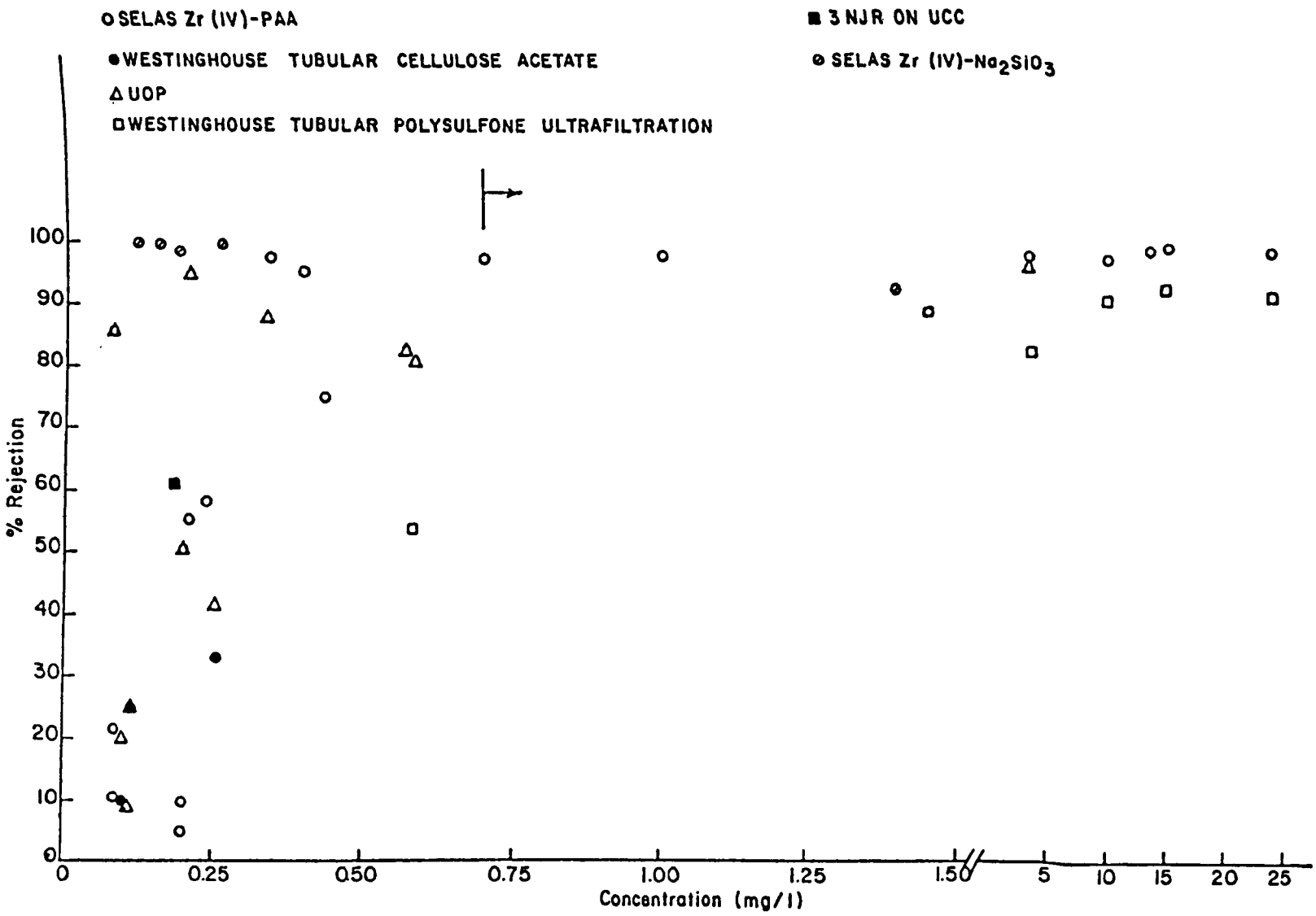

Figure A-12 Percent Rejection versus Concentration for Chromium.

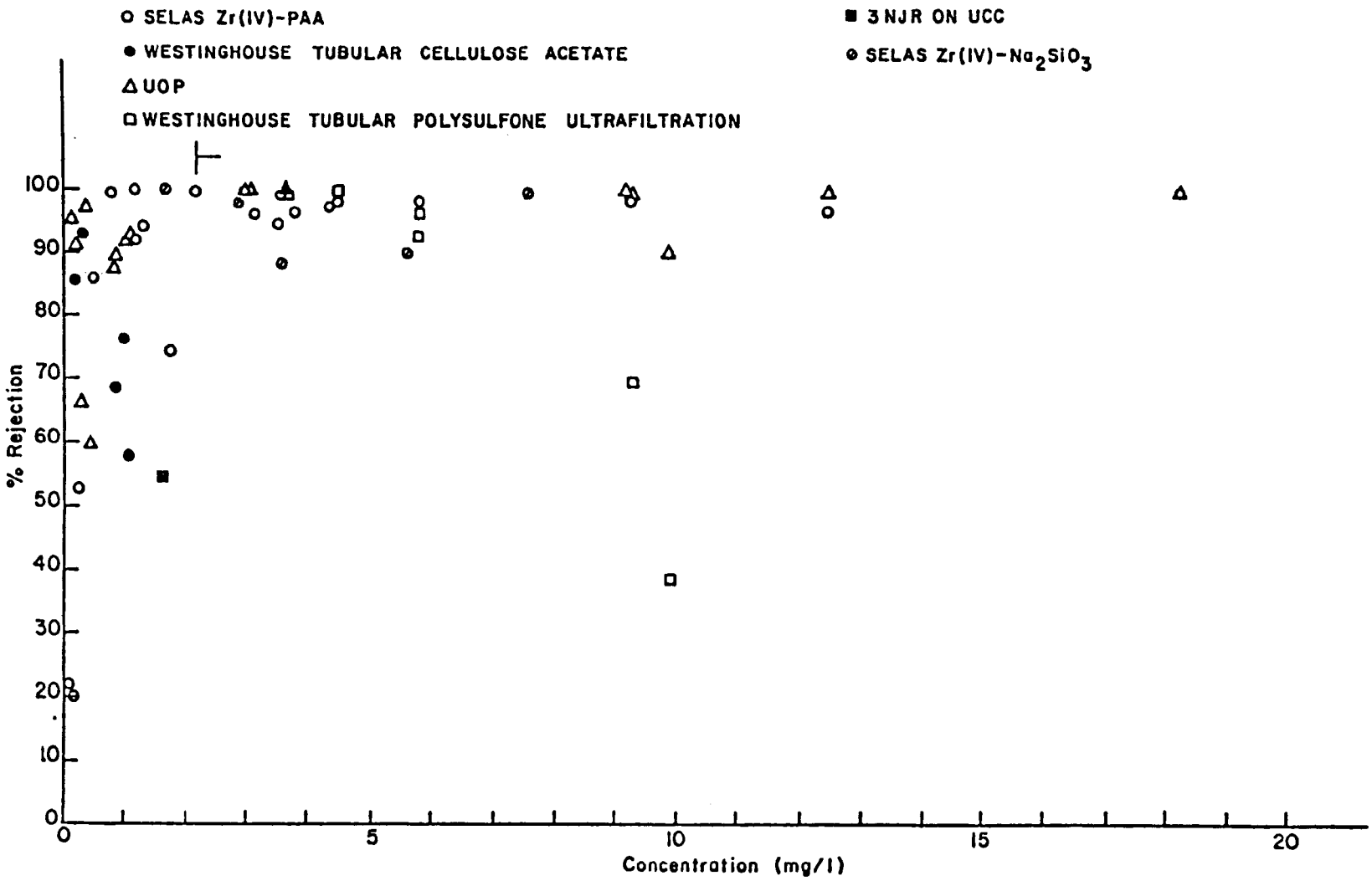

Figure A-13 Percent Rejection versus Concentration for Zinc.

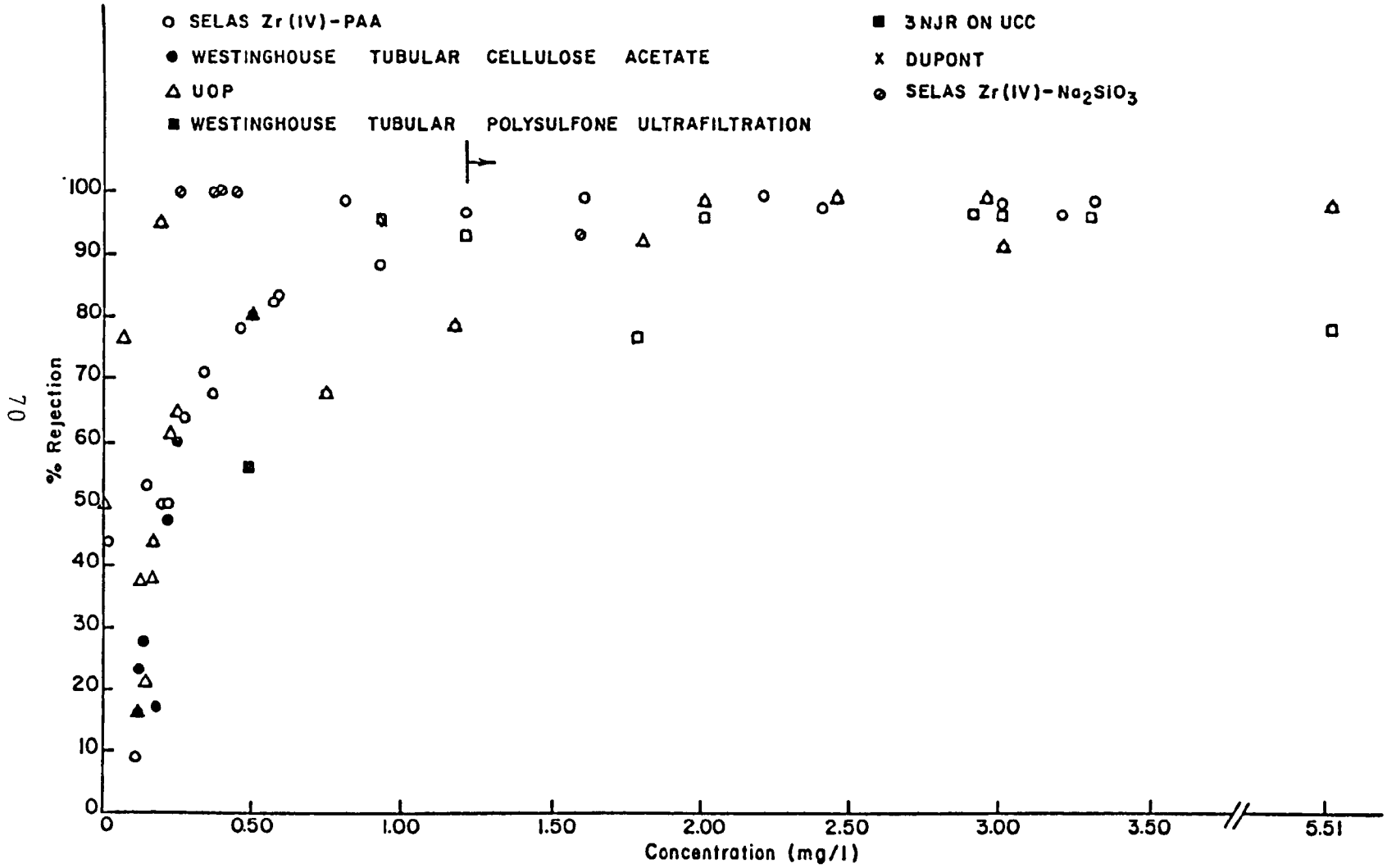

Figure A-14 Percent Rejection versus Concentration for Cooper.

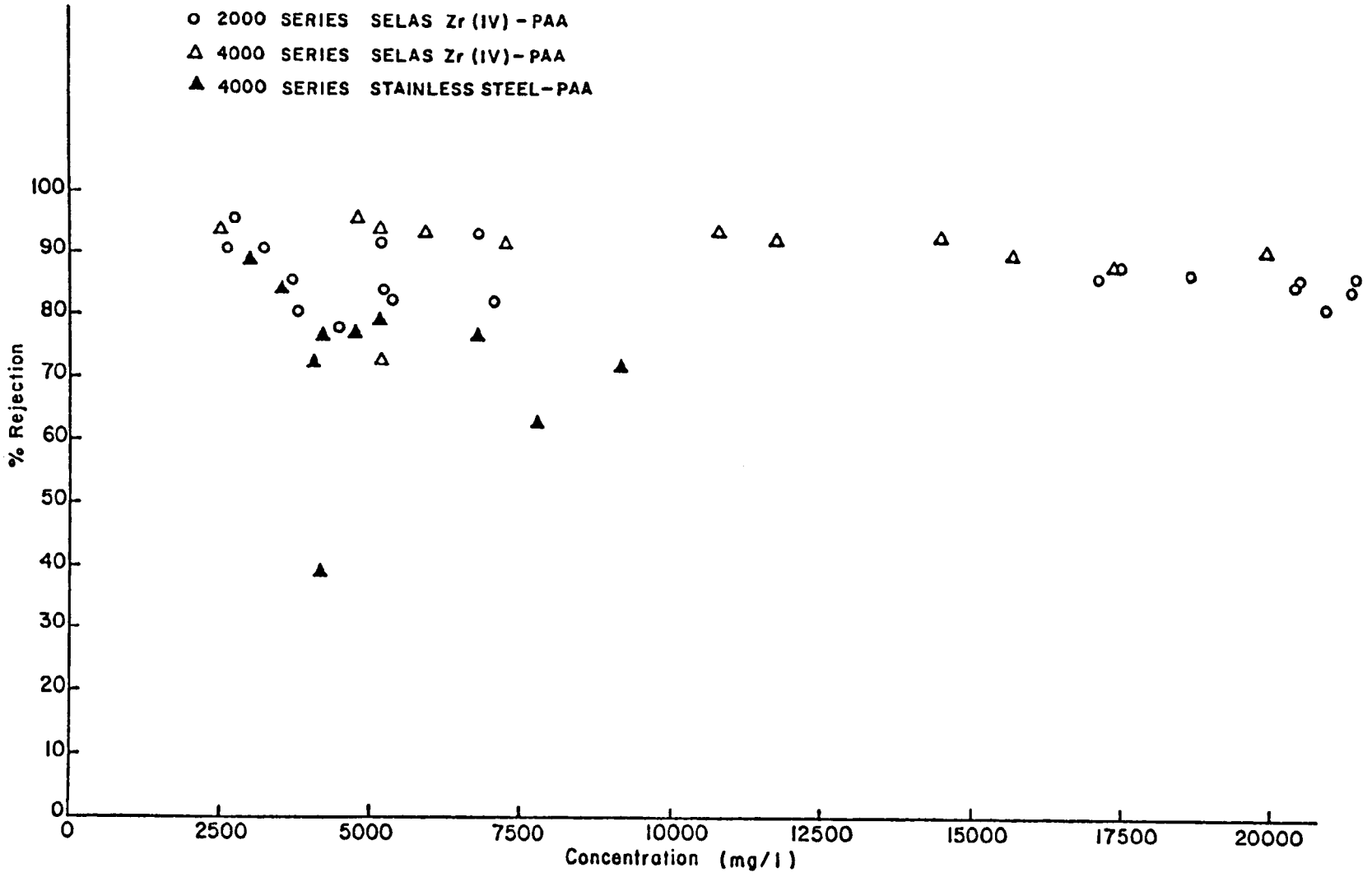

Figure A-15 Percent Rejection versus Concentration for Total Solids.

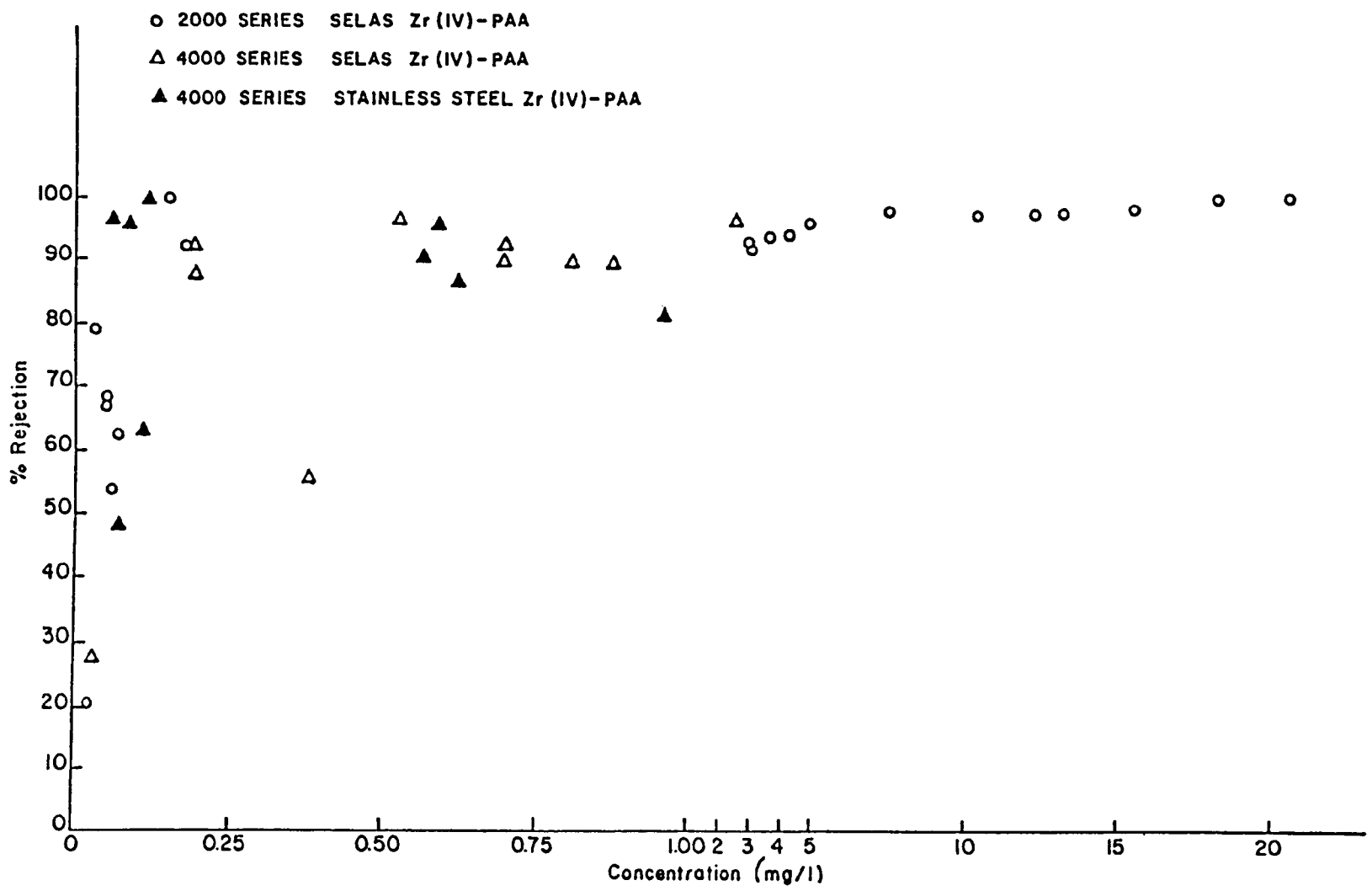

Figure A-16 Percent Rejection versus Concentration for Copper.

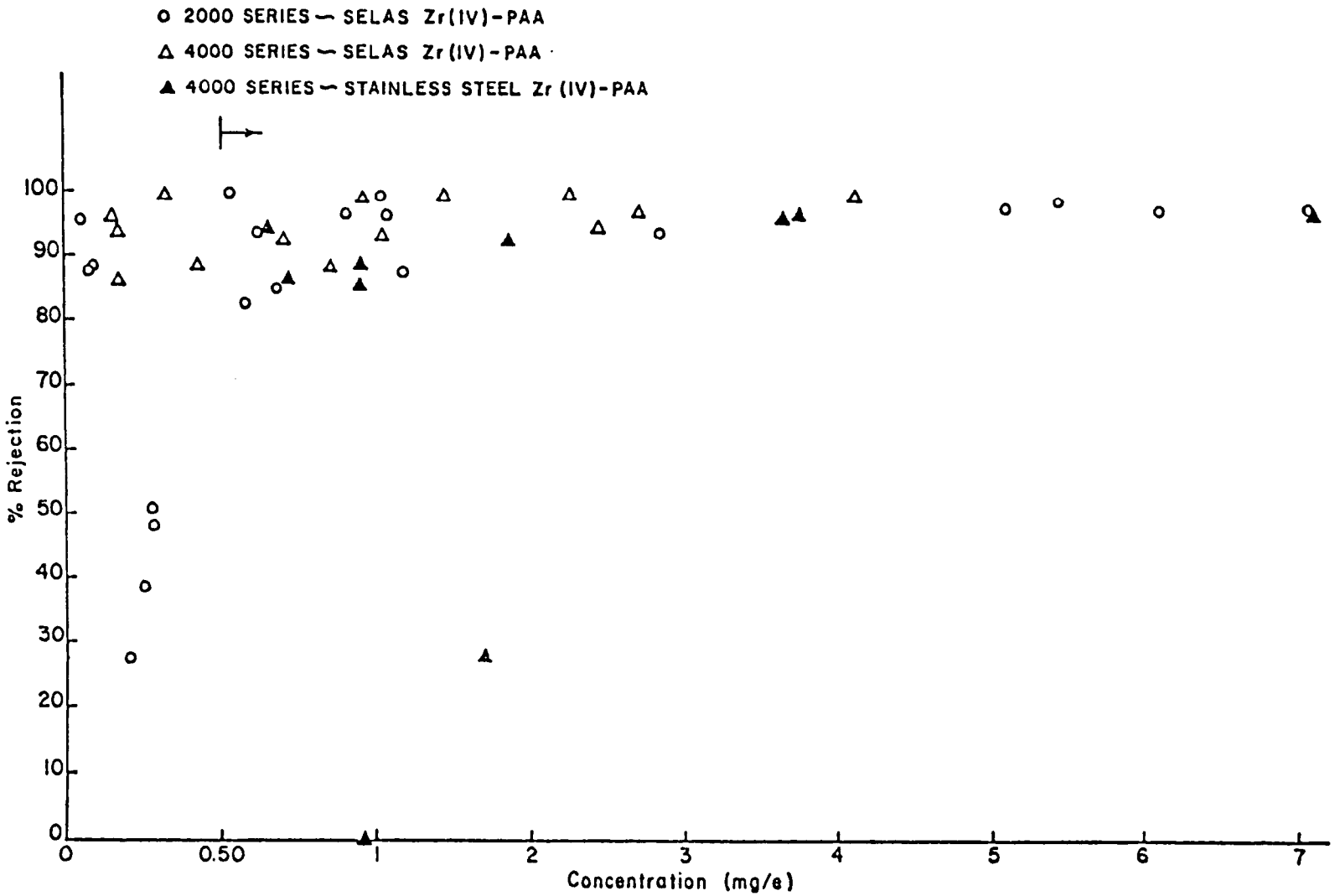

Figure A-17 Percent Rejection versus Concentration for Iron.

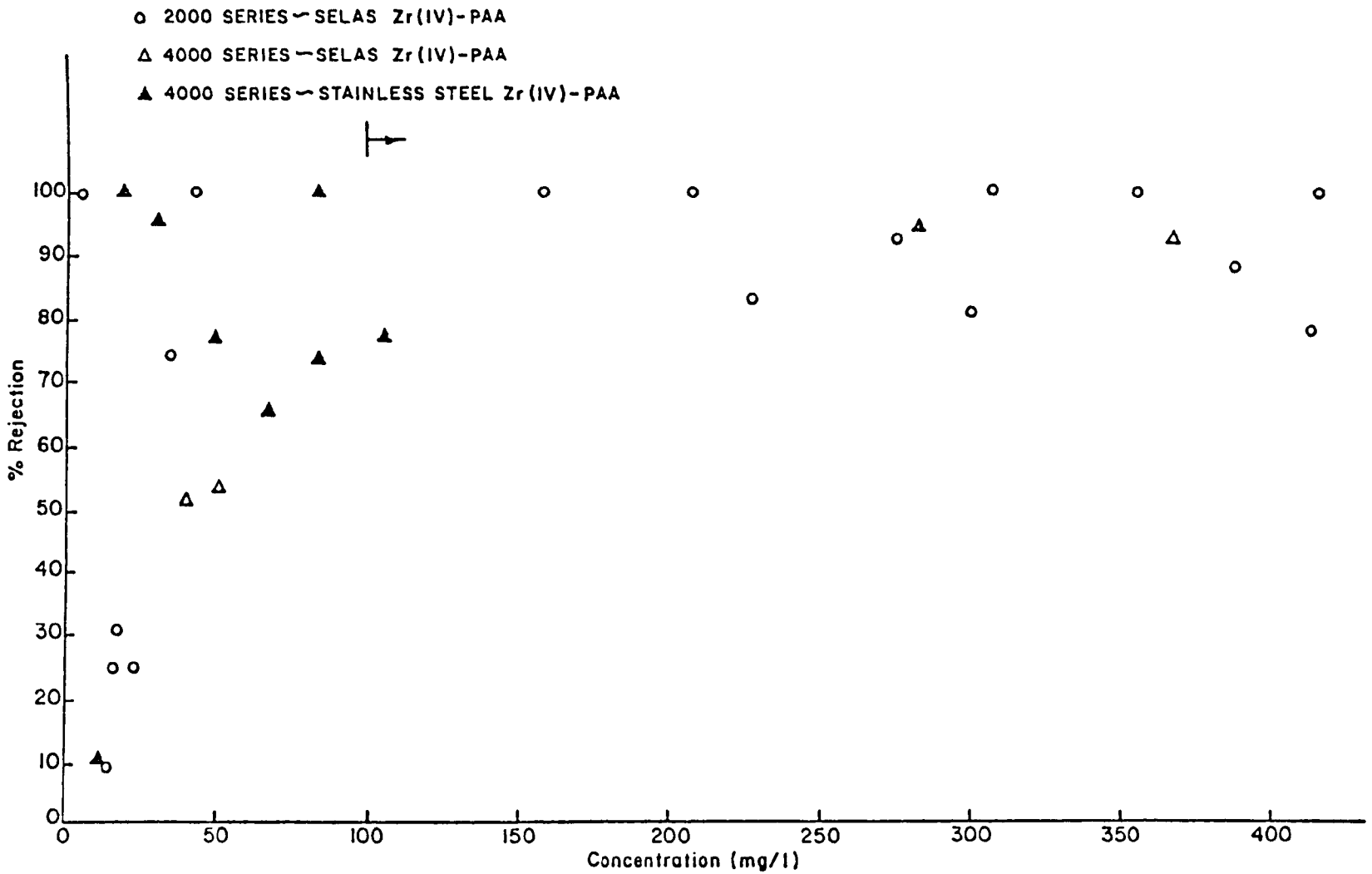

Figure A-18 Percent Rejection versus Concentration for Chromium.

Appendix B

PREDICTION OF OSMOSIS MEMBRANE SEPARATION EFFICIENCIES FOR SOLUTES IN DILUTE AQUEOUS SOLUTIONS

RTI/1430/29-01F

PREDICTION OF OSMOSIS MEMBRANE SEPARATION EFFICIENCIES FOR SOLUTES IN DILUTE AQUEOUS SOLUTIONS

by

Anton Schindler

Research Triangle Institute
P. O. Box 12194
Research Triangle Park, North Carolina 27709

Contract No. 68-02-2612, Task 29

EPA Task Officer: Dr. Max Samfield

Industrial Environmental Research Laboratory
Office of Energy, Minerals, and Industry
Research Triangle Park, NC 27711

Prepared for

U. S. ENVIRONMENTAL PROTECTION AGENCY
Office of Research and Development
Washington, DC 20460

CONTENTS

LIST OF SYMBOLS

E_{coh} . . . . . cohesive energy

e_{coh} . . . . . cohesive energy density

K_a . . . . . dissociation constant of an acid

K_b . . . . . dissociation constant of a base

M_i . . . . . molecular weight of solute

P . . . . . pressure

R_i . . . . . solute rejection in reverse osmosis

RO . . . . . reverse osmosis (hyperfiltration)

S . . . . . Small number

V . . . . . molar volume

α . . . . . degree of dissociation

δ . . . . . solubility parameter (general)

δ_s . . . . . solubility parameter of solvent

δ_p . . . . . solubility parameter of polymer

δ_i . . . . . solubility parameter of solute

δ_m . . . . . solubility parameter of membrane

Δ_{im} . . . . . difference between solubility parameters of solute and membrane (absolute value)

σ . . . . . Hammet constant

σ^* . . . . . Taft constant

Δv . . . . . band shift for hydroxyl groups in infrared spectra

SECTION I

ABSTRACT

The EPA has set maximum concentration levels for many environmental pollutants in water. Most of these pollutants are nonelectrolytes being present in low concentrations albeit still exceeding the maximum permissible level. Hyperfiltration possesses a high potential for large volume separation of pollutants in industrial unit operation effluents. The objective of this report was to present a critical evaluation of methods permitting the predictions of separation efficiencies in hyperfiltration for different non-electrolytes from their chemical structure. The evaluation was based on two criteria important for practical applications: universality and facile accessibility of the required correlation parameters.

SECTION II

CONCLUSIONS AND RECOMMENDATIONS

The most extensive investigations of establishing correlations between solute parameters and hyperfiltration efficiency (solute rejection) were carried out by Sourirajan and Matsuura on cellulose acetate membranes. Although this work represents extremely valuable contributions to the problem by initiating and stimulating the search for predictibility parameters in hyperfiltration, the choice of solute parameters was very unfortunate for practical applications. Generally, the parameters lack universality, i.e., solutes possessing the same parameter value but being of different chemical structure exhibit different behavior in hyperfiltration. As a consequence, as many individual correlations have to be established as there are structurally distinguishable groups of solutes. In addition most of the solute parameters proposed are not accessible for compounds of which only the chemical structure is known.

The above objections were circumvented in the correlation studies of Spencer and Gaddis by selecting the solubility parameter of the solute as the correlation parameter for predicting hyperfiltration efficiencies. These correlations represent the best and simplest approach toward predicting membrane performance so far obtained. For practical applications the method only requires knowledge of the solubility parameters of solute and membrane. The latter value, which would be nearly impossible to calculate, can be obtained from a small number of hyperfiltration tests performed with solutes covering a fair range of solubility parameter values. Solubility parameters of solutes are either accessible from extensive compilations in the literature or can be calculated from the chemical structure and the density of the solute.

In all fairness toward Sourirajan and Matsuura it has to be pointed out that the correlation by Spencer and Gaddis practically fails in the case of

cellulose acetate membranes. One may conclude that the hyperfiltration properties of cellulose acetate membranes cannot be described by one-parametric correlations comprising solutes of widely differing chemical structures. Since cellulose acetate membranes represent the most commonly used membrane type, further investigations, especially of commercial membranes, are required.

Presently, predictions of membrane performances according to Spencer and Gaddis are solely based on estimates of solute distributions between membrane and feed solution. Transport properties of the hyperfiltration system are not considered in this treatment. This deficiency permits the use of a single parameter in the correlation but necessarily restricts the applicability of the correlation to a limited pressure range.

Despite this minor deficiency the correlation proposed by Spencer and Gaddis presently represents the simplest and the most generally applicable method for predicting hyperfiltration performance of membranes with the exception of cellulose acetate membranes. With the latter type of membranes the correlation is not satisfactory although it is still applicable with some reservations. Especially the facile accessibility of the required solubility parameters of the solutes should make the correlation method of Spencer and Gaddis the preferred one for practical applications.

SECTION III

INTRODUCTION

Reverse osmosis (RO) is an efficient water purification process of low energy consumption. In the application of RO for water desalination membrane characterization with respect to solute separation does not present too severe a problem due to the predictable composition of the feed solution. Complications arise in the application of RO for purification of industrial wastewaters containing organic impurities. The great number of possible organic compounds which can be present in industrial wastewater precludes, at least at the present time, the application of experimental data to describe membrane performance. It is therefore pertinent to investigate the possibility of predicting membrane performance in RO from easily accessible solute parameters which can be related to the chemical structure of the solute.

The most extensive investigations in this direction were carried out by Sourirajan and Matsuura.[1] These authors based the choice of characteristic solute parameters on their sorption-capillary flow model describing membrane performance (Figure 1). According to this model, RO is governed by interfacial phenomena on the feed side of the RO membrane, i.e., either the water or the solute is preferentially sorbed on the feed-membrane interface. As a consequence, the membrane surface will be in contact with a solution differing in concentration from the bulk of the feed. If water is preferentially sorbed then an interfacial layer results on the feed side of the membrane which is depleted in solute with respect to the bulk of the feed (Figure 1A). This interfacial layer of low solute concentration is then transported through the capillaries of the membrane by the applied pressure (Figure 1B). Continuous removal of the interfacial layer by flow under pressure (hydraulic flow) and reformation of the layer by preferential sorption of water results in a permeate of lower solute concentration than the feed, i.e., the membrane rejects the solute.

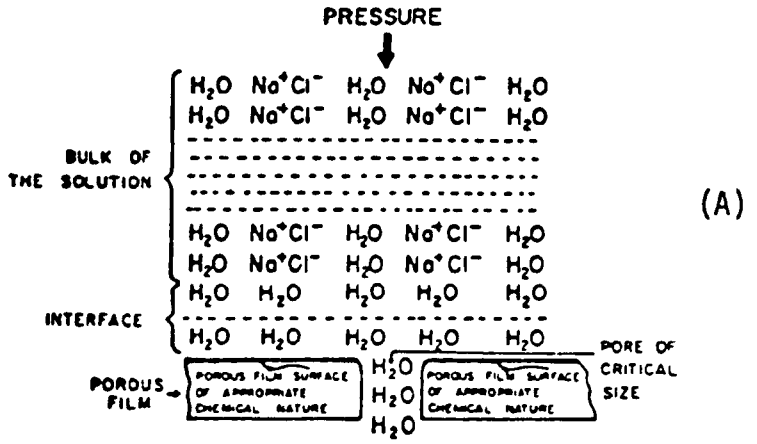

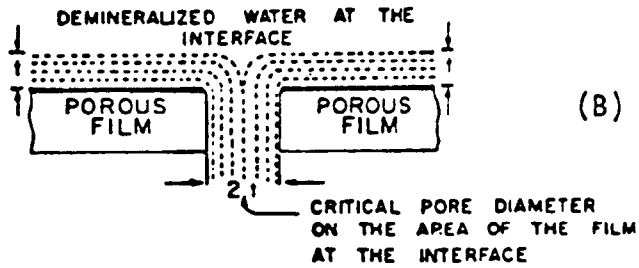

Figure 1. Schematic representation of the sorption-capillary flow mechanism in hyperfiltration. (A) Sorption mechanism on feed-membrane interface, (B) Transport mechanism.

Solutes which exhibit sorption behavior comparable to that of water or solutes which are even more strongly sorbed than water will not be separated under RO conditions.

According to the model of Sourirajan and Matsuura the membrane performance in RO is a function of solute-solvent-membrane interaction at the interface. These interactions are assumed to arise from the polar-, steric, nonpolar- and/or ionic character of each of the three components in the RO system. Proper selection of interaction parameters should provide means for predicting RO separations for a wide range of different solutes. Indeed, Surirajan and Matsuura succeeded in establishing correlations between RO performance and solute parameters by restricting themselves to water as the solvent and cellulose acetate as the membrane material. With these constraints RO performance should be a sole function of solute properties characterized by some physicochemical parameters.

Solute parameters for predicting solute separations in RO should meet two conditions. First, in agreement with the proposed model of membrane transport, the parameters should be relevant in describing sorption phenomena. Secondly, it should be possible to calculate the parameters from the known chemical structure of the solute, i.e., the parameters should be accessible from group contributions.

Five solute parameters were investigated by Sourirajan and Matsuura in their correlation studies.

1. Band shifts in IR spectra of OH groups ($\Delta\nu$)
2. Dissociation constants of carboxylic acids (K_a)
3. Hammett constants of aromatic compounds (σ)
4. Taft constants of aliphatic compounds (σ^*)
5. Small's number (S))

All of the parameters are not applicable to all solutes but the latter have to be classified into chemically related groups. Inside each group of solutes good correlation between the applicable solute parameter and solute separation in RO could be experimentally established.

It must be pointed out that the good correlations between solute parameters and solute separations in RO observed for many solutes does not represent a proof for the validity of the sorption-capillary flow mechanism proposed

by Sourirajan and Matsuura. Indeed, this mechanism has met strong criticisms by several authors. Nevertheless, the established correlations are experimental facts and consequently demonstrate the existence of relationships between specific solute parameters and solute properties under RO conditions. From this point of view the investigations of Sourirajan and Matsuura represent extremely valuable contributions by initiating and stimulating the search for predictbility parameters in RO although the underlying theory can be considered only as a working hypothesis.

According to the sorption-capillary flow model of the authors it is only the sorbed layer on the membrane interface at the feed side which participates in the hydraulic flow through the membrane, i.e., the composition of the sorbed layer determines the composition of the effluent.

According to hydrodynamic theories the first molecular layers on a liquid-solid interface do not particpate in the flow of the liquid but remain at rest, i.e., the flow of the liquid encompasses only subsequent layers. One has now to consider that forces which govern preferential sorption of either water or solute on the membrane interface are of short-range, i.e., their acting distance will not extend beyond one or two molecular layers. At larger distances the solution will be of uniform concentration since at this distance a solute molecule will be unaware of the presence of the membrane surface. Since the layer being affected in its composition by sorption will not participate in the hydraulic flow, it is difficult to understand how the composition of this layer should determine the composition of the solution flowing through the membrane capillaries (pores) under hydraulic pressure.

The solute parameters on which the correlation studies of Sourirajan and Matsuura are based are not specific for sorption processes but are of general validity in describing interactions between solutes and solvents. Consequently, the same correlations could be expected to exist if the RO process were based on a solution-diffusion model in which the partition of the solute between aqueous solution and membrane plays the decisive role. A solute which is strongly sorbed on the membrane surface will also migrate into the membrane due to the favorable interaction with the membrane material, i.e., the partition coefficient of such a solute will be relatively high. As a consequence of the relatively high solute concentration in the membrane the solute rejection will be low.

Solutes which are less compatible with the membrane material will possess a low partition coefficient, i.e., a low equilibrium concentration will establish inside the membrane. Such solutes will be highly rejected by the membrane.

Compatibility (miscibility) of solvents and polymers is described best by their respective solubility parameters. Although these parameters are not providing quantitative relationships with respect to the amounts of solute imbibed by the membrane, they permit a relative classification of different solutes with respect to their compatibilities with a given membrane material. It is somewhat surprising that no direct use of solubility parameters was made by Sourirajan and Matsuura in their correlation studies inasmuch as Spencer and Gaddis[2] could demonstrate good correlations to exist for a number of different membranes. Indeed, the correlations obtained by Spencer and Gaddis for different membranes could be unified thus permitting a comparison of rejection properties of different membrane materials with respect to a given solute.

SECTION IV

SOLUTE PARAMETERS

A considerable number of different solute parameters were investigated by Sourirajan and Matsuura[1,3-6] with respect to their correlation with solute rejection under RO conditions. Unfortunately, nearly all of these parameters do not meet the most important conditions required for practical applications: universality and facile accessibility.

The condition of universality of a parameter would mean that solutes differing in their chemical structure but possessing the same parameter value should exhibit very similar rejection properties with respect to the same membrane. If this condition is not met but correlations exist only for solutes belonging to the same structurally related group (e.g., alcohols, aldehydes, ketones, esters, ethers, etc.) prediction of membrane performance requires as many individual correlations as there are structurally distinguishable groups. This unfortunate situation exists for nearly all of the solute parameters investigated by Sourirajan and Matsuura. For example a Taft number of zero corresponds to solute separations of 60% with aldehydes, 50% with ethers, 30% with esters, and 20% with ketones.[5] The same pronounced differences are observed with Small numbers in the case of hydrocarbons.[6]

The second condition of facile accessibility of the solute parameter is also not always met by the parameters selected by Sourirajan and Matsuura. Very often practical applications of RO will be concerned with compounds of which only the chemical structure is known, and this sparse information has to suffice for the estimation of the correlation parameters. Under these conditions the choice of solubility parameters by Spencer and Gaddis[2] is of advantage. Solubility parameters for an extremely large number of solvents are listed in the literature, e.g., Hoy[7] lists close to 700 compounds. Values for unlisted compounds can be estimated from the chemical structure by means of the additivity rule for group[7-9] or atomic[10] contributions to the molar attraction constant.

The different solute parameters investigated by Sourirajan and Matsuura and by Spencer and Gaddis are discussed in subsequent sections.

A. Polar Parameters

The polar parameters describe the proton-donating or the proton-accepting properties of the solute. Numerical values related to these properties can be derived from (i) infrared spectra of alcohols and phenols, (ii) dissociation constants of carboxylic acids, and (iii) reaction rates under standard conditions.

(1) Infrared Spectra

Infrared spectra supply numerical values for the strength of hydrogen bond formation under standard conditions. If the solute is a proton-donor (alcohols or phenols) spectroscopic measurements are performed with diethyl ether as the proton-acceptor. The relative shift, $\delta\nu$ (acidity), in the absorption maximum of the hydroxyl group represents a quantitative measure for the hydrogen bonding ability of the solute, i.e., the larger $\Delta\nu$, the stronger the acidity of the solute.

If the solute is a proton-acceptor (aldehydes, ketones, ethers, or esters) deuterated methanol (CH_3OD) is used as the standard proton-donor. In this case the relative shift in the absorbance maximum of the OD group, $\Delta\nu$ (basicity), expresses the hydrogen bonding ability of the solute, i.e., the larger $\Delta\nu$, the stronger the basicity of the solute.

(2) Dissociation Constants

In the case of carboxylic acids, amines, and aminoacids, the acidity or the basicity of the solute is quantiatively described by its dissociation constants, K_a or K_b, respectively.

Acid:
$$HA + H_2O \rightleftharpoons H_3O^+ + A \qquad (1)$$
$$K_a = [H_3O^+][A^-]/[HA] \qquad (2)$$

Base:
$$B + H_2O \rightleftharpoons HB^+ + OH^- \qquad (3)$$
$$K_b = [HB^+][OH^-]/[B] \qquad (4)$$

The degree of dissociation, α, expressed as the fraction of total acid or base being present in ionized form is then given by

$$K = \alpha^2 C_{total}/(1-\alpha) \qquad (5)$$

The degree of dissociation of weak acids and weak bases is pH dependent which has to be considered in the prediction of solute separation by RO.

(3) Hammet or Taft Numbers

Hammett numbers describe the polar effect of substitutents in m- or p-position of aromatic compounds. The values are obtained either from equilibrium determinations or from rate measurements under standard conditions. In the first case dissociation constants of differently m- or p-substituted benzoic acids are compared. If K_o and K are the dissociation constants of unsubstituted and substituted benzoic acid, respectively, the Hammett constant σ, is given by:

$$\sigma = (1/\rho)\lg(K/K_o) \qquad (6)$$

where ρ is a constant, in this case referring to measurements of dissociation constants. The value of ρ changes with the kind of physico-chemical measurement, e.g., if one compares rate constants of ester hydrolysis, but taking this change into account the same σ value is obtained for each substituent.

Taft numbers are defined analogously for aliphatic and o-substituted aromatic compounds. Also in this case the Taft number σ^* is a measure of the polar effect of the substituent.

Both solute parameters, Hammett and Taft numbers represent group contributions, i.e., for solutes possessing more than one substituent, Hammett or Taft number of the solute are equal to the sum of the Hammett or Taft numbers of each of the substituent groups. Consequently, it is possible to calculate Hammett or Taft numbers if the chemical structure of the solute is known.

Since the dissociation constants, K_a, represents the total polar effect of the acid molecule and σ or σ^* represent the contribution of the substitutent groups to this total effect, a relationship exists between K_a and σ or σ^* for aromatic and aliphatic monocarboxylic acids, respectively. From this relationship dissociation constants of monocarboxylic acids can be estimated from the chemical structure of the acid.

There exists also a correlation between σ or σ^* numbers and spectroscopically determined $\Delta\nu$ values for reasons analogous to those given for the correlation between K_a and σ or σ^*.

Because of the existing relationships between different polar parameters correlation of solute separation in RO with either the Hammett or the Taft number of the solute will suffice.

B. Small Numbers

Hydrocarbon solutes are hydrophobic and essentially non-polar. The cellulose acetate membrane has both polar and non-polar character. The polar character of the membrane arises from hydroxyl and ester groups and is responsible for the ability of hydrogen bond formation. The non-polar character arises from the hydrocarbon backbone and the hydrocarbon groups in the ester part. Consequently, the membrane may be expected to attract both the polar solvent (water) and the non-polar solute (hydrocarbon). According to the sorption-capillary flow mechanism of Sourirajan and Matsuura the relative extents of these attractions determine the solute separation in RO.

For the purpose of correlation of RO data both the molar solubility of the solute in water or the Small number of the solute were used to express the degree of hydrophobicity or of non-polar character of the solute. From a practical point of view, it was desirable to use a solute parameter which can be calculated from the chemical structure of the solute. This is the case with Small numbers but not with solubilities which require experimental determinations.

The Small numbers are related to the cohesive energies of liquids, E_{coh}, which are defined as the energies necessary to break all the intermolecular contacts per mole of the liquid. The cohesive energy of a liquid is closely related to its molar heat of evaporation, ΔH_{vap}.

$$E_{coh} = \Delta H_{vap} - P\Delta V \qquad (7)$$

Quantities derived from the cohesive energy of a liquid are, vis.:

the cohesive energy density: $e_{coh} = (E_{coh}/V)$, (8)

the solubility parameter: $\delta = (E_{coh}/V)^{1/2}$, and (9)

the molar attraction constant (Small Number):

$$S = (VE_{coh})^{1/2} = V\delta \qquad (10)$$

In the above expressions V is the molar volume at standard temperature of 298 K (25°C) and is given by molecular weight divided by density. The dimension of the solubility parameters is $[J^{1/2}\ m^{3/2}]$ with 1.0 $(J/m^3)^{1/2}$ = 4.88 x 10^2 $(cal/cm^3)^{1/2}$.

In the final analysis the calculation of solubility parameters or Small numbers revolves around obtaining the value of the heat of evaporation from vapor pressure data. The procedure used in the calculation of solubility parameters for 680 compounds from vapor pressure data is outlined by Hoy.[7]

The additive property of the cohesive energy, E_{coh}, was demonstrated as early as 1928 by Dunkel.[11] Small[8] demonstrated the usefulness of the molar attraction constant as an additive quantity. His set of values is still frequently used with some refinements by other authors.[7-9] A comparison of values derived by different authors is given by Van Krevelen.[10] The latter author also devised a list of atomic attraction constants[10] which considerably simplify calculations.

Generally, solubility parameters derived from vapor pressure data should be preferred in correlation studies over those calculated by the additivity method from group contributions. The total cohesive energy, E, which holds a liquid together and which is derived from vapor pressure data, can be divided into contributions from dispersive forces (London forces), E_d, dipole-dipole forces, E_p, and hydrogen bonding forces, E_h.

$$E = E_d + E_p + E_h \qquad (11)$$

Multiplying this equation by the molar volume of the compound one obtains

$$VE = VE_d + VE_p + VE_h \qquad (12)$$

or with $VE = S^2$ from equ. 10

$$S^2 = S_d^2 + S_p^2 + S_y^2 \qquad (13)$$

The value of S calculated from group contributions strongly depends on the way the individual group values were derived with respect to equ.(13). For example, Small obtained a value of 170 for the OH group which was derived from the contribution of an ether oxygen (70) and a hydrocarbon hydrogen (100). This value represents only the contribution to the cohesive energy derived from dispersion forces but neglects the considerably high contribution resulting from hydrogen bonding which does not exist in hydrocarbons from which the value of 100 for hydrogen was derived. According to Konstam and Feairheller[9] the value for a single OH group is 399 which yields good agreement between calculated and experimental solubility parameters of alcohols (see Table I).

Problems arise with compounds containing more than one functional group. In some cases, e.g., OH in diols, Cl in CCl_2 or CCl_3, modified group contibutions are reported,[9] but generally the additive method yields ambigous results if applied to polyfunctional compounds.

Table 1. COMPARISON OF SOLUBILITY PARAMETERS OF SELECTED COMPOUNDS OBTAINED BY DIFFERENT METHODS

Compound	Molar Volume (m^3/kmol)	Solubility Parameter in $(J/m^3)^{1/2} \times 10^3$		
		Hoy (Ref. 7)	VanKrevelen (Ref. 10)	Konstam et. al. (Ref. 9)
Alcohols				
Methanol	40.66	29.7	31.9	30.9
Ethanol	58.60	26.2	27.0	26.1
n-Propanol	75.11	25.0	24.8	24.1
i-Propanol	*78.82*	*23.4*	*22.0*	*22.2*
n-Butanol	91.53	23.8	23.4	22.7
n-Pentanol	99.41	22.8	24.4	23.6
3-Pentanol	104.27	20.8	21.0	21.0
Ethyleneglycol	55.92	34.9	34.5	32.5
Propyleneglycol	73.70	30.7	30.0	27.7
Glycerol	73.19	36.3	34.9	34.3
Benzylalcohol	103.82	24.7	25.8	25.0
Esters				
Methylacetate	79.88	19.4	17.0	18.9
Ethylacetate	98.54	18.3	16.6	18.1
Ethylbenzoate	144.20	20.0	19.0	19.8
Ketones				
Acetone	74.01	19.7	20.7	21.1
Butanone	90.19	19.4	20.1	20.3
Aldehydes				
Acetaldehyde	57.13	20.2	21.8	22.1
Propionaldehyde	73.44	19.3	20.8	20.9
Acids				
Acetic acid	57.26	26.7	-	26.4
Propionic acid	74.99	25.6	-	23.8
Butyric acid	92.45	24.5	-	22.3
Acrylic acid	69.30	26.4	-	24.4
Ethers				
Diethylether	104.78	15.4	15.8	19.1
Isopropylether	142.33	14.5	15.6	17.2
Amines				
Diethylamine	104.30	16.5	17.6	-
Triethylamine	139.95	15.2	15.0	-
Triethylenetetramine	149.83	22.8	25.1	-
Ethylenediamine	66.57	25.3	23.0	29.6
Hydrocarbons				
n-Hexane	131.61	14.9	14.9	14.9
Cyclohexane	108.79	16.8	16.6	16.9
Benzene	89.42	18.8	18.6	17.0
Toluene	106.88	18.3	18.2	18.2

The usefulness of solubility parameters for predicting solute rejections in RO was pointed out by Spencer and Gaddis[2] and is based on the fact that these parameters describe the solubility of a solute in a polymer. According to theoretical concepts developed by Hildebrand[12] the solubility parameters of solvent, δ_s, and polymer, δ_p, determine the compatibility of both. The larger the difference $\delta_p - \delta_s$ the less compatible the components whereas close similarity of δ_p and δ_s assures complete miscibility.

SECTION V

PREDICTION OF SOLUTE SEPARATION

A. Polar Parameters of Sourirajan and Matsuura

Although several of the polar parameters selected by Sourirajan and Matsuura show good correlations with solute rejections in RO, these results are more of academic interest and are not useful for practical applications.

Band shifts in infrared spectra cannot be predicted from the chemical structure of the solute but would require individual determinations. Furthermore, the range from zero rejection to over 80% rejection is compressed inside a range of 20 units in Δv, thus small changes in the parameter cause extremely large changes in the rejection value.

A similar criticism applies to the use of Taft numbers. Also in this case the Taft number would have to be known to three significant digits to be useful for predicting solute rejections. In addition, as pointed out previously, structurally different compounds possessing the same Taft number exhibit widely differing rejection properties. Consequently, a great number of correlation curves would be required for practical applications.

B. Small Numbers

Small numbers of different aliphatic and aromatic hydrocarbons were correlated with their rejection properties by Sourirajan and Matsuura.[6] No correlation existed between Small numbers and rejections if all of the compounds were considered. Some improvement could be obtained by grouping the solutes according to chemically related groups, e.g., paraffins, olefins, aromatics, etc.

The usefulness of Small numbers as correlative parameters is doubtful. With structurally related compounds for which correlations are observed, the Small numbers generally increase linearly with molecular weight as a consequence of their additive nature. Such a dependence is shown in Figure 2 for hydrocarbons, but also exists for alcohols, esters, ketones, etc. Because of

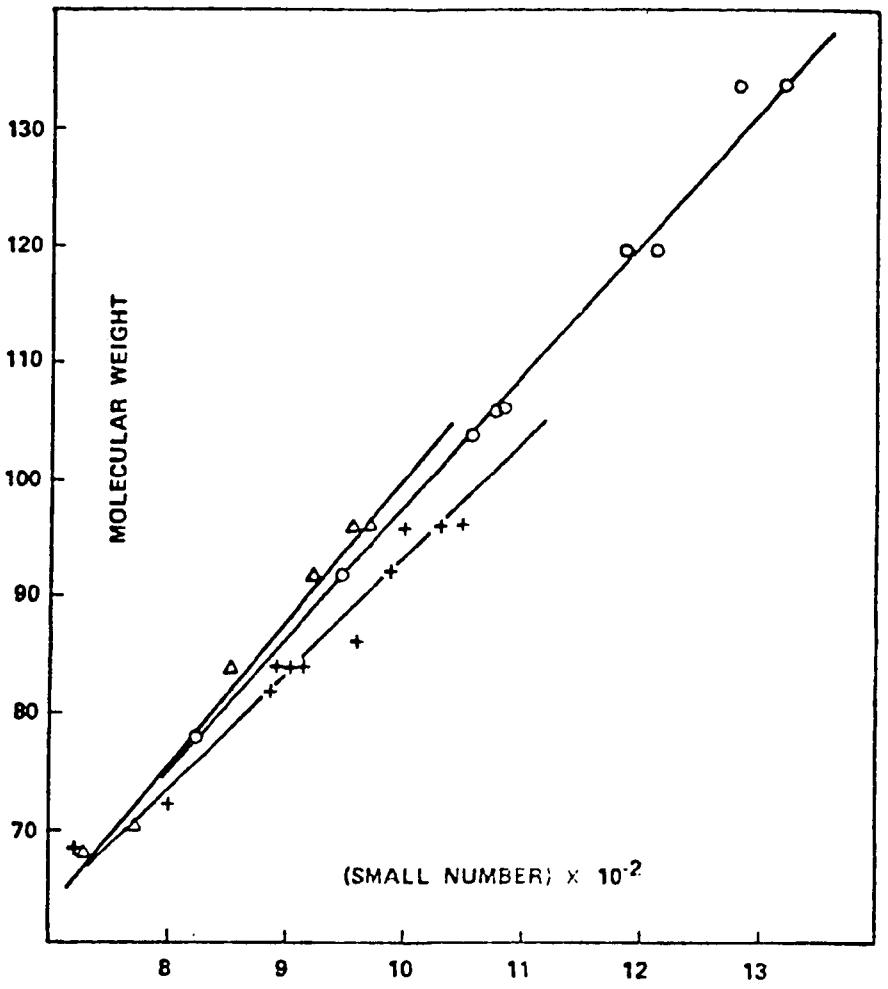

Figure 2. Molecular weight dependence of Small numbers for structurally related compounds, Aliphatic (+), cycloaliphatic (Δ), and aromatic (∘) hydrocarbons.

this linear relationship molecular weights of solutes can be substituted for Small numbers without change in the shape of the correlation curve, i.e., correlation of solute rejection with molecular weight of the solute will be as good as correlation with Small numbers.

C. Solubility Parameters

Correlation of solute rejections, R_i, in RO with solubility parameters of the solute, δ_i, was proposed by Spencer and Gaddis (2). This correlation is based on the assumption that the concentration of solute available for transport across the membrane depends on the difference between the solubility parameters of solute, δ_i, and membrane material, δ_m.

$$\Delta_{im} = \delta_i - \delta_\mu \qquad (14)$$

Consequently, R_i should be a function of Δ_{im} and a membrane should exhibit maximum rejection properties for solutes which differ strongly in the δ_i value from that of the membrane material. Contrarily, minimum rejection or no rejection at all will be observed with solutes possessing δ_i values equal to that of the membrane.

Correlation plots of R_i vs δ_i for three different membranes were found in good agreement with the predicted dependence of R_i on δ_i. The plots exhibited minima which permitted the estimation of the δ_m values of the three membranes. It was further observed that close to 100% rejection is obtained if the δ_i value of a solute differed $\pm 0.01\ (J/m^3)^{1/2}$ from the δ_m value of the membrane. Inside the intermediate range of δ_i values the R_i values showed a linear correlation with respect to δ_i.

Since the Δ_{im} values observed for onset of 100% rejection were found to be the same for the three membranes, their correlation plots could be superimposed by changing the independent variable δ_i to Δ_{im}, i.e., by using the δ_m values as the common origin. The resulting correlation plot in its generalized form is shown in Fig. 3.

The correlation by Spencer and Gaddis between R_i and δ_i represents the best and simplest correlation so far obtained for predicting membrane performance in RO. For practical applications the method only requires knowledge of δ_i of the solute (See Section IV-B) and of δ_m of the membrane. The latter value, which would be nearly impossible to calculate, can be obtained from few hyperfiltration tests with solutes of differing δ_i values.

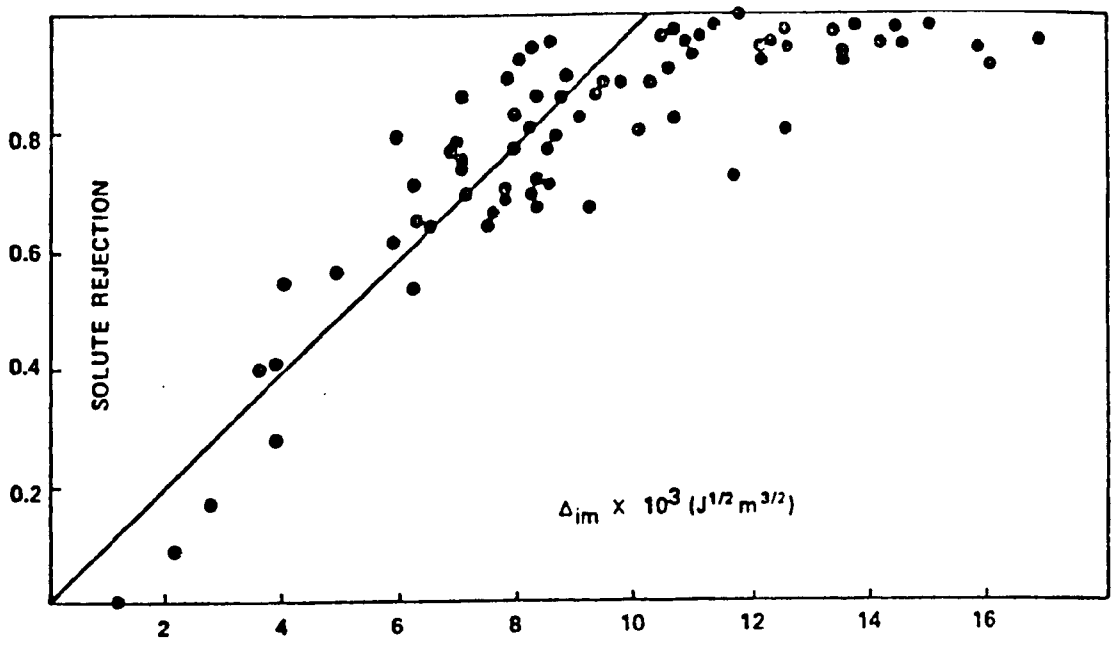

Figure 3. Dependence of solute rejection on the difference between the solubility parameters of solute and membrane. Data from Ref. 2.

The correlation shown in Fig. 3 does not include R_i values obtained with cellulose acetate membranes. Such values are shown in Fig. 4. Also in this case 100% rejection approximately corresponds to a Δ_{im} value of 0.01 $(J/m^3)^{1/2}$ but the scatter of data is considerably stronger than for the three combined membranes of Fig. 3. Solute rejection by cellulose acetate membranes can be predicted only with some reservations.

As pointed out by Spencer and Gaddis (2) their approach toward predicting membrane performance in RO is solely based on estimating the distribution of the solute between the separating membranes and the bulk of the feed. This treatment does not include a parameter describing the transport properties of the hyperfiltration system.

A possible effect of a changing transport parameter is indicated if one compares rejection data obtained with the same membrane at widely differing pressures. In Table II, data by Chian and Fang (13) are presented which were obtained with a polyamide membrane at three different operating pressures. In Fig. 5 the rejection values are plotted versus δ_i values of the solutes. Although data are insufficient to permit the estimation of the δ_m value of the membrane, they clearly demonstrate that at low pressure the rejection is much less sensitive to changes in δ_i than at high pressure. Probably for this reason the correlation between R_i and δ_i is somewhat lost at higher pressures.

D. Molecular Weight

The value of solute molecular weights, M_i, as a parameter for predicting the rejection of non-electrolytes in RO was pointed out by Spencer et al (14). Most highly rejecting hyperfiltration membranes effectively reject non-electrolytes in the molecular weight range exceeding a limiting value of about 70. This is demonstrated for data by Cadotte et al (15) shown in Fig. 6. Solutes with molecular weights exceeding a value of 60 exhibit an average rejection of 93.2 ± 4.1%.

Hyperfiltration results presented in Fig. 5 are replotted in Fig. 7 in dependence of solute molecular weights. Data obtained at lowest operating pressure show very weak correlation but the correlation improves by going to higher pressures. If one neglects two solutes, methanol and methylacetate, which show decreasing rejection with increasing pressure, the average rejection for solutes with M_i >60 is 91%.

Table 2. EFFECT OF OPERATING PRESSURE ON SOLUTE REJECTION BY A POLY(AMIDE)MEMBRANE.

Solute	Molecular Weight (kg/kmol)	Solubility Parameter[a] $(J/m^3/^{1/2} \times 10^3$	Percent Solute Rejection at Operating Pressure in MPa[b]		
			2.75	4.13	10.34
Methanol	32	29.7	28	19	5
Ethanol	46	26.2	36	28	57
i-Propanol	60	25.0	90	89	95
Acetone	58	19.7	53	72	72
Diethylether	74	15.4	58	90	92
Glycerol	92	36.3	88	88	88
Aniline	93	(21.3)	47	78	82
Methylacetate	74	19.4	57	54	45
Acetic acid	60	26.6	31	70	82
Phenol	94	(23.5)	45	80	89
Formaldehyde	30	(28.5)	21	52	69

[a] Solubility parameters from Ref. 7, values in parenthesis calculated according to Ref. 10.
[b] Rejection values from Ref. 13.

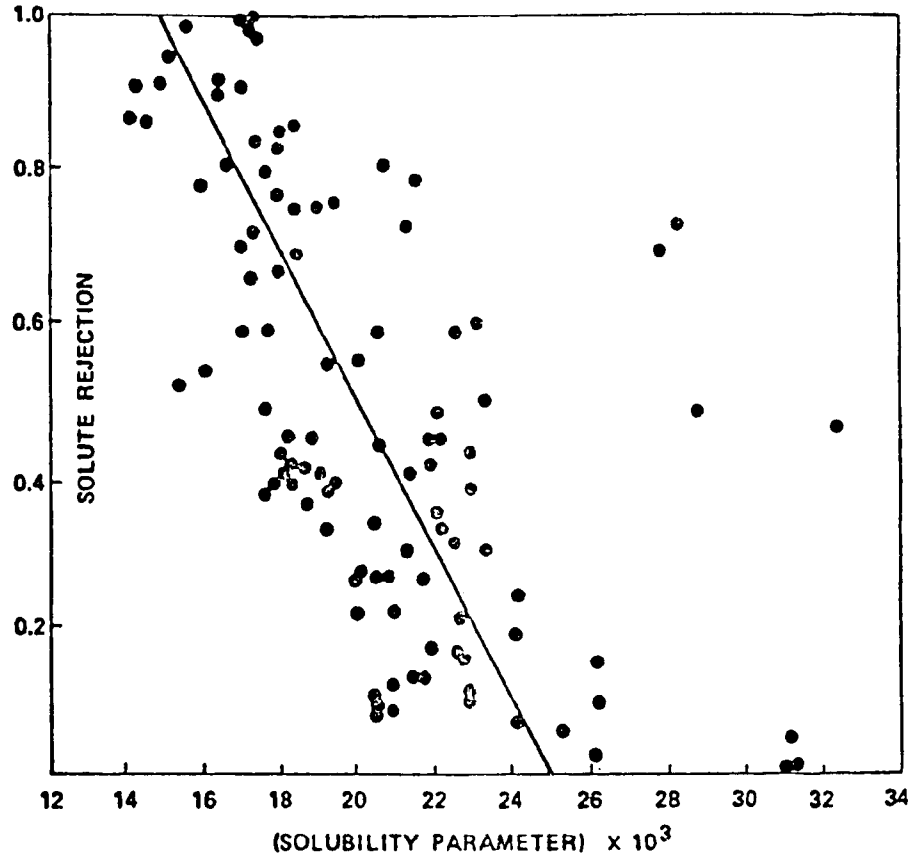

Figure 4. Solute rejection by cellulose acetate membranes in dependence of the solubility parameters of the solute. Data from Ref. 2.

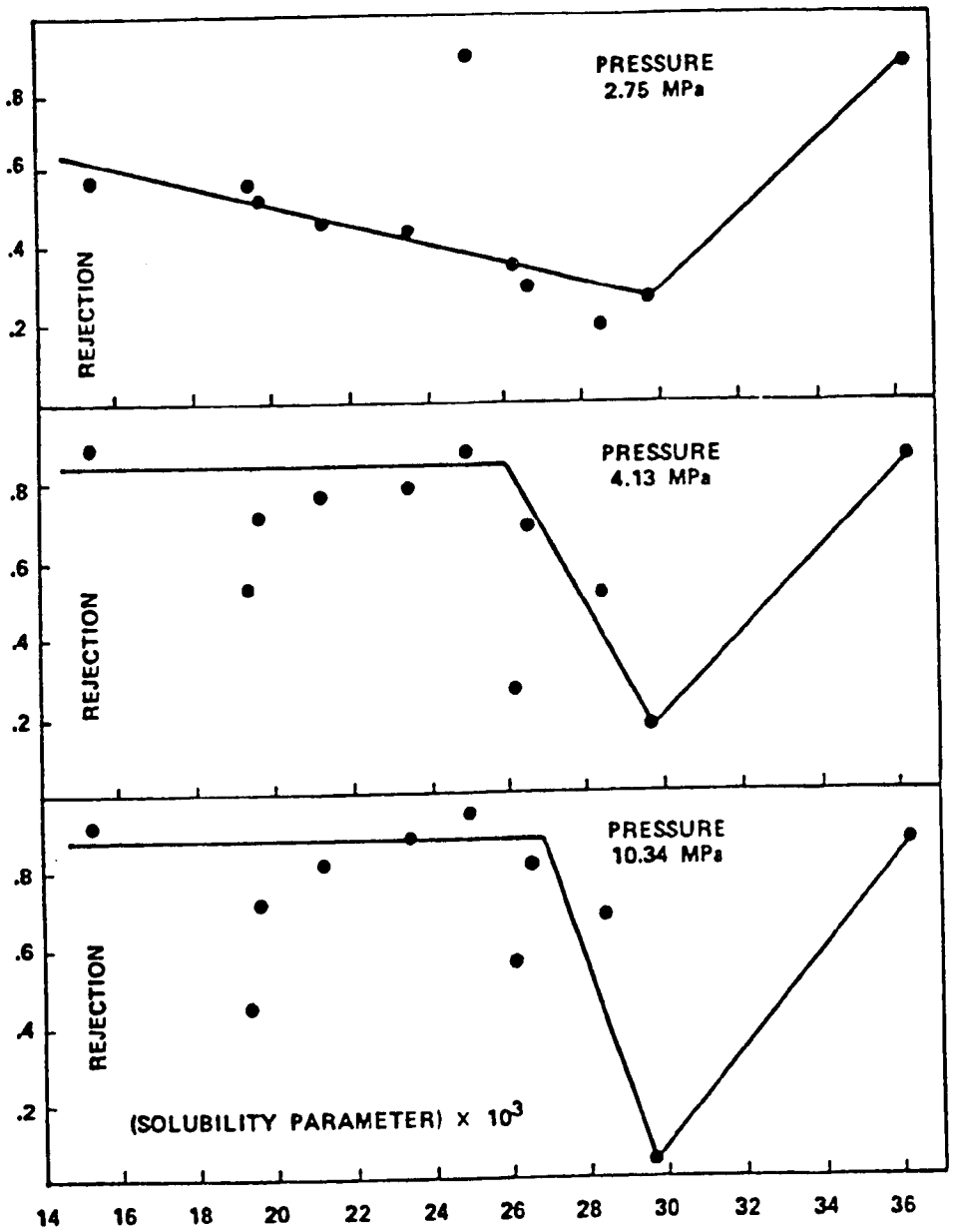

Figure 5. Solute rejections for three operating pressures in dependence on the solubility parameters of the solutes. Data from Table II.

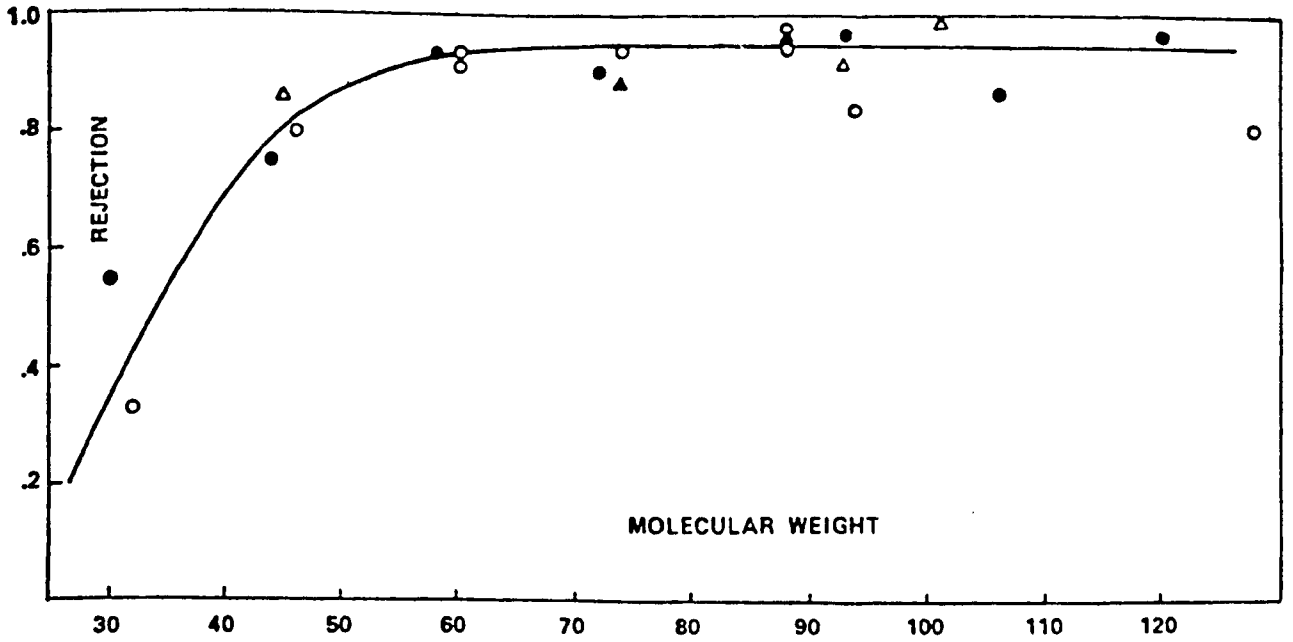

Figure 6. Solute rejection in dependence on the molecular weight of solutes for NS-1 membrane at 5.52 MPa operating pressure. Data from Ref. 15. Alcohols (∘), aldehydes and ketones (•), amines (Δ), and esters (▲).

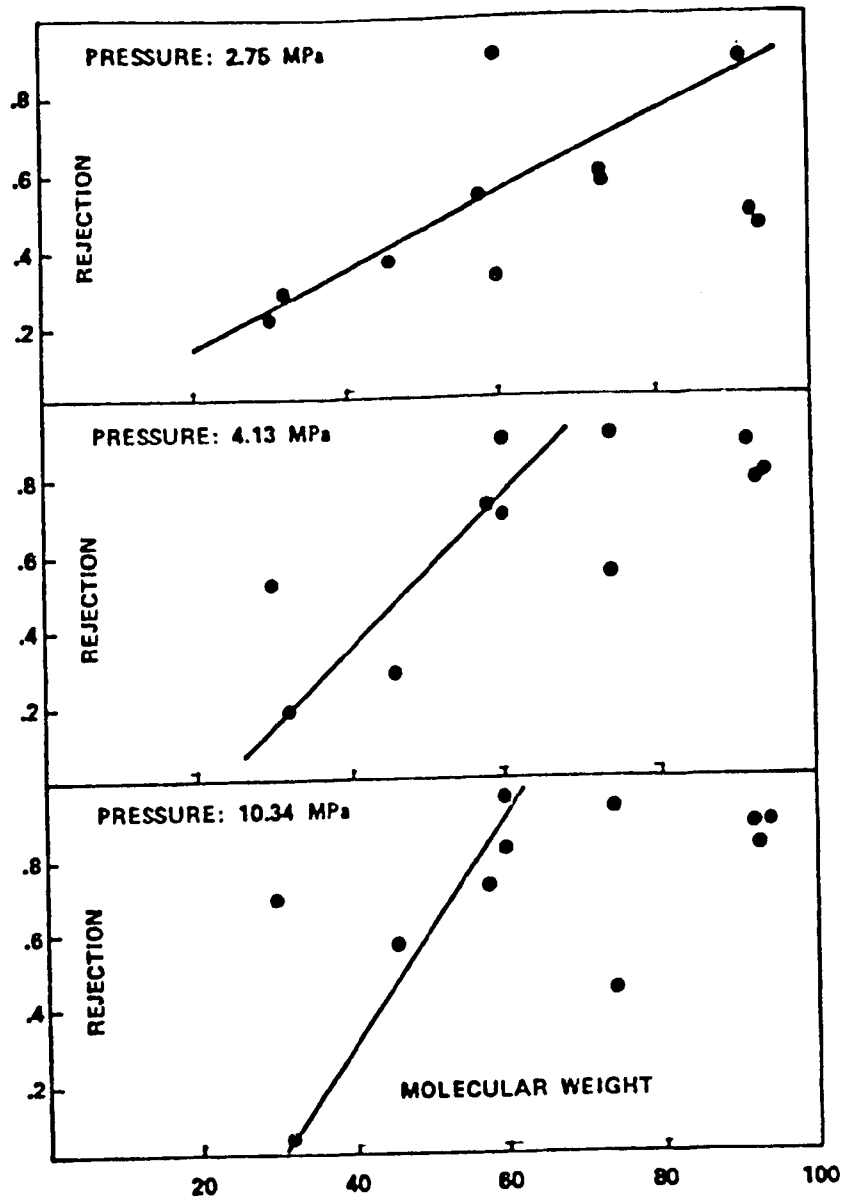

Figure 7. Solute rejection for three operating pressures in dependence on the molecular weight of the solute. Data from Table II.

As demonstrated by Spencer and Gaddis, (2) no correlation between R_i and M_i exists for cellulose acetate membranes. With other membrane systems the molecular weight of the solute can be considered to represent a useful parameter for estimating solute rejection in RO.

References

1. S. Sourirajan and T. Matsuura, in "Reverse Osmosis and Synthetic Membranes", S. Sourirajan, Ed., National Research Council of Canada Publication, Ottaw, Canda, 1977, Chapter 2.
2. H. G. Spencer and J. L. Gaddis, EPA Grant Number R805777-1.
3. T. Matsuura and S. Sourirajan, J. Appl. Polymer Sc., 15, 2905 (1971).
4. T. Matsuura and S. Sourirajan, J. Appl. Polymer Sci., 17, 1043 (1973).
5. T. Matsuura and S. Sourirajan, J. Appl. Polymer Sci., 16, 1663 (1972).
6. T. Matsuura and S. Sourirajan, J. Appl. Polymer Sci., 17, 3683 (1973).
7. K. L. Hoy, J. Paint Techn., 42, 76 (1970).
8. P. A. Small, J. Appl. Chem., 3, 71 (1953).
9. H. H. Konstam and W. R. Feairheller, AIChE J., 16, 837 (1970).
10. D. W. Van Krevelen and P. J. Hoftyzer, "Properties of Polymers", Elsevier Publishing Co., Amsterdam, Netherlands, 1972, Chapter 8.
11. M. Dunkel, Z. physik. Chem., A138, 42 (1928).
12. J. H. Hildebrand and R. L. Soctt, "The Solubility of Non-Electrolytes", Reinhold, New York, 1959.
13. E. S. K. Chian and H. H. P. Fang, Annual Report 1973, U. S. Army Medical Res. and Development Command, Contract No. DADA 17-73-C-3025.
14. H. G. Spencer, J. L. Gaddis, and C. A. Brandon, Membrane Separation Technology Seminar, Clemson University, Clemson, S.C., 1977.
15. J. E. Cadotte, C. V. Kopp, K. E. Cobian, and L. T. Rozelle, Progress Report June 19 to Office of Water Research and Technology, U. S. Dept. of the Interior.

Appendix C

COMPUTER CODE LISTING

```
      REAL LTUBE,LCHNL,LCHNT,LTUBT
      REAL MAREA,MRC,MOMC
      DIMENSION PIN(99,3),CIN(99,3),POUT(99,3),COUT(99,3),CPRM(99,3),
     x   RF(99,3),FTRJ(99,3),FTPM(99,3),CPMOA(99,3),ISTG(3),FIN(99,3),
     x   NTB(99,3),NTBS(99,3)
C
      COMMON/PRAM/IMDUL,DIF,B
      COMMON/TGEOM/      LTUBT,RTUBT,WCHNT,TCHNT,LCHNT
      COMMON/TCOND/CFDT,QFDT,TFDT,PFDT
      COMMON/COND/QFEED,TFEED
      COMMON/GEOM/RTUBE,LTUBE,RFCTR,WCHNL,TCHNL,LCHNL,ATUBE,ACHNL,RHYDR
      COMMON/MSPEC/PERM,STP
C
C     INPUT SECTION
C     READ TYPE OF MODULE(TUBULAR MEMBRANE=1, SHEET MEMBRANE=2)
 1000 CONTINUE
      READ(5,3) IMDUL
      IF (IMDUL.EQ.0) GO TO 2000
      READ(5,4) TREJ,TFLUX
      GO TO (20,21) , IMDUL
   20 READ(5,2)LTUBT,RTUBT
      GO TO 22
   21 READ(5,2) WCHNT,TCHNT,LCHNT
   22 CONTINUE
      READ(5,5) DIF,CFDT,QFDT,TFDT,PFDT,B
C     READ INITIAL CONDITIONS
      READ(5,1)PFEED,QFEED,CFEED,TFEED
C     READ SYSTEM SPECIFICATION
      GO TO (30,31), IMDUL
   30 READ(5,2) RTUBE,LTUBE,RFCTR
```

```
      GO TO 32
   31 READ(5,2) UCHNL,TCHNL,LCHNL,RFCTR
   38 CONTINUE
      READ(5,2) DPRF,DFLOW,DREJ
C     READ CONSTANTS FOR TRANSPORT COEFFICIENTS
      READ(5,2) UCC,UMRC,UMOMC,EPUMP,ERATE,UWC,UEC
C
    1 FORMAT(2F10.4,E10.4,F10.4)
    2 FORMAT(8F10.4)
    3 FORMAT(16I5)
    4 FORMAT(F10.4,E10.4)
    5 FORMAT(2E10.4,4F10.4)
      TFLUX=TFLUX*(PFEED/PFDT)*EXP(-4500.*(1./(TFEED+459.)-
     *   1./(TFDT+459.)))
C
      CALL MBSPEC(TREJ,TFLUX,PERM,STP)
      WRITE(6,52)
   52 FORMAT('1TEST MODULE DATA')
      WRITE(6,53) IMDUL
   53 FORMAT(//,' IMDUL=',I5,'(TUBULAR=1,SHEET=2)')
      WRITE(6,54) TREJ,TFLUX
   54 FORMAT(/,' TEST REJECTION=',F10.4,2X,'TESTFLUX=',E15.8,2X,
     *    'FT/SEC')
      WRITE(6,55)
   55 FORMAT(/,' TEST MODULE GEOMETRY')
      GO TO (56,57), IMDUL
   56 WRITE(6,58) LTUBT,RTUBT
   58 FORMAT(' LENGTH=',F10.4,2X,'RADIUS=',F10.4)
      GO TO 59
   57 WRITE(6,60) UCHNT,TCHNT,LCHNT
```

```
   60 FORMAT(' WIDTH=',F10.4,2X,'THICKNESS=',F10.4,2X,'LENGTH=',F10.4)
   59 CONTINUE
      WRITE(6,61)
   61 FORMAT(/,' TEST CONDITIONS')
      WRITE(6,62) CFDT,QFDT,TFDT,PFDT
   62 FORMAT(' CFDT=',E10.4,'QFDT=',F10.4,'TFDT=',F10.4,'PFDT=',F10.4)
      WRITE(6,50)
      WRITE(6,51) PERM,STP
   50 FORMAT(/,' TRANSPORT PARAMETER')
   51 FORMAT(' PERMEABILITY=',E15.8,2X,'SOLUTE TRNS. PARA.=',E15.8,2X,
     X       'FT/SEC')
C     CALCULATE TUBE CROSS SECTION AREA AND HYDROLIC RADIUS
      GO TO (33,34), IMDUL
   33 ATUBE=3.141593*RTUBE**2.
      RHYDR=RTUBE/2.
      GO TO 35
   34 ACHNL=WCHNL*TCHNL
      RHYDR=TCHNL/2.
   35 CONTINUE
C
C
      CR=CFEED*(1.-DPRF+DPRF*DREJ)/(1.-DPRF)
      CP=CFEED*(1.-DREJ)
C
      J=1
      I=1
      PIN(I,J)=PFEED*144.
      CIN(I,J)=CFEED
C
  154 CONTINUE
```

```
C
C
      CALL MODUL(PIN(I,J),CIN(I,J),POUT(I,J),COUT(I,J ,CPRM(I,J),
     *   RF(I,J))
      IF(I.GT.1) GO TO 151
      FTRJ(1,J)=1.-RF(1,J)
      FTPM(1,J)=1.-FTRJ(1,J)
      CPMOA(1,J)=CPRM(1,J)
      GO TO 152
  151 FTRJ(I,J)=FTRJ(I-1,J)*(1.-RF(I,J))
      FTPM(I,J)=1.-FTRJ(I,J)
      CPMOA(I,J)=FTPM(I-1,J)*CPMOA(I-1,J)/FTPM(I,J)
     *   +(FTPM(I,J)-FTPM(I-1,J))*CPRM(I,J)/FTPM(I,J)
C
  152 CONTINUE
      IF(J.EQ.3) GO TO 150
      IF(CPMOA(I,J).LT.CP) IP=I
      IF(COUT(I,J).GT.CR) GO TO 153
      GO TO 149
  150 IF(COUT(I,J).GT.CFEED) GO TO 159
  149 CONTINUE
      PIN(I+1,J)=POUT(I,J)
      CIN(I+1,J)=COUT(I,J)
      I=I+1
      GO TO 154
C
  153 CONTINUE
      III=I
      IX=(III+IP)/2
C
```

```
  155 CONTINUE
      ISTG(2)=III-IX
      ISTG(1)=IX
C
C
      ISTG1=ISTG(1)
      ISTG2=ISTG(2)
C
      DO 157 I=1,ISTG2
      PIN(I,2)=PIN(IX+I,1)
      CIN(I,2)=CIN(IX+I,1)
      POUT(I,2)=POUT(IX+I,1)
      COUT(I,2)=COUT(IX+I,1)
      CPRM(I,2)=CPRM(IX+I,1)
      RF(I,2)=RF(IX+I,1)
      IF(I.GT.1) GO TO 158
      FTRJ(1,2)=1.-RF(1,2)
      FTPM(1,2)=1.-FTRJ(1,2)
      CPMOA(1,2)=CPRM(1,2)
      GO TO 157
  158 FTRJ(I,2)=FTRJ(I-1,2)*(1.-RF(I,2))
      FTPM(I,2)=1.-FTRJ(I,2)
      CPMOA(I,2)=FTPM(I-1,2)*CPMOA(I-1,2)/FTPM(I,2)
     *   +(FTPM(I,2)-FTPM(I-1,2))*CPRM(I,2)/FTPM(I,2)
  157 CONTINUE
C
C
      I=1
      J=3
      PIN(I,J)=PFEED*132.
```

```
      CIN(I,J)=CPMOA(ISTG2,2)
      GO TO 154
  159 CONTINUE
      NSTG=J
      ISTG(J)=I
      ISTG3=ISTG(3)
C
C
      AAA=FTPM(ISTG1,1)/(1.-FTRJ(ISTG1,1)*FTPM(ISTG2,2)*FTRJ(ISTG3,3))
      BBB=FTRJ(ISTG1,1)*FTPM(ISTG2,2)*FTPM(ISTG3,3)/
     *   (1.-FTRJ(ISTG1,1)*FTPM(ISTG2,2)*FTRJ(ISTG3,3))
      CCC=AAA+BBB
      CX=AAA/CCC*CPMOA(ISTG1,1)+BBB/CCC*CPMOA(ISTG3,3)
      E=CX-CP
      TOL=0.010*CFEED
      IF(ABS(E).LT.TOL) GO TO 160
      IF(E.LT.0.) IX=IX+1
      IF(E.GT.0.) IX=IX-1
      GO TO 155
C
C
  160 CONTINUE
      FIN(1,1)=DFLOW/(1.-FTRJ(ISTG1,1)*FTPM(ISTG2,2)*FTRJ(ISTG3,3))
      FIN(1,2)=FTRJ(ISTG1,1)*FIN(1,1)
      FIN(1,3)=FTPM(ISTG2,2)*FIN(1,2)
      NTEST=0
      DO 167 J=1,3
      ISTGJ=ISTG(J)
      DO 166 I=1,ISTGJ
      IF(I.EQ.1) GO TO 166
```

```
      FIN(I,J)=FIN(1,J)*FTRJ(I-1,J)
  169 CONTINUE
      NTB(I,J)=FIN(I,J)/QFEED+1
      IF(I.GT.1) GO TO 170
      NTBS(1,J)=NTB(1,J)
      GO TO 168
  170 NTBS(I,J)=NTBS(I-1,J)+NTB(I,J)
  168 CONTINUE
      NTBST=NTBST+NTBS(I,J)
  167 CONTINUE
C
C
      WRITE(6,84)
   84 FORMAT('1SUMMARY OF DESIGN AND PERFORMANCE OF THE SYSTEM',///,
     *   ' MODULE DESIGN SPECIFICATIONS AND OPERATING CONDITIONS',
     *   1X,'SPECIFIED')
      GO TO (95,96), IMDUL
   95 WRITE(6,85) RTUBE,LTUBE,RFCTR,QFEED,TFEED,PFEED
   85 FORMAT(/,' TYPE OF MEMBRANE=',11X,'TUBULAR',/,
     *   ' RADIUS OF TUBE=',10X,E12.5,' FT',/,
     *   ' LENGTH OF TUBE=',10X,E12.5,' FT',/,
     *   ' TUBE WALL ROUGHNESS FACTOR=',F5.2,/,
     *   ' TUBE FEED RATE=',10X,E15.8,' GPM',/,
     *   ' FEED TEMPERATURE=', 8X,F8.2,' DEG F',/,
     *   ' PUMP OUTLET PRESSURE=',5X,F8.2,' PSIG')
      GO TO 97
C
   96 WRITE(6,86) WCHNL,TCHNL,LCHNL,RFCTR,QFEED,TFEED,PFEED
   86 FORMAT(/,' TYPE OF MEMBRANE=SHEET OR SPIRAL WOUND',/,
     *   ' WIDTH OF CHANNEL=',E12.5,' FT'/,
```

```
     &    ' LENGTH OF CHANNEL=',E12.5,' FT',/,
     &    ' TUBE WALL ROUGHNESS FACTOR=',F5.2,/,
     &    ' TUBE FEED RATE=',E15.8,' GPM',/,
     &    ' FEED TEMPERATURE=',F8.2,' DEG F',/,
     &    ' PUMP OUTLET PRESSURE=',F8.2,' PSIG')
   97 CONTINUE
C
      WRITE(6,87)
   87 FORMAT(/,' SYSTEM DESIGN SPECIFICATIONS AND OPERATING CONDITIONS',
     &   1X,'SPECIFIED')
      WRITE(6,88) DFLOW,DREJ,DPRF
   88 FORMAT(/,' DESIGN FLOW RATE=',15X,E15.8,' GPM',/,
     &    ' DESIGN REJECTION=',14X,F8.2,/,
     &    ' DESIGN PRODUCT RECOVERY FACTOR=',F8.2)
C
      WRITE(6,89)
   89 FORMAT('1SUMMARY OF NUMERICAL RESULTS',/,
     &   3X,'J',4X,'I',5X,'NTB',4X,'NTBS',5X,'FIN',10X,'PIN',9X,
     &   'POUT', 8X,'CIN',9X,'COUT',6X,'CPMOA',6X,'FTPM',/,29X,'(GPM)',
     &   8X,'(PSFA)',6X,'(PSFA)',2X,'(MOLE/CUFT)',2X,'(MOLE/CUFT)',2X,
     &   '(MOLE/CUFT)',/)
      DO 90 J=1,NSTG
      ISTGJ=ISTG(J)
      DO 91 I=1,ISTGJ
      WRITE(6,92) J,I,NTB(I,J),NTBS(I,J),FIN(I,J),PIN(I,J),POUT(I,J),
     &   CIN(I,J),COUT(I,J),CPMOA(I,J),FTPM(I,J)
   92 FORMAT(2I5,2I7,7E12.5)
   91 CONTINUE
   90 CONTINUE
C
```

```
      WRITE(6,93) CX,AAA,BBB
   93 FORMAT(//,' CX=',E12.5,/,
     *   'PERMEATE FRACTION FROM STAGE 1 =',F5.2,/,
     *   'PERMEATE FRACTION FROM STAGE 3 =',F5.2)
      MAREA=RTUBE**2.*LTUBE*FLOAT(NTBST)
      TCC=UCC*MAREA
      CAF=0.013345
C *** CAPITAL AMORTIZATION FACTOR, CAF=0.013345 FOR 10 PERCENT INTEREST
C *** RATE AND TEN YEAR LIFE.
      CACOST=2.315*CAF*TCC/DFLOW
C *** CALCULATE MEMBRANE REPLACEMENT COST, CENTS/KGAL.
      MRC=UMRC*MAREA/(DFLOW*1440.)
C *** CALCULATE OTHER O+M COSTS, CENTS/KGAL.
      MOMC=UMOMC*MAREA/(DFLOW*1440.)
C *** CALCULATE PUMPING POWER REQUIREMENT, KW.
      PKW=(PFEED/3.117*(DFLOW+FIN(1,3))+DFLOW*QFEED**2.*1.406E-8/
     *   RTUBE**4.+(PFEED-POUT(ISTG3,3)/144.)/3.117*(FIN(1,1)-DFLOW)+
     *   (PFEED-POUT(ISTG1,1)/144.)/3.117*FIN(1,2))/EPUMP/737.56
C *** CALCULATE PUMPING COST, CENTS/KGAL.
      PCOST=PKW*ERATE*16.67/DFLOW
C *** CALCULATE CREDIT FOR RECOVERED WATER.
      WCRDT=UWC*DPRF
C *** CALCULATE CREDIT FOR RECOVERED ENERGY.
      ECRDT=UEC*(TFEED-70.)*4.185E-3
C *** CALCULATE TOTAL PRODUCT COST, CENTS/KGAL.
      TCOST=PCOST+MOMC+MRC+CACOST-WCRDT-ECRDT
C *** PRINT ECONOMIC RESULTS.
      WRITE(6,70)
   70 FORMAT('1SUMMARY OF SYSTEM ECONOMICS')
      WRITE(6,71) TCC,NTBST,MAREA,MRC,MOMC,PCOST,CACOST,WCRDT,
```

```
     *   ECRDT,TCOST
    71 FORMAT(/,' TOTAL INSTALLED CAPITAL COST,DALLARS=', E15.5,
     *   /,' TOTAL NUMBER OF TUBES=',I8,
     *   /,' TOTAL MEMBRANE AREA,SQ FT=',E15.5,
     *   /,' MEMBRANE REPLACEMENT COST,CENTS/KGAL=',F10.2,
     *   /,' OTHER O+M COST,CENTS/KGAL=',F10.2,
     *   /,' PUMPING POWER COST,CENTS/KGAL=',F10.2,
     *   /,' CAPITAL AMORTIZATION COST,CENTS/KGAL=',F10.2,
     *   /,' CREDIT FOR RECOVERED WATER,CENTS/KGAL=',F10.2,
     *   /,' CREDIT FOR RECOVERED ENERGY,CENTS/KGAL=',F10.2,
     *   /,' TOTAL UNIT COST,CENTS/KGAL=',F10.2)
C
      GO TO 1000
 2000 CONTINUE
      STOP
      END

      SUBROUTINE MBSPEC (TREJ,TFLUX,PERM,STP)
      COMMON/TGEOM/      LTUBE,RTUBE,WCHNL,TCHNL,LCHNL
      COMMON/TCOND/ CFEED,QFEED,TFEED,PFEED
      COMMON/PRAM/IMDUL,DIF,B
      REAL LCHNL,LTUBE
C
C     CALCULATE TUBE CROSS SECTION AREA AND HYDROLIC RADIUS
      GO TO (33,34), IMDUL
   33 ATUBE=3.141593*RTUBE**2.
      RHYDR=RTUBE/2.
      GO TO 35
   34 ACHNL=WCHNL*TCHNL
      RHYDR=TCHNL/2.
```

```
   35 CONTINUE
C
      GO TO (36,37), IMDUL
   36 UBAR=QFEED/ATUBE/448.86
      GO TO 38
   37 UBAR=QFEED/ACHNL/448.86
   38 CONTINUE
C    CALL PROPW AND CALCULATE DENSITY AND VISCOSITYOOF SOLUTION.  IT IS
C    ASSUMED THAT THESE PROPERTIES ARE THE SAME AS THOSE FOR PURE WATER.
      CALL PROPW(TFEED,DENS,VIS)
C
C     CALCULATE REYNOLDS NUMBER
      RENR=4.*RHYDR*UBAR*DENS/VIS
C     CALCULATE SCHMIDT NUMBER
      SCNR=VIS/( DENS*DIF)
      GO TO(39,40), IMDUL
   39 X=LTUBE
      GO TO 41
   40 X=LCHNL
   41 CONTINUE
C
C     CALCULATE SHERWOOD NUMBER
      CALL SHWDNR(RTUBE,TCHNL,LCHNL,IMDUL,X,RENR,SCNR,SHNR)
C
C     CALCULATE MASS TRANSFER COEFFICIENT
      TCM=SHNR*DIF/(4.*RHYDR)
      P=PFEED*138.
      C=DENS/18.
C
      STP=TFLUX*(1.-TREJ)/TREJ*EXP(-TFLUX/TCM)
```

```
      PERM=STP*TFLUX*C**8./(C*P*STP-TFLUX*B*CFEED*(1.-TREJ))
      RETURN
      END
      SUBROUTINE MODUL(PINTL,CINTL,P,CA1,CA3AV,RF)
      COMMON/COND/QFEED,TFEED
      COMMON/GEOM/RTUBE,LTUBE,RFCTR,WCHNL,TCHNL,LCHNL,ATUBE,ACHNL,RHYDR
      COMMON/PRAM/IMDUL,DIF,B
      COMMON/MSPEC/PERM,STP
      REAL LTUBE,LCHNL,LAMDA
      DIMENSION TCA1(3),TCA3(3),E(3),GTHET(3)
C
C     INITIALIZE VARIABLES
      X=0.
      XPRNT=0.
      CA3VVS=0.0
      VVS=0.0
      P=PINTL
      GO TO (39,40), IMDUL
   39 UINTL=QFEED/ATUBE/448.86
      GO TO 41
   40 UINTL=QFEED/ACHNL/448.86
   41 CONTINUE
      UBAR=UINTL
      CA1=CINTL
      UC=UBAR*CA1
C     DEFINE INTEGRATION STEP SIZE
      DXX=0.125
C     PRINT INTERVAL
      DXP=2.5
C     WRITE(6,7)
```

```
    7 FORMAT('1 MODULE PERFORMANCE SIMULATION RESULTS',/,2X,'X',10X,
     *   'P',12X,'UBAR',12X,'CA1',12X,'CA2',12X,'CA3',11X,'CA3AV',8X,
     *   'REJ',4X,'REC',/,' (FT)',4X,'(LB/SQFT)',8X,'(FT/SEC)',5X,
     *   '(MOLE/CUFT)',4X,'(MOLE/CUFT)',4X,'(MOLE/CUFT)',4X,
     *   '(MOLE/CUFT)',/)
C
C     INITIALIZE RKG
      L=1
      CALL RKG(X,DXX,L)
C
C   CALL PROPW AND CALCULATE DENSITY AND VISCOSITYOOF SOLUTION.  IT IS
C   ASSUMED THAT THESE PROPERTIES ARE THE SAME AS THOSE FOR PURE WATER.
      CALL PROPW(TFEED,DENS,VIS)
C
C     CALCULATE REYNOLDS NUMBER
  103 RENR=4.*RHYDR*UBAR*DENS/VIS
C     CALCULATE FANNING FRICTION FACTOR
      FFF=0.08*RFCTR/RENR**0.25
C     CALCULATE SCHMIDT NUMBER
      SCNR=VIS/( DENS*DIF)
C
C     CALCULATE SHERWOOD NUMBER
      CALL SHWDNR(RTUBE,TCHNL,LCHNL,IMDUL,X,RENR,SCNR,SHNR)
C
C     CALCULATE MASS TRANSFER COEFFICIENT
      TCM=SHNR*DIF/(4.*RHYDR)
C
C     CALCULATE MOLAR DENSITY OF SOLUTION
      C=  DENS/18.
C
```

```
C     CALCULATE DIMENSIONLESS VARIABLES
      LAMDA=TCM/STP
      GAMMA=B/C/P
      VUSTR=PERM*P/C
      THETA=STP/VUSTR
C
C
C     CALCULATE CA3 BY NEWTON RAPHSON METHOD
C     INITIALIZE TRIAL FOR CA3
      TCA3(1)= 0.5*CA1
      TCA3(2)= 0.4*CA1
C      TOLERENCE FOR N-R CONVERGENCE
      TOL=0.005*CA1
      II=0
      DO 50 I = 1,2
      GTHET(I)=GAMMA*TCA3(I)+THETA
      TCA1(I)=TCA3(I)*(1.+1./GTHET(I)*EXP(-1./LAMDA/GTHET(I)))
   50 E(I)=CA1-TCA1(I)
   52 II=II+1
C     WRITE(6,5) (E(I),I=1,2),(TCA3(I),I=1,3),(TCA1(I),I=1,2)
    5 FORMAT(7E15.8)
C     CHECK CONVERGENCE
      IF(ABS(E(2)).LE.TOL) GO TO 51
      IF(II.EQ.100) GO TO 500
      TCA3(3)=TCA3(2)-E(2)*(TCA3(2)-TCA3(1))/(E(2)-E(1))
      TCA3(1)=TCA3(2)
      TCA3(2)=TCA3(3)
      E(1) =E(2)
      GTHET(2)=GAMMA*TCA3(2)+THETA
      TCA1(2)=TCA3(2)*(1.+1./GTHET(2)*EXP(-1./LAMDA/GTHET(2)))
```

```
      E(2)=CA1-TCA1(2)
      GO TO 52
   51 CA3=TCA3(2)
      UU=VUSTR*(1.-GAMMA*CA3/(GAMMA*CA3+THETA))
      UUS=UU+UUS
      CA3UUS=CA3*UU+CA3UUS
      CA3AV=CA3UUS/UUS
C     CALCULATE CA2
      CA2=CA3*(1.+1./(GAMMA*CA3+THETA))
      REJ=(CA1-CA3)/CA1
      RF=(UINTL-UBAR)/UINTL
C     LOGIC TO STOP PROGRAM
      GO TO (36,37), IMDUL
   36 IF(X.GE.LTUBE) GO TO 100
      GO TO 38
   37 IF(X.GE.LCHNL) GO TO 100
   38 CONTINUE
C
C     OUTPUT SECTION
      IF(X.LT.XPRNT) GO TO 101
C     WRITE(6,4)X,P,UBAR,CA1,CA2,CA3,CA3AV,REJ,RF
    4 FORMAT(  F6.1,6E15.8,2F7.3 )
      XPRNT=XPRNT+DXP
  101 CONTINUE
C     EXECUTE RKG 4 TIMES
      DO 102 I=1,4
      L=2
C
C
C     DEFINE DIFFERENTIAL EQUATIONS
```

```
      GC=32.2
      DX=1.
      DUBAR=-1./RHYDR*VV
      DUC=-1./RHYDR*CA3*VV
      DP=-DENS*(UBAR**2.*FFF/(GC*RTUBE)-1.*VV*UBAR/(GC*RHYDR))
C     CALL RKG FOR EACH VARIABLES
      CALL RKG(X,DX,L)
      CALL RKG(P,DP,L)
      CALL RKG(UBAR,DUBAR,L)
  102 CALL RKG(UC,DUC,L)
C     WRITE(6,20) X,DX,P,DP,UBAR,DUBAR,UC,DUC
   20 FORMAT(///,8E14.8,///)
      CA1=UC/UBAR
C     GO TO NEXT STEP
      GO TO 103
  100 CONTINUE
C     WRITE(6,4) X,P,UBAR,CA1,CA2,CA3,CA3AV,REJ,RF
      RETURN
  500 WRITE(6,6)
    6 FORMAT(/,' N-R NOT CONVERGING')
      STOP
      END
      SUBROUTINE RKG(Z,DZ,L)
      DIMENSION Q(50)
      GO TO (1,2,3),L
    1 N=50
      A2=1.-SQRT(0.5)
      A3=2.-A2
      A4=1./6.
      DO 4 I=1,N
```

```
    4 Q(I)=0.
      H=DZ
      J=1
      RETURN
    2 GO TO(10,20,30,40),J
   10 A=0.5
      B=2.
      GO TO 11
   20 A=A2
      GO TO 12
   30 A=A3
   12 B=1.
   11 C=A
      GO TO 13
   40 A=A4
      B=2.
      C=0.5
      J=0
   13 J=J+1
      L=3
      I=0
    3 I=I+1
      DX=H*DZ
      US=A*(DX-B*Q(I))
      Q(I)=Q(I)+3.*US-C*DX
      Z=Z+US
      RETURN
      END
      SUBROUTINE PROPU(T,DENS,VIS)
C***
```

```
C***THIS SUBROUTINE CALCULATES VISCOSITY AND DENSITY OF WATER AS A FUNCT
ION
C***OF TEMPERATURE.
C***
      REAL LOGT,LOGT2
      D1=62.717763
      D2=-0.38152986E-2
      D3=-0.48932777E-4
      DENS=D1+D2*T+D3*T**2.
C
C
      V1=22.216036
      V2=-16.460588
      V3=3.0949585
      LOGT=ALOG10(T)
      LOGT2=LOGT**2.
      VIS=(V1+V2*LOGT+V3*LOGT2)/3600.
      RETURN
      END
      SUBROUTINE SHWDNR(RTUBE,TCHNL,LCHNL,I,X,RENR,SCNR,SHNR)
C***
C***
C***  THIS SUBROUTINE CALCULATES SHERWOOD NUMBER.  THE EXPRESSIONS ARE O
BTAINED
C***  FROM THE LITERATURE.
C***
C***
      REAL       LCHNL
C
C
C     CHECK REYNOLS NUMBER
      IF(RENR.LT.2100.) GO TO 100
```

```
C
C     TURBULENT FLOW CASE
C     CHECK TYPE OF MODULE
      GO TO (10,20),I
C
C     FOR TUBULAR MEMBRANE
   10 A1=0.127*(1.-60./RENR**0.875)**0.5
      SHNR=0.18*A1*RENR**(7./8.)*SCNR**0.25
      RETURN
C
C     FOR SHEET MEMBRANE
   20 SHNR=0.44*RENR**(7./12.)*(SCNR*TCHNL/2./LCHNL)**(1./3.)
      RETURN
C
C     LAMINAR FLOW CASE
C     CHECK TYPE OF MODULE
  100 GO TO (30,40),I
C
C     FOR TUBULAR MEMBRANE
   30 A3=1.95
      SHNR=A3*(RENR*SCNR*2.*RTUBE/X)**(1./3.)
      RETURN
C
C     FOR SHEET MEMBRANE
   40 A4=3.24
      SHNR=A4*(RENR*SCNR*2.*TCHNL/X)**(1./3.)
      RETURN
      END
```

TECHNICAL REPORT DATA
(Please read Instructions on the reverse before completing)

1 REPORT NO. EPA-600/2-79-195	2.
3. RECIPIENT'S ACCESSION NO.	
4 TITLE AND SUBTITLE Hyperfiltration Processes for Treatment and Renovation of Textile Wastewater	5. REPORT DATE October 1979 6. PERFORMING ORGANIZATION CODE
7 AUTHOR(S) S.M. Ko and J.A. Tevepaugh	8. PERFORMING ORGANIZATION REPORT NO.
9 PERFORMING ORGANIZATION NAME AND ADDRESS Lockheed Missiles and Space Co. Huntsville Research and Engineering Center Huntsville, AL 35807	10. PROGRAM ELEMENT NO. 1BB-610 11. CONTRACT/GRANT NO. 68-02-2614, Task 009
12 SPONSORING AGENCY NAME AND ADDRESS EPA, Office of Research and Development Industrial Environmental Research Laboratory Research Triangle Park, NC 27711	13. TYPE OF REPORT AND PERIOD COVERED Final; 10/78 - 8/79 14. SPONSORING AGENCY CODE EPA/600/13

15. SUPPLEMENTARY NOTES IERL-RTP project officer is Max Samfield, Mail Drop 62, 919/541-2547.

16. ABSTRACT The report describes a computer program developed for the design and simulation of a multistage hyperfiltration system for renovation of textile wastewater. The program is capable of practical design, parametric simulation, and cost projection of the multistage hyperfiltration system with tapered innerstages. The mathematical model is based on Sourirajan's preferential sorption and solute diffusion theory. Experimental rejection and flux data of a test hyperfiltration module are required as inputs. Empirical correlations and test results available from recent EPA-sponsored programs are used to calculate membrane transport parameters. Computed results for sample cases using cellulose acetate and dynamic membranes are presented. Various designs and operations are considered in the computations to show their effects on system economics. The program is readily adaptable for evaluation of other reverse osmosis/hyperfiltration applications.

17. KEY WORDS AND DOCUMENT ANALYSIS

a. DESCRIPTORS		b. IDENTIFIERS/OPEN ENDED TERMS	c. COSATI Field/Group
Pollution	Design	Pollution Control	13B
Textiles	Cost Analysis	Stationary Sources	11E 14A
Waste Water	Osmosis	Hyperfiltration	
Filtration		Reverse Osmosis	07D
Water Treatment			
Renovating			09B
Computer Programs			

18. DISTRIBUTION STATEMENT Release to Public	19. SECURITY CLASS (This Report) Unclassified 20. SECURITY CLASS (This page) Unclassified
	21. NO. OF PAGES 128 22. PRICE

EPA Form 2220-1 (9-73)